

**Genetics of siderophore assembly line biosynthesis
in *Vibrio anguillarum*.**

by

Manuela Di Lorenzo

A DISSERTATION

Presented to the Department of Molecular Microbiology and Immunology
and the Oregon Health and Science University

School of Medicine

in partial fulfillment of

the requirements for the degree of

Doctor of Philosophy

June 2005

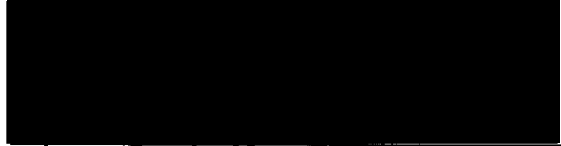
School of Medicine
Oregon Health Sciences University
Department of Molecular Microbiology & Immunology

CERTIFICATE OF APPROVAL


This is certify that the Ph.D. thesis of

Manuela Di Lorenzo


has been approved



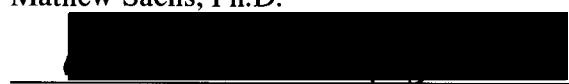
Jorge H. Crosa, Ph.D., Professor in charge of thesis



Richard Brennan, Ph.D.



Mathew Sachs, Ph.D.



Fred Heffron, Ph.D.



David Farrell, Ph.D.



Eric Barklis, Ph.D.

TABLE OF CONTENTS

Table of contents	i
Table of abbreviations	vii
Acknowledgements	xiv
Abstract	xv
Chapter 1	1
1.0. Introduction	2
1.1. Bacterial iron acquisition systems	5
1.1.1. Utilization of iron proteins of the host	7
1.1.2. Siderophore-mediated iron uptake systems	10
1.2. Nonribosomal peptide synthetases and siderophore synthesis	15
1.3. Regulation of bacterial iron uptake systems	21
1.4. <i>Vibrio anguillarum</i> iron acquisition systems	24
1.5. Virulence plasmids and iron acquisition systems	32
1.6. Summary of the work presented in this thesis	34
Chapter 2	62
2.0. Abstract	63
2.1. Introduction	64
2.2. Materials and methods	66
2.2.1. Bacterial strains, plasmids, and growth conditions	66
2.2.2. Determination of the pJM1 sequence	66
2.2.3. Nucleotide sequences accession number	67

2.3. Results	68
2.3.1. Nucleotide composition	68
2.3.2. ORF analysis	68
2.3.3. Utilization of iron	69
2.3.4. Insertion elements and transposon	74
2.3.5. Replication and partition	75
2.3.6. The microheterogeneity of pJM1-like plasmids in strains of <i>V. anguillarum</i>	76
2.4. Discussion	77
2.5. Acknowledgements	81
Chapter 3	91
3.0. Abstract	92
3.1. Introduction	93
3.2. Materials and methods	95
3.2.1. Bacterial strains, plasmids, and growth conditions	95
3.2.2. General methods	95
3.2.3. Construction of the complementing clone	96
3.2.4. Site-directed mutagenesis	97
3.2.5. Construction of <i>V. anguillarum</i> mutant strains by allelic-exchange	98
3.2.6. Determination of DHBA and anguibactin production	99
3.2.7. AngBp protein expression and purification	99
3.2.8. Expression and purification of EntC, Sfp and Vibe	100

3.2.9. Assay for isochorismate lyase activity	101
3.2.10. Analysis of covalent [¹⁴ C] salicylation of the ArCP domain	101
3.2.11. Nucleotide sequences accession number	102
3.3. Results	103
3.3.1. Identification of a chromosomal <i>angB</i> gene in strain 775	103
3.3.2. Mutational analysis of the <i>angBp</i> gene in strain 775	104
3.3.3. Mutational analysis of the <i>angBc</i> gene in strain 775 and generation of a double <i>angB</i> mutant in strain 775	105
3.3.4. Characterization of the AngB functions in vivo	106
3.3.5. ICL and ArCP domain activities in vitro	108
3.4. Discussion	110
3.5. Acknowledgements	113
Chapter 4	127
4.0. Abstract	128
4.1. Introduction	129
4.2. Materials and methods	131
4.2.1. Bacterial strains, plasmids, and growth conditions	131
4.2.2. General methods	131
4.2.3. Construction of the complementing clone	132
4.2.4. Site-directed mutagenesis	133
4.2.5. Construction of promoter fusions in pKK232-8	133

4.2.6. Construction of <i>V. anguillarum</i> strains by conjugation and allelic-exchange	134
4.2.7. Growth in iron-limiting conditions and detection of anguibactin	134
4.2.8. Fish infectivity assays	135
4.2.9. CAT assay	135
4.2.10. RNA isolation	135
4.2.11. Primer extension	136
4.2.12. RNase protection assay	136
4.3. Results	138
4.3.1. Sequencing and analysis of a transposon insertion in the <i>angM</i> gene	138
4.3.2. Construction of an <i>angM</i> mutant in plasmid pJM1 and complementation with the cloned <i>angM</i> gene	138
4.3.3. PCP and C domains of AngM are essential for anguibactin biosynthesis	140
4.3.4. Effect of <i>angM</i> mutations on the virulence phenotype of <i>V. anguillarum</i> 775	141
4.3.5. Transcription and regulation of the <i>angM</i> gene	141
4.4. Discussion	144
4.5. Acknowledgements	148
Chapter 5	165
5.0. Abstract	166

5.1. Introduction	167
5.2. Materials and methods	169
5.2.1. Bacterial strains and plasmids	169
5.2.2. General methods	169
5.2.3. Mobilization of the #120 insertion mutant in <i>angN</i> from pJHC-T2612 to the pJM1 plasmid	170
5.2.4. Construction of the complementing clone	170
5.2.5. Site-directed mutagenesis	171
5.2.6. Growth in iron-limiting conditions and detection of anguibactin	171
5.2.7. Fish infectivity assays	172
5.2.8. RNA isolation	172
5.2.9. Primer extension	173
5.2.10. Ribonuclease protection assays	173
5.3. Results	175
5.3.1. Analysis of the AngN sequence	175
5.3.2. Disruption of the <i>angN</i> gene and complementation with a wild type <i>angN</i> gene	175
5.3.3. Effect of site-directed modification of the <i>angN</i> gene on anguibactin production	176
5.3.4. AngN cyclization domains and the virulence of <i>V. anguillarum</i>	178
5.3.5. Transcription and regulation of the <i>angN</i> gene	178

5.4. Discussion	181
5.5. Acknowledgements	184
Chapter 6	197
6.0. Discussion	198
6.1. Summary and conclusions	207
References	210

TABLE OF ABBREVIATIONS

A (DNA context)	deoxyadenosine
A (protein context)	alanine
A (NRPS domain)	adenylation
α	alpha
ABC	ATP binding cassette
AcCoA	acetyl coenzyme A
ACP	acyl carrier protein
ADP	adenosine diphosphate
Ap	ampicillin
ArCP	aryl carrier protein
ATP	adenosine triphosphate
ATPase	adenosine triphosphatase
β	beta
bp	base pairs
BSA	bovine serum albumin
C (DNA context)	deoxycytosine
C (protein context)	cysteine
C (NRPS domain)	condensation
C-	carboxy-
$^{\circ}\text{C}$	degree Celsius
CAS	chrome azurol S

CAT	chloramphenicol acetyl transferase
Cl	chloride
Cm	chloramphenicol
CoA	coenzyme A
cpm	counts per minute
Cy	cyclization
D	aspartic acid
Da	dalton
DHB	2,3-dihydroxybenzoyl
DHBA	2,3-dihydroxybenzoic acid
DHBS	2,3-dihydroxybenzoylserine
DHP	dihydroxyphenyl
DHPT	dihydroxyphenylthiazolyl
DNA	deoxyribonucleic acid
DNase	deoxyribonuclease
DTT	dithiothreitol
E (protein context)	glutamic acid
E (NRPS domain)	epimerization
ϵ	extinction coefficient
ECF	extracytoplasmic function
EDDA	ethylenediamine-di-(<i>o</i> -hydroxyphenyl acetic acid)
EDTA	ethylenediaminetetraacetate

E2p	dihydrolipoyl transacetylases
F	phenylalanine
FAD	flavin adenine dinucleotide
Fe	iron
Fe ²⁺	ferrous iron
Fe ³⁺	ferric iron
G (DNA context)	deoxyguanosine
G (protein context)	glycine
g	gram
γ	gamma
Ga	gallium
Gm	gentamycin
H (protein context)	histidine
H (chemical compounds)	hydrogen
h	hour
I	isoleucine
ICL	isochorismate lyase
IPTG	isopropyl-β-D-thiogalactoside
IS	insertion sequence
ITB	iron transport biosynthesis
K (protein context)	lysine
K (chemical compounds)	potassium
kb	kilobase pairs

kDa	kiloDalton
Km	kanamycin
L	leucine
λ	lambda
LB	Luria-Bertani medium
LD ₅₀	50% lethal dose
LDH	L-lactate dehydrogenase
M (protein context)	methionine
M	molar
Mg	magnesium
mg	milligram
μ g	microgram
MIC	minimal inhibitory concentration
min	minute
ml	milliliter
μ l	microliter
mM	millimolar
μ M	micromolar
mOX	methyloxazolinyl
mRNA	messenger RNA
MT	methylation
N	asparagine
N-	amino-

Na	sodium
NADH	nicotinamide adenine dinucleotide
NADPH	nicotinamide adenine dinucleotide phosphate
ng	nanogram
nM	nanomolar
nm	nanometer
nmol	nanomole
NRPS	nonribosomal peptide synthetase
NSPD	norspermidine
O	oxygen
OD _x	optical density at x nm
OMR	outer membrane receptor
ORF	open reading frame
Ox	oxidase
P	proline
PAGE	polyacrylamide gel electrophoresis
PBP	periplasm binding protein
PCP	peptidyl carrier protein
PCR	polymerase chain reaction
%	percent
pITBO	promoter of the iron transport biosynthesis operon

PMF	proton motive force
PP	phosphopantetheinyl
Q	glutamine
R	arginine
Red	reductase
Rif	rifampicin
RNA	ribonucleic acid
RNase	ribonuclease
S	serine
s	seconds
SDS	sodium dodecyl sulfate
Sp	spectinomycin
T (protein context)	threonine
T (DNA context)	deoxythymidine
TAF	transacting factor
Tc	tetracycline
TCA	trichloroacetic acid
TCEP	tris(carboxyethyl)phosphine
TE	thioesterase
Tp	trimethopim
TSBS	trypticase soy broth with 1% NaCl
TSAS	trypticase soy agar with 1% NaCl
UTP	uridine triphosphate

V	valine
W	tryptophan
Y	tyrosine
Zn	zinc

Acknowledgements.

I would like to thank Jorge and Lidia Crosa for all their support and the way they always made me feel at home.

Also many thanks to Marcelo Tolmasky and Luis Actis for the fruitful and fun discussions on my thesis project but also on several non-scientific subjects.

To Kirsten Mattison and the past and present members of the lab, I owe gratitude for the help they gave me in the progress of this work.

I am also grateful to the members of my committee for their support in the development of my project.

I could have not done much of the work for this thesis without the assistance of Jeff Vandehey and Chris Langford during my many computer crises.

I also want to thank my parents: Grazie per aver condiviso ogni mia ambizione e per l'aiuto che mi avete sempre dato, anche in questa avventura in terra straniera.

Finally, I am very glad for the presence in my work and private life of Michiel Stork that always supports me and helps me overcoming any obstacle.

Abstract

The pathogen *Vibrio anguillarum* causes a fatal hemorrhagic septicemia in salmonid fishes and many isolates of this bacterium possess a plasmid-mediated iron uptake system that has been shown to be essential for virulence. This iron acquisition system centers on the siderophore anguibactin that is synthesized from 2,3-dihydroxybenzoic acid, cysteine and histidine via a nonribosomal peptide synthetase mechanism. Nonribosomal peptide synthetases (NRPSs) are multimodular proteins that assemble peptides in the absence of an RNA template. A wide variety of compounds, such as siderophores and antibiotics, have been shown to be produced by these enzymes that operate as an assembly line in which the order of the modules is colinear to the order of the amino acids in the final product. NRPS synthesis of peptides is more versatile than the classic tRNA based assembly since they have at their disposal a larger number of monomers that are also modified once incorporated in the compound.

In this thesis I analyzed the sequence of plasmid pJM1 harbored by the virulent *V. anguillarum* strain 775 and showed that the biosynthesis genes for the siderophore anguibactin are all harbored on this plasmid. These genes encode proteins with domains highly similar to NRPSs involved in the synthesis of siderophores produced by other bacteria. I determined the role that some of these gene products have in anguibactin assembly and showed that the domain organization of this system is unusually fragmented. Functionality of the domains was also assessed by genetic analysis introducing residue substitutions in highly conserved motifs within the domains and testing the resulting mutant strains for their ability to produce anguibactin and establish infection in the fish host. I also initiated the biochemical determination of the domain

activities and showed a correlation of the results obtained by the in vivo and in vitro approach.

CHAPTER 1

Introduction

Part of the topics presented in this introduction were published in:

Vibrio

Manuela Di Lorenzo, Michiel Stork, Alejandro F. Alice, Claudia S. López, and Jorge H. Crosa

Chapter 16 (p. 241-255) in J. H. Crosa, A. R. Mey and S. M. Payne (ed.)

Iron transport in bacteria. ASM Press Washington D.C. USA.

1.0. Introduction

Iron is a very abundant metal on the Earth's crust and displays remarkable chemical properties mainly due to its wide range of redox potentials (23). In most organisms many essential cellular functions, such as respiration, nitrogen fixation, photosynthesis and DNA precursor biosynthesis, are performed by iron containing proteins thus this metal is an essential element for the growth of nearly all living organisms. The amount of iron required for growth varies between 10^{-6} and 10^{-7} M (145). Iron is highly insoluble at neutral pH in the presence of oxygen and in nature is primarily found as part of ferric-hydroxide complexes (136). Furthermore, if not complexed iron can be extremely toxic to cells since in its ferrous form (Fe^{2+}) it can react with superoxides and hydrogen peroxide and generate highly reactive hydroxide radicals (24, 69).

In the vertebrate biological fluids the amount of total iron is quite high, however the amount of iron freely available is extremely low, about 10^{-18} M, because most of it is bound by high-affinity iron-binding proteins that store and transport iron (136, 193).

Furthermore, the majority of iron in vertebrates is found inside the cells bound to ferritin and heme, with the latter mainly found in erythrocytes as part of the protein hemoglobin. In case of red blood cell lysis, the free hemoglobin in the blood is rapidly bound by haptoglobin and the resulting complexes removed from circulation by reticuloendothelial cells (141). If circulating haptoglobin is saturated, heme is released from hemoglobin by oxidation. Unbound-heme is complexed by the proteins hemopexin and albumin, but only heme bound to hemopexin can be removed from the serum by

hepatic parenchymal cells. The heme-albumin complexes instead continue circulating in the blood stream until heme can be transferred to apo-hemopexin and cleared (176).

Ferritins are intracellular iron-storage proteins found in most animal and plant tissues. Ferritins are water-soluble high molecular weight protein complexes (24 protein subunits of 19-21 kDa) that can accommodate a prosthetic group of iron hydroxide-phosphate composed of more than 4,000 atoms of ferric iron (Fe^{3+}) (136). At physiological pH, ferritins can solubilize iron by binding the highly toxic ferrous iron, oxidizing it to ferric iron and thus sequestering the metal in its less toxic form (168). Bacterial ferritins and bacterioferritins perform in the bacterial cell the same function of iron storage and iron detoxification as ferritins in the eukaryotic cell (155).

The extracellular iron is bound by lactoferrin in secretions and transferrin in serum. The association constant of these proteins for iron is about 10^{22} M and they are normally only partially saturated with iron, as a consequence, even when the iron concentration is above normal values, it can be complexed by the high-affinity iron-binding proteins to keep the amount of free iron limited (136, 193).

Transferrins are single-chain glycoproteins with molecular weights of 75-80 kDa and they have two similar but not identical binding sites for iron. In the blood about 95% of iron is bound to the transferrins that are saturated with iron only 30-40% in normal conditions (136, 193). The main role of transferrin is to transport iron from the area where it is released to another area where it can be either utilized or stored. Transferrins can be transported in the eukaryotic cells where they release the ferric ions without been degraded and they are then recycled to the extracellular fluids (193). Lactoferrins have a

structure similar to transferrins and have an analogous function in mucosal secretions such as milk, tears, nasal mucus and saliva (10).

1.1. Bacterial iron acquisition systems

The necessity of vertebrates to complex iron to overcome the solubility and toxicity issues of this element resulted in the evolution of an environment very poor in free iron that does not allow growth of invading microorganisms. To establish an infection, pathogenic bacteria must possess one or more efficient iron-scavenging systems to acquire the complexed-iron from the host (187).

Obviously iron is not the only factor required for bacteria to establish an infection. Several components are required for pathogenesis and determinants of virulence include various factors that allow the colonization of a specific niche in the host, invasion of tissues and/or cells and the synthesis of metabolites that are advantageous for the invading bacteria and could be detrimental for the host.

Pathogenic bacteria have evolved several mechanisms to compete with or to mine the iron transport and storage mechanisms of the host. These mechanisms are also utilized in any other environment in which iron availability is a limiting factor for growth and they are expressed only when necessary for survival (23, 136, 145, 193).

Mechanisms of microbial iron uptake can be divided into two main groups: those mediated by siderophores that scavenge iron from the high-affinity iron-binding proteins of the host and those that employ cell surface receptors that specifically recognize host iron proteins (136, 193).

Systems from both groups require outer membrane receptors with high affinity for their cognate ligands (Fig. 1.1). Transport through these receptors is an active process and requires energy for iron internalization. Unlike the inner membrane, the outer membrane does not have any of the classical means to generate energy for transport, such

as ATP hydrolysis or an established ion gradient. Thus, transport through the outer membrane receptors is energized by the proton motive force (PMF) of the inner membrane and it requires a complex of proteins, the TonB system (132). The TonB system consists of three proteins, TonB, ExbB and ExbD that interact at the cytoplasmic membrane and transduce the PMF energy to the outer membrane receptors (Fig. 1.1). TonB is the actual energy transducer of the complex and it consists of three distinct functional domains: the amino-terminal, the central and the carboxy-terminal domain. The amino-terminal domain of TonB is the transmembrane domain and it has been shown to be important for energy transduction. On the other hand, the carboxy-terminal domain is essential for the interaction with the outer membrane transporters. The central region spans most of the periplasmic space and possesses a proline-rich domain that seems to play a structural role more than having any direct involvement in transducing the energy to the outer membrane. Although the TonB protein is a cytoplasmic membrane protein it has been found almost in equal amounts associated with the outer membrane where it interacts with the ligand-bound receptor (93). The model for energy transduction to the outer membrane receptor proposes that the TonB protein exist in two basic conformations: the uncharged TonB that is associated with ExbB and ExbD in the inner membrane and the charged TonB generated by the combined action of ExbB, ExbD and PMF. This energized conformation of TonB is able to shuttle to the outer membrane and directly contact the ligand-bound receptor, transducing the PMF energy and allowing active transport of the ligand into the periplasmic space. The discharged TonB returns to the cytoplasmic membrane in a process that requires ExbB and ExbD (132).

As shown in Figure 1.1, once in the periplasm the ligand is recognized by soluble periplasmic binding proteins (PBPs) that serve as high-affinity carriers to escort ligands to the inner membrane transporters (89). Since the PBPs target substrates to their cytoplasmic membrane transporters, the binding affinity of these proteins for the substrates they transport into the cytoplasm, is not necessarily strong. Transport across the inner membrane requires additional energy and occurs by means of an ABC transporter (89). ABC transporters consist of four domains, two hydrophobic domains and two hydrophilic membrane-associated ATP binding domains (Fig. 1.1). One or two proteins, forming homo- or heterodimers in the inner membrane, constitutes the hydrophobic portion of the membrane-spanning transporter while two copies of the same protein harboring the ATP-binding cassette are usually found associated with each monomer. ATP hydrolysis provides the energy to transport the ligands delivered by the PBPs across the inner membrane into the cell cytosol (89).

1.1.1. Utilization of iron proteins of the host

A quite diverse array of receptors for host iron proteins (transferrins, lactoferrins and hemoglobin) can be found in a growing number of bacterial pathogens (136).

The transferrin receptors have been very well characterized in *Neisseria* species and in *Haemophilus influenzae* (148, 149). In both bacteria the receptor constitutes of two proteins, TbpA and TbpB, which form a complex at the outer membrane able to recognize Fe³⁺-transferrin. TbpA is a TonB-dependent outer membrane transporter and *Neisseria* mutants that do not express TbpA were unable to grow in media containing transferrin as the sole iron source. TbpB has been shown to be a lipoprotein and it has been proposed that its lipid tail tethered it to the outer leaflet of the outer membrane.

Mutants in either *tbpA* or *tbpB* are still able to bind transferrin at the outer membrane with the *tbpB* mutant still showing iron uptake from transferrin though at a lower rate than the wild type (33). TbpB binds transferrin in a 1:1 ratio, while two molecules of TbpA appear to bind each molecule of transferrin. Furthermore, a different affinity for ferric-transferrin was observed in the two proteins with TbpB binding preferentially diferric-transferrin and TbpA showing no preference for the iron status of its ligand (33). Based on these observations a model has been proposed for the mechanism of recognition and iron extraction from transferrin by the TbpA and TbpB proteins of *Neisseria* (34, 136). In this dynamic model TbpB initially recognizes and binds holotransferrin that is then presented to the TbpA dimer in the outer membrane. Association of both receptor proteins with the ferrated ligand may induce conformational changes in the transferrin resulting in iron release. Each ferric-iron ion is then internalized to the periplasm through one of the TbpA molecules in an event that requires energy transduced from the TonB complex. Once in the periplasm iron is bound by the periplasmic binding protein FbpA that then interacts with the FbpB and FbpC proteins in the inner membrane. FbpB resembles a permease while FbpC is the ATPase that provides the energy to facilitate the passage of iron through FbpB to the cytoplasm (136). *Neisseria* species also express a receptor for lactoferrin that is, in many respects, similar to the transferrin receptor TbpBA (34).

The ability to use heme as an iron source is associated with a growing number of pathogenic bacteria (136). Not surprisingly, since heme is ubiquitous in the living matter, heme acquisition systems have been also identified in nitrogen-fixing bacteria, such as *Sinorhizobium meliloti* and *Rhizobium leguminosarum* (127). In the blood, bacterial

access to heme and hemoglobin is limited due to the host sequestration mechanisms. To increase the concentration of these iron sources, some bacteria secrete hemolysins and cytolytins that release the heme and the hemoglobin from red blood cells (127).

All heme uptake systems have a strict requirement for the presence of an outer membrane receptor but different systems show variability in their components as well as in the substrates recognized. Nevertheless, two common mechanisms can be found in heme transport in bacteria (136). Some bacteria secrete hemophores that bind heme or hemoproteins with high affinity and deliver them to the outer membrane receptor. The other mechanism is non-hemophore-dependent and the heme or the hemoproteins bind directly the bacterial cell surface through the outer membrane transporters (44, 136). These receptors differ in their ability to recognize heme alone or heme in the context of the host hemoproteins (hemoglobin, hemoglobin-haptoglobin, heme-hemopexin, heme-albumin and myoglobin), with few of these transporters limited to only one or a few structurally similar substrates (136). Recognition of the hemoproteins seems to occur mainly through heme and not the surrounding protein scaffold (127).

The best-characterized hemophore is the HasA protein of *Serratia marcescens* (44, 136). HasA is a 19 kDa protein that binds one molecule of heme with high affinity in a solvent-exposed pocket. Two residues in this pocket (histidine 32 and tyrosine 75) are the axial iron ligands and bind heme in a fashion similar to the majority of hemoproteins (44, 136). HasA captures heme by interacting with hemoglobin. This interaction reduces the affinity of the globin for the heme ligand allowing transfer of heme to the binding pocket of HasA (44, 136). Hemophores can also capture heme from hemopexin and myoglobin although in some cases only one heme carrier protein can be

recognized by a specific hemophore, e.g. hemopexin is the only substrate for *H. influenzae* hemophore (136). The heme-hemophore complexes bind the receptor and heme must be transferred to the transporter since only the intact heme ligand is taken up by the cell. Conformational changes that reduce the affinity for heme must occur in the hemophore upon binding since the receptor has a lower affinity for heme than the hemophore. A possible involvement in the heme-stripping step of the energy transducing TonB complex has been proposed (44).

Similarly, when hemoproteins directly bind to TonB-dependent receptors, heme needs to be released from the protein scaffold to be transported to the periplasm. Histidine residues in the receptor could act as axial ligands for heme and play a major role in internalization (136). Once heme has crossed the outer membrane it is recognized by the PBP and shuttled to a heme-specific ABC transporter in the inner membrane. The heme-specific ABC transporter differs from the non-heme ABC transporter in having only one permease protein that does not form a dimer in the cytoplasmic membrane (44). The heme delivered in the cytoplasm can be directly incorporated into enzymes or the iron can be removed by heme oxygenases that degrade the porphyrin ring.

1.1.2. Siderophore-mediated iron uptake systems

Siderophores are low molecular weight compounds (< 1,000 Da) that contain side chains and functional groups that can coordinate ferric-iron ions with high affinity and specificity, with their dissociation constants ranging from 10^{-22} to 10^{-50} M (136, 137, 193). The siderophore affinity for iron is sufficiently high to remove Fe^{3+} from transferrin, lactoferrin and ferritin but not to remove the iron from the heme proteins. Ferric iron has a valence of 3 and to be thermodynamically stable requires hexadentate

coordination (137). To be able to coordinate iron, siderophores need functional groups possessing a lone pair with good electron donor properties. Three main functional groups of siderophores have been identified: catecholates, hydroxamates and hydroxycarboxylates (137, 182). However, the variety of functional groups identified (oxazoline, thiazoline, hydroxypyridinone, α - and β -hydroxy acids and α -keto acid) is growing with the increasing number of siderophore structures solved (137, 182).

Catecholate and phenolate siderophores are characterized by the presence of functional phenolic hydroxyl groups. The main catechol and phenol ring found in siderophore structures are 2,3-dihydroxybenzoic acid (DHBA) and 2-hydroxybenzoic acid, also known as salicylate (137, 182). These two compounds are made from chorismic acid, the central intermediate of aromatic amino acid biosynthesis, by specialized enzymes that in conditions of iron limitation reroute the flux of chorismate to the production of siderophore precursors. Chorismic acid conversion to DHBA requires three enzymes, isochorismate synthase, isochorismate lyase (ICL) and 2,3-dihydro-2,3-DHBA dehydrogenase (Fig. 1.2), that have been well characterized in the *Escherichia coli* enterobactin system, *entABC* (100, 117, 140). DHBA is the precursor of several other siderophores such as vibriobactin of *Vibrio cholerae* and vulnibactin of *V. vulnificus*, and the same enzymes identified for the pathway of DHBA biosynthesis in *E. coli* are encoded by genes found within the gene clusters for these siderophores (99, 194). Salicylate is produced from chorismic acid by *Pseudomonas* species making pyochelin in a two-enzyme pathway (60, 154) that does not require the dehydrogenase (Fig. 1.2). Since in *Yersinia* species that produce yersiniabactin only one gene, *ybtS*, has been identified in the pathogenicity island for the salicylate pathway, formation of this

phenolate from chorismic acid may follow a different reaction mechanism in these bacteria (62). Interestingly, all the siderophores mentioned above, with the exception of enterobactin, possess besides the catecholate or phenolate functional group, five-member heterocyclic rings, such as oxazoline and thiazoline (Fig. 1.3) that have been shown to be involved in the coordination of ferric iron (182).

Enterobactin, a cyclic trimer of 2,3-dihydroxybenzoylserine (DHBS), is the most studied siderophore system and it is found in most enteric bacteria (36, 125).

Enterobactin is assembled via a nonribosomal peptide synthetase mechanism (see section 1.2.) from DHBA and serine by the products of the *entBDEF* genes, as shown in Figure 1.4 (182). The genes required for DHBA biosynthesis, *entABC*, are also encoded by this system and they are found with the other *ent* genes and the genes encoding the transport proteins, *fep*, organized in 7 transcriptional units (51). The EntB protein is a bifunctional protein required for DHBA production but also intervening in enterobactin biosynthesis (61). Once synthesized enterobactin is secreted into the environment probably through EntS a member of the major facilitator superfamily of export pumps (59). Enterobactin has the highest dissociation constant for iron, 10^{-52} M, of all siderophores studied so far and can readily acquire ferric iron from transferrins and other iron-chelating compounds (51, 137). Ferric-enterobactin is recognized by the outer membrane receptor FepA and internalized in a TonB-dependent process (51). The other Fep proteins, FepBCDG, complete the transport to the cytoplasm of iron still bound to the siderophore (51). Once in the cytoplasm iron is released from enterobactin by the activity of Fes, an esterase that hydrolyzes the siderophore molecule at its three ester bonds thus reducing the affinity of

enterobactin for ferric iron (51). Some bacteria do not produce enterobactin but express a receptor for it that enables them to utilize this siderophore whenever present (46).

Hydroxamate siderophores are observed with both linear and cyclic backbones with typically two hydroxamate groups per molecule (Fig. 1.5). Alcaligin from *Bordetella* species and ferrichrome from the fungus *Ustilago sphaerogena* are examples of macrocyclic hydroxamate siderophores while aerobactin found in enteric bacteria has a linear structure (53, 108, 114). Although hydroxamates can be the only functional group present in a siderophore, several structures have been described in which additional iron-chelating functional groups were found in conjunction with hydroxamate groups, e.g. mycobactin of *Mycobacterium tuberculosis*, pyoverdine from *Pseudomonas aeruginosa* and ornibactin of the closely related *Burkholderia cepacia* (1, 64, 160). The lone pair of hydroxamate oxygens are extremely good nucleophiles due to the proximity of the lone pair of electrons on the nitrogen. As a result hydroxamate groups are highly efficient in coordinating ferric iron. The hydroxyl is derived from molecular oxygen reduced by two electrons to generate the hydroxamate (137, 182). Monooxygenase catalyze the amine oxygenation reaction and the best-characterized enzyme is IucD, the lysine: N⁶-hydroxylase of the aerobactin system. IucD functions as a tetramer with a FAD cofactor that accepts electrons from NADPH the preferred source of reducing equivalents (167).

Aerobactin is assembled from two molecules of lysine and one molecule of citrate that serves as a central linker (Fig. 1.6). The aerobactin system is organized in a single operon of 5 genes *iucABCDiutA* that encode the enzymes for the synthesis of the siderophore, *iuc*, and the receptor for ferric-aerobactin, *iutA* (42). During synthesis the lysine molecules are converted to N⁶-hydroxylysine by the product of the *iucD* gene, as

described above. This intermediate is the substrate for IucB, which N-acetylates the hydroxamate with an acetyl group derived from acetyl-CoA (42). IucA and IucC are the α and β subunits of the synthetases that assemble the two N⁶-acetyl-N⁶-hydroxylysine molecules onto the citrate in two discrete steps (42). Following aerobactin synthesis and secretion, the ferric-aerobactin is recognized by the IutA receptor and it is internalized in a TonB-dependent process (42). Additional proteins are required to complete the transport of ferric-aerobactin to the cytoplasm, FhuB, the PBP, and FhuCD, the ABC transporter. These proteins are part of the ferrichrome transport system and their genes, *fhuBCD*, form a genetic cluster that is not linked to the aerobactin cluster or any other siderophore biosynthesis genes (22).

Although aerobactin has a dissociation constant for ferric iron of 10^{-23} M that is lower than that of enterobactin, aerobactin seems to be more effective than enterobactin in competing for iron with the host iron-binding proteins in vivo (191). The main difference between the two siderophores lies in the ability of the host to recognize, bind and inactivate enterobactin through albumin and lipocalin (a protein associated with the immune response) limiting, in the blood, the effectiveness of enterobactin in supplying iron to the bacterium (57). It is then not surprising that *E. coli* strains associated with extraintestinal infections express aerobactin in addition to enterobactin and production of the former siderophore has been associated with virulence (184, 191).

1.2. Nonribosomal peptide synthetases and siderophore synthesis

Most siderophores are synthesized via a nonribosomal peptide synthetase (NRPS) mechanism that catalyzes the formation of peptides such as siderophores and antibiotics in the absence of an RNA template (85, 177). The NRPS precursors are exceedingly diverse (more than 300 have been identified to date) and allow the synthesis of a wide variety of secondary metabolites. In contrast, the mRNA-dependent ribosomal synthesis of peptides is restricted to the incorporation of only 20 amino acid precursors (21 when selenocysteine is included) clearly limiting the variability of the compound primary structures (103, 115).

Three domain types are required for peptide bond formation, the adenylation (A), the peptidyl carrier protein (PCP) and the condensation (C) domains (Fig.1.7). Although a wide variety of domain arrangements have been identified in the different systems, the following description represents a “typical” NRPS in which repeats of A-PCP-C are found tethered to each other. Each repeat constitutes a module that is responsible for the incorporation of one amino acid into the final product through a step-by-step elongation process (159). Modules are semiautonomous units carrying all the information for recognition, activation and tethering of one substrate and these units are organized colinearly with the order of the amino acids in the peptide (83). Thus, NRPSs are multimodular enzymes that work as an enzymatic assembly line in which the order and the number of the modules determine the sequence and the length of the peptide (178).

Each step of the synthesis requires that the amino acid substrate is activated by ATP hydrolysis to its adenylate form (Fig. 1.7). Activation of the substrate as aminoacyl adenylate is mediated by the A domain at the expense of Mg^{2+} -ATP (32, 103). The

aminoacyl adenylate is an unstable intermediate that is transferred and bound as a thioester to the PCP domain of the same module (Fig. 1.7). The adenylation domain is the major determinant of specificity of each module and as a consequence it is the A domain arrangement that dictates the sequence of the peptide (103, 182).

The site of tethering of the substrate onto the PCP domain is at the enzyme-bound 4'-phosphopantetheinyl (4'-PP) cofactor (157). The site of cofactor binding of PCP domains has a signature sequence LGx(HD)SL that is highly homologous to the same site of acyl carrier proteins (ACP) of modular fatty acid and polyketide synthases (103, 157). Although the ACP and PCP proteins perform similar functions, the homology between these two groups of proteins is limited only to the site of tethering of 4'-PP. This cofactor is posttranslationally added to the PCP domains by 4'-PP transferases that use coenzyme A (CoA) and carrier protein domains as substrates (92). This superfamily of proteins catalyze the conversion of apo-proteins to their holo forms by nucleophilic attack of the β -hydroxy side chain of the conserved serine in the signature sequence of ACP and PCP domains on the pyrophosphate bond of CoA. The 4'-PP arm is transferred on the attacking serine and 3',5'-ADP is released (92). Protein-protein interactions seem to determine specificity of the 4'-PP transferases for the carrier protein domains and each NRPS system identified so far has a gene encoding a dedicated 4'-PP transferase associated with the peptide synthetase operons (51, 135, 194). Experimental evidence has accumulated proving the essential role of the serine residue in the function of PCP domains (147, 157).

The C domain catalyzes formation of a peptide bond between two activated substrates tethered on PCP domains of different modules (97, 139). Therefore, although

modules can act independently of each other, their concerted action is required for peptide elongation. The activated amino acid of the upstream module is transferred to the substrate on the PCP of the downstream module (Fig. 1.7). The growing peptide is translocated with each elongation step along the NRPS from its N-terminus to the C-terminal end (103). A mechanism for C domains has been proposed based on the homology of these domains with the chloramphenicol acetyltransferases (CAT) and dihydrolipoyl transacetylases (E2p), part of the pyruvate dehydrogenase multienzyme (16, 81). The homology of the C domains to CAT and E2p is limited to a core motif (HHxxxDG) and the second histidine of this motif is thought to act as the general base promoting nucleophilic attack of the hydroxy molecule of chloramphenicol in CAT and of the thiol group of CoA in the E2p catalytic domain (the first histidine of the motif is not conserved in E2p) (103). The conservation of the HHxxxDG motif and the similar reaction catalyzed by the C domain may indicate a similar function of the second histidine in this NRPS domain. Mutations in this residue resulted in a drastic reduction of condensation activity of the C domain of VibF of the vibriobactin system and TycB of the tyrocidine A biosynthetic pathway, supporting the essential role of the second histidine in the active site (16, 106). In the case of VibH, the free-standing C domain of the vibriobactin system, the results obtained with a mutant in which the histidine was replaced by an alanine do not coincide with a critical role of this residue for the reaction (80, 81). It should be noted that the second histidine is still in the active site of VibH as determined by X-ray diffraction analysis and the role played by this histidine may be different in each C domain depending on the donor and acceptor involved in the peptide bond formation (80, 81).

At the C-terminal end of the module that adds the last amino acid to the peptide, a region with homology to thioesterases is usually found in place of the C domain. The thioesterase (TE) domain releases the synthesized peptide from the PCP domain of the last module by transfer to a water molecule for linear products (Fig. 1.7) or to a nucleophile on the peptide itself in the case of cyclic products (18, 182). In association with NRPS systems, TE domains encoded by a distinct gene and not as part of a module can be found. These enzymes, called type II TE, are involved in clearing mischarged PCP domains that are blocked by a non-specific thioesterification of their 4'-PP cofactor (150, 196).

Besides the domains just described several other domains can be found in a given module that modify the corresponding amino acids to be inserted in the peptide (86, 181). Cyclization (Cy) domains are specialized C domains that form five-member heterocyclic rings using amino acids possessing β -carbon nucleophiles, such as cysteine, serine and threonine (50, 106). Heterocyclization occurs in two steps, the first of which is the initial amide bond formation similar to the condensation carried out by typical C domains (Fig. 1.8). In the second step cyclodehydration occurs; the thiol group of cysteine or the β -OH of serine/threonine attack the carbonyl group of the newly formed amide creating a tetrahedral intermediate that by loss of water generates the cyclic thiazoline/oxazoline rings (Fig. 1.8). The epimerization (E) domain converts the L-amino acids to their D form by racemization of the α -carbon. Substrate epimerization can occur at different stages of peptide bond formation including direct activation and tethering on the PCP domain of the D-amino acid (96, 124, 181). Methylation (MT), oxidase (Ox) and reductase (Red) domains are auxiliary domains that add to the amino acid functional diversity often

critical to the biology of the peptide (103, 182). Additional variability to the compounds is acquired by incorporation of non amino acid monomers. Although only amino acids are capable of upstream and downstream attachment, carboxylic acid can be utilized as the initial monomer of the peptide and amine can be the final acceptor for transfer of the peptide. Several siderophores can be found that are N-capped with carboxylic acids or C-capped with amines (79, 133). In the case of siderophore containing carboxylic acid monomers, an additional domain is required for tethering of the activated substrate, the aryl carrier protein (ArCP) domain, while when an amine is the acceptor for the peptide there is no need for a TE domain to catalyze the release of the final product.

In the typical NRPS all modules are incorporated in one single polypeptide and transfer of the growing peptide between modules occurs intramolecularly (or in *cis*) within the same multimodular protein. This organization is not the most common found in siderophore systems that tend to distribute the modules on multiple proteins. In these instances, peptide bond formation can become an intermolecular (or in *trans*) event in which the growing peptide is transferred from one protein to another. Furthermore, some systems can extend this fragmentation to extremes in which divisions occurs even within modules forcing intermolecular interactions of the single domains (103, 182).

Vibriobactin biosynthesis is described in the following section as an example of a siderophore produced via a NRPS mechanism, albeit a nonstandard one (Fig. 1.9).

Vibriobactin is synthesized from three molecules of DHBA, two molecules of L-threonine and one molecule of norspermidine (NSPD). NSPD, the backbone of the vibriobactin molecule, has no free carboxylate moiety for thioester attachment to the PCP domain of an NRPS. As a consequence, intermediates to the finished product need to be

free, soluble molecules instead of phosphopantetheine-tethered thioesters of typical NRPSs (Fig. 1.9).

The free-standing A domain, VibE, activates DHBA and tethers it onto the 4'-PP arm of the ArCP domain of the bifunctional ICL/ArCP protein VibB (79). One of the three DHBA is transferred directly to one of the primary amines of the NSPD molecule in a reaction catalyzed by the condensation domain, VibH (80). The other two DHBA residues are linked to L-threonine by the VibF protein. The 270 kDa VibF NRPS with its predicted six domains, Cy₁-Cy₂-A-C₁-PCP-C₂, is the core of the vibriobactin assembly line (106). The A domain of VibF activates L-threonine and installs it on the PCP domain of the same protein. Both Cy domains of VibF are required to catalyze condensation of DHBA with the amino group of the L-threonine and heterocyclization of threonine to an oxazoline ring to yield dihydroxyphenyl-methyloxazoliny (DHP-mOX) loaded on the PCP domain of VibF (106). The requirement for both Cy domains of VibF to yield the DHP-mOX intermediate is a consequence of the division of functions between these two domains with the Cy₂ domain in charge of the condensation step and the Cy₁ domain taking over the cyclodehydration. This distribution of labors is not found in other Cy domains like those present in the pyochelin and yersiniabactin systems that catalyze both steps, condensation and cyclodehydration, to yield the heterocyclic ring (124, 166). In the next step of vibriobactin synthesis, the C₂ domain of VibF transfer the heterocyclic acyl DHP-mOX group to the primary amine of DHB-norspermidine generating a free intermediate (DHP-mOX-NS-DHB). A second DHP-mOX group is then transferred by the same C₂ domain to the secondary amine of DHP-mOX-NS-DHB to yield the final product vibriobactin (79).

1.3. Regulation of bacterial iron uptake systems

Expression of the genes involved in iron acquisition is tightly regulated in response to the iron status of the cell. The Fur (ferric uptake regulator) protein is a global regulator that represses gene transcription in the presence of intracellular ferrous iron (43). Fe^{2+} binds directly to the Fur protein that only when in complex with iron acquires a conformation capable of binding specific DNA sequences, the Fur box. When the concentration of ferrous iron is low, Fe^{2+} dissociate from Fur and this results in a drastic decrease of the protein affinity for the Fur box (43). As a consequence Fur-regulated genes are expressed under iron-limiting conditions. Determination of the three-dimensional structure of Fur protein suggested how the binding of ferrous iron to Fur affects the ability of this protein to recognize its DNA binding sites. The Fur protein from *P. aeruginosa* possesses two domains: an N-terminal DNA binding domain and a C-terminal dimerization domain. One structural Zn atom is found in the linker region between these two domains, while the site for the Fe^{2+} ion is probably in the dimerization domain (43). Metal binding at the dimerization domain could lead to a conformational change affecting the relative orientation of the DNA-binding domains of the dimer increasing the affinity for the target DNA (43). The Fur box consists of a 19 bp inverted repeat as determined by DNase I footprinting analyses of several Fur-binding sites. It is not clear how the Fur- Fe^{2+} dimer binds to this sequence and how many nucleotide repeats are required for a fully functional repression (43). Although several Fur-DNA recognition models have been proposed so far, no definitive mode of binding could be proposed to explain the results obtained at different promoters.

Some iron acquisition systems possess additional levels of regulation downstream of the Fur protein. Extracytoplasmic function (ECF) sigma factors have been identified in many bacteria. The ECF sigma factors respond to specific extracellular signals and regulate expression of several gene clusters (12). In *E. coli* the *fec* system (*fecIR* and *fecABCDE*) of iron dicitrate transport is repressed by Fur and induced by the FecI-FecR system in response to ferric-dicitrate (101). FecI is the ECF sigma factor and FecR is an integral membrane protein that acts as an anti-sigma factor. When the outer membrane receptor FecA binds ferric-dicitrate, a conformational change occurs in the transporter and it is transmitted to FecR. FecI is then released from the complex with FecR and activates transcription of the *fec* genes. Besides inhibiting the action of FecI by binding to it, the FecR protein seems to play a role also in converting the sigma factor to a conformation competent for transcriptional activation (101). ECF sigma factor/anti-sigma factor systems have been identified in *P. aeruginosa* to induce expression of the pyoverdine-mediated iron acquisition system only in the presence of the siderophore in the extracellular milieu in a mechanism similar to the dicitrate system of *E. coli* (13). A difference between the dicitrate system and the pyoverdine system is that in the FecI-FecR system only the genes for the transport proteins are present and induced while in the pyoverdine system also the biosynthesis genes are induced. Two sigma factors are present in *P. aeruginosa*, PvdS and FpvI, and they both interact with the same anti-sigma factor FpvR (13). FpvI controls expression of the pyoverdine receptor, FpvA, while PvdS induces expression of the *pvd* biosynthesis genes and the other genes required for transport of the ferric-siderophore. In this system, the *pvd* biosynthesis and transport genes are not directly controlled by Fur. Iron regulation of the *pvd* genes occurs

indirectly, through the sigma factor PvdS, as a result of Fur control of *pvdS* expression (13).

Other regulatory mechanisms have been identified that do not involve ECF sigma factors. Regulation of pyochelin production and the ferric-pyochelin receptor (*fptA*) in *P. aeruginosa* is controlled by Fur and by the positive regulator PchR (71). PchR is an AraC family regulator necessary for the expression of the *fptA* and the pyochelin biosynthesis genes (*pch*). The siderophore pyochelin also plays a positive role in the expression of these genes in a process mediated by PchR (71). Siderophore-dependent expression of the cognate transport genes seems to be a common theme in *P. aeruginosa* that allows to up-regulate expression only of the most appropriate iron acquisition system in this bacterium that can utilize a wide variety of endogenous and heterologous siderophores and xenosiderophores, i.e. siderophores produced by other microorganisms.

1.4. *Vibrio anguillarum* iron acquisition systems

The Gram-negative bacterium, *V. anguillarum*, is a polarly flagellated comma-shaped rod that causes the fish disease vibriosis, a highly fatal hemorrhagic septicemic disease (4). Vibriosis generally occurs at temperatures above 10°C, particularly when the surface of the fish is damaged or there are other stress-related conditions present. This pathogen can invade the fish epithelium at multiple sites, including the skin and the intestinal tract (4). In the first stages of infection, bacteria can be observed in the lower intestine and colon, where *V. anguillarum* can adhere to the intestinal mucus and proliferate using it as a nutrient source. Colonization of the intestinal tract is followed by accumulation of fluid and severe tissue damage in these areas as a result of toxin production by the bacteria. As the infection progresses, bacteria are transported across the intestinal epithelium by endocytosis to the surrounding tissues and to the bloodstream (4). Once the disease becomes systemic, the infection quickly spreads throughout the fish and at the later stages of infection, *V. anguillarum* can be isolated from liver, kidney and muscle tissue of rainbow trout (*Oncorhynchus mykiss*).

Several virulence factors have been identified in *V. anguillarum* and the role that these determinants play in the establishment and progress of the infection has been determined. The polar flagellum plays a role in the first step of vibriosis pathogenesis when chemotactic motility is required for colonization. Mutations resulting in the loss of the flagellum (flagellin-deficient mutants and mutants in the *rpoN* gene, a regulator of flagellar biosynthesis) or in a defect in chemotactic motility (mutants in the *cheR* gene, encoding a chemotaxis methyl transferase) affected the ability of *V. anguillarum* to spread in the intestinal tract (113, 118, 119). Interestingly, these attributes were essential

for virulence only when fish were immersed in water harboring the bacteria, but not when bacteria were injected intraperitoneally, suggesting that chemotactic motility is needed for colonization but not proliferation within the host.

In addition to chemotactic motility, an extracellular metalloprotease has also been shown to be an important factor necessary for early steps in the infection process. When the gene encoding this metalloprotease, *empA*, is mutated the resulting strain is 1000-fold less virulent than the wild type when infection is initiated by immersion or anal intubation, but only 10-fold less virulent when fish are infected intraperitoneally (112). It has been suggested that bacterial proteases act as virulence factors by causing massive tissue damage in the host thereby aiding in host cell entry (112).

Once in the bloodstream, the ability to utilize iron complexed by the high affinity iron-binding proteins of the host becomes an essential requirement for multiplication and spreading of *V. anguillarum* to several organs. *V. anguillarum* possesses several different mechanisms for iron acquisition including the utilization of heme and hemoglobin as iron sources and siderophore-mediated uptake system.

A cluster harboring genes necessary for the uptake of heme and hemoglobin as well as a gene encoding a hemolysin have been identified in *V. anguillarum*. The process of heme uptake is probably important during the septicemic stage of infection when the bacteria encounter abundant erythrocytes and the ability to produce a hemolysin could increase the availability of free heme/hemoglobin in the blood. One of the genes identified in the heme uptake cluster of *V. anguillarum* encodes an outer membrane protein, HuvA that is essential for heme uptake (107, 116). A mutant in the *huvA* gene showed a dramatic decrease in virulence when compared to the wild type strain, however this

happened only in experimental infections in which fishes were overloaded with heme, suggesting that heme is not an essential iron source during the infection (116).

For many pathogenic serotype O1 *V. anguillarum* strains, the key feature to survive and cause an infection in the vertebrate host is the possession of a ~65 kb virulence plasmid (172). The plasmid provides the bacterium with an iron sequestering system consisting of the siderophore anguibactin and a specific transport complex for the ferric-siderophore (37, 39, 183). On the other hand, serotype O1 strains without a virulence plasmid and serotype O2 strains of *V. anguillarum* rely on a chromosomal-encoded siderophore system that is different from that encoded by the plasmid (94). The siderophore vanchrobactin, encoded on the chromosome of *V. anguillarum* strains was shown to possess catechol groups, most likely DHBA, and to be similar to enterobactin. Strains producing vanchrobactin are unable to synthesize and/or utilize anguibactin while strains harboring the plasmid-encoded system, although not producing vanchrobactin, could utilize it as an iron source (94). The chromosomal genes encoding the biosynthesis and transport proteins of vanchrobactin have not yet been identified.

The siderophore anguibactin is synthesized from DHBA, L-cysteine and histidine (29, 170, 188) (Fig. 1.10). The structure of anguibactin has been characterized as ω -N-hydroxy- ω -N-[[2'-(2'',3''-dihydroxyphenyl)thiazolin-4'-yl]carboxy]histamine by crystal X-ray diffraction studies and chemical analysis (2, 77). Thus, the anguibactin molecule contains three types of iron-chelating groups, the hydroxyl group of the catechol moiety of DHBA, the nitrogen of the thiazoline ring and the N-hydroxyl group of hydroxyhistamine, all in a compact siderophore structure (Fig. 1.10). As shown in Figure 1.11, from the structure determination of anguibactin complexed with Ga^{3+} , used in place

of ferric iron, anguibactin binds to ferric iron in a 1:1 stoichiometry in which all three functional groups of the siderophore coordinate the metal ion. The additional groups needed for the hexadentate coordination of Fe^{3+} are provided by the deprotonated nitrogen of the imidazole ring and by two molecules of water that are packed between two molecules of anguibactin in complex with two metal ions (77).

From a transposon insertion collection in a plasmid derivative harboring a 25 kb region of the virulence plasmid of *V. anguillarum* strain 775, several mutants were isolated that were affected in anguibactin production and/or transport (169). Analyses of some of these mutants led to the identification of an operon containing the *fatDCBAangRT* genes (Fig. 1.12). Most of the studies of the anguibactin iron uptake system have focused on this operon including the role of each gene product and regulation of expression.

As shown in Figure 1.12, the *fatDCBA* genes encode the energy-dependent transport system that internalizes the iron-anguibactin complex (88). The ferric-anguibactin receptor FatA is an 86 kDa protein that is essential for anguibactin transport. The FatA amino acid sequence is similar to other receptors involved in iron transport like FhuA and FepA of *E. coli* and a TonB box can be identified at its amino terminal end (3).

V. anguillarum harbors two *tonB* systems: *tonB1* and *tonB2*, both chromosomally encoded (163). The presence of multiple *tonB* systems has been shown to be a characteristic of *Vibrio* species (153, 163). Only the TonB2 protein is able to energize transport through the FatA receptor while both TonBs are proficient in the uptake of heme/hemoglobin through the HuvA receptor (163).

Once in the periplasm the ferric-anguibactin is bound by the periplasmic binding protein FatB, a 35 kDa lipoprotein that is anchored in the inner membrane (5). FatB shuttles ferric-anguibactin to the permeases FatC and FatD in the inner membrane that internalize the ferric-anguibactin complex to the cytoplasm, using the energy generated by ATP hydrolysis (6). The ATP-binding component of this ABC transporter has not yet been identified.

Mutations in the *angR* gene resulted in an anguibactin deficient phenotype suggesting a role for this gene in biosynthesis of the siderophore (190). In line with this assumption, the product of this gene, AngR, possesses three domains found in NRPSs, Cy-A-PCP, as shown in Figure 1.12. This latter domain seems to be defective in the AngR protein since the highly conserved serine necessary for attachment of the 4'-PP cofactor is naturally replaced by an alanine (190). It is possible that the 110 kDa AngR protein provides the A domain required for the adenylation of cysteine, while thioester tethering of cysteine may require another protein to provide the essential PCP domain in view of the fact that the PCP domain of AngR could be defective. The N-terminal Cy domain of AngR may form the thiazoline ring identified in the anguibactin structure. An interesting finding is that in *V. anguillarum* strain 531A, AngR harbors a histidine to asparagine change at position 267 (H267N) and this amino acid substitution results in overproduction of the siderophore anguibactin in strain 531A (171).

A role in siderophore biosynthesis has also been proposed for the *angT* gene found downstream of *angR* (190). The *angT* gene encodes a predicted protein with similarity to a type II TE domain of NRPSs, and deletion of the gene results in a decrease, but not in a complete shutoff of anguibactin production. This phenotype is not

surprising since type II TE domains are not essential for biosynthesis but affect the efficiency of the system.

From the transposition mutagenesis experiment, an additional gene was identified that is not part of the iron transport biosynthesis (ITB) operon but is located in a contiguous region on the pJM1 plasmid. This gene, *angH*, encodes a histidine decarboxylase enzyme that produces histamine from histidine by release of a carbon dioxide molecule (11, 170). Mutants in the *angH* gene do not produce histamine or anguibactin and are unable to grow in iron-limiting conditions. Growth under iron starvation of the *angH* mutants could be restored by addition of histamine to the medium further confirming that histamine is a precursor in the biosynthesis of the siderophore (170).

The anguibactin precursors DHBA and histamine are dedicated metabolites made by *V. anguillarum* for siderophore production. The enzymatic activity required for histamine production is encoded directly on the plasmid as explained above, while the enzymatic activities that convert chorismic acid to DHBA are encoded by chromosomal genes since a plasmidless derivative of *V. anguillarum* strain 775 could still produce this catechol. Some variability in the ability to produce DHBA has been observed in serotype O1 strains cured from the virulence plasmid (29). The plasmidless derivatives of some strains do not produce DHBA while they are perfectly proficient in the production of this catechol when the plasmid is present (188). The virulence plasmid of one of these strains, strain 531A, harbors genes of the DHBA pathway, one of which, the *angB* gene, is essential for DHBA and anguibactin production (188). The AngB protein was shown to be bifunctional, with its amino end conferring an ICL activity required for the

production of DHBA and its carboxyl end serving as an ArCP domain functioning in anguibactin assembly. Furthermore, the carboxy-terminal end of AngB can be synthesized as an independent polypeptide that, like AngB, also functions as an ArCP domain (188).

Virulence experiments with *V. anguillarum* mutants lacking either the ability to synthesize or utilize the siderophore anguibactin showed an approximate 10,000-fold decrease in LD₅₀ when tested by intramuscular injection (163, 190, 192). These results proved that this iron scavenging system is absolutely necessary for virulence in this pathogen, in contrast with the heme iron uptake system.

As in many other Gram-negative bacteria, the siderophore-mediated iron uptake system in *V. anguillarum* is negatively regulated by the chromosomal-encoded Fur (180, 189). It has been shown that upon binding at the Fur box of the ITB operon promoter Fur bends the DNA blocking RNA polymerase from binding in a mechanism quite different than the proposed simple repressor model (26). Furthermore the anguibactin system of *V. anguillarum* was the first example of the presence of additional regulators modulating the expression of siderophore biosynthesis and transport genes (Fig.1.12). Additionally to the negative regulator Fur, two positive regulators, the AngR protein and products encoded in the Transacting Factor (TAF) region, were shown to act at the same promoter (55, 169). Thus, AngR is a bi-functional protein that besides its role in the biosynthesis of anguibactin, is also involved in regulation. The TAF product is encoded in a region of the virulence plasmid noncontiguous to the ITB operon (169). Besides the positive regulators AngR and TAF, expression of the ITB operon is also positively regulated by the siderophore anguibactin itself (31).

Expression of this operon is also regulated posttranscriptionally by two antisense RNAs encoded within the same operon but on the opposite strand. RNA α is a long untranslated RNA molecule encoded within *fatB* open reading frame in the opposite orientation, while the other antisense RNA, RNA β , is a 427 nt molecule that is transcribed across the intergenic region between *fatA* and *angR*, starting within *angR* and ending in *fatA* (30, 142, 143, 179). These two antisense RNAs control the levels of specific mRNA within the ITB operon by interaction with the transcribed polycistronic message.

1.5. Virulence plasmids and iron acquisition systems

Genes associated with virulence in bacteria are often harbored by mobile genetic elements such as phages, transposons and plasmids. These elements can mediate the transfer of entire gene clusters that once acquired endow the bacteria with a complete new array of virulence attributes.

Plasmids are extrachromosomal elements that code for additional information that is not necessary for the survival of the bacteria containing the plasmid but gives a selective advantage in a specific environment for example plasmids encoding nitrogen fixation gene clusters found in symbiotic *Rhizobium* species (65). The majority of plasmids are circular DNA molecules of varied size encoding all the functions necessary for their maintenance in a bacterial population. They can autonomously replicate in the bacterial cells and distribute in both daughter cells at each cell division. Each plasmid depending on the bacteria and the growing conditions is maintained in a specific number per cell, defined as copy number, and this number is determined by the plasmid origin of replication.

A wide variety of virulence factors has been found associated with virulence plasmids, the most common of which are the R plasmids that encode antibiotic resistance genes. Iron utilization systems are also found encoded on plasmids but they are limited to only two families of plasmids: the pJM1-like and the pColV-K30-like plasmids. pJM1-like plasmids are found in *V. anguillarum* strains and the anguibactin system encoded on these plasmids has been shown to be an essential virulence factor during the septicemic disease vibriosis (see section 1.4.). A similar association with virulence has been found for the ColV plasmids of *E. coli* strains associated with bacteremia of humans

and domestic animals (184, 185). The pColV-K30-like plasmids also harbor a siderophore-mediated iron uptake system, the aerobactin system (see section 1.1.2.) that can also be found encoded in the chromosome (108). Plasmids of the pColV-K30 family have been found in many invasive strains of *Shigella*, *Salmonella* and *Klebsiella* (185).

1.6. Summary of the work presented in this thesis

This work focuses on the pJM1 plasmid and the biosynthesis of the siderophore encoded by this virulence plasmid.

In Chapter 2, the complete sequence of the pJM1 plasmid of strain 775 is presented with the annotation of the 59 ORF identified. pJM1 is the first virulence plasmid encoding an iron uptake system to be completely sequenced. Sequencing of the plasmid revealed that all the genes required for the biosynthesis of the siderophore anguibactin from its precursors are encoded on pJM1. Furthermore, only one of the functions required for the synthesis of the two metabolites, DHBA and histamine, is missing from this plasmid making this plasmid almost an independent unit for the assembly of a siderophore. Another interesting feature of pJM1 is that a high percentage of the ORFs (32%) have homology with proteins involved in iron metabolic functions. Several gene clusters on the plasmid show a transposon-like organization, that together with their G+C content, suggest that these clusters were acquired by pJM1 as modules, with a marked bias toward those containing iron acquisition genes. Taking advantage of the information obtained from the plasmid sequence, I proposed a pathway for anguibactin biosynthesis.

In Chapter 3, I identified a homologue of the plasmid-encoded *angB* on the chromosome of strain 775 and analyzed the functions of each homologue in DHBA and anguibactin production. Both proteins, thus both ICL domains, are functional in the production of DHBA in *V. anguillarum* as well as in *E. coli* but only the plasmid-encoded ArCP domain can participate in anguibactin production. These results suggest a system specificity of the NRPS domains in which interaction occurs only amongst the proteins of

the same system. The identification of an *angB* gene in the chromosome allows also some speculation on the evolution of the different siderophore-mediated iron uptake systems of *V. anguillarum* strains. This study was the first example of site-directed mutagenesis of an ICL domain associated with an ArCP domain and I could clearly show that a mutant in the ICL domain does not affect the function of the ArCP domain and vice versa. Furthermore the mutants were tested for their functions using in vivo and in vitro approaches that generated results that were in agreement.

In Chapter 4, I examined the product of one of the genes identified on the pJM1 plasmid that shows homology with NRPS proteins. The domain organization of this putative NRPS, called AngM, is quite intriguing since the PCP and C domains found in this protein are not associated with an A domain. I first demonstrated that the *angM* gene is essential for anguibactin production since an insertion mutant in this gene resulted in the complete abolition of this siderophore's synthesis. I further characterize the role of AngM by substituting with alanine serine 215 in the PCP domain and histidine 406 in the C domain. The residue mutated in each domain had been previously shown to be essential for the activity of the domains and I wanted to demonstrate the functionality of the two domains of AngM. Each mutant results in an anguibactin-deficient phenotype underscoring the importance of these two domains in the function of this protein and in the production of the siderophore. As expected all the mutants in *angM* affecting anguibactin production resulted in a dramatic attenuation of the virulence of *V. anguillarum* 775 highlighting the importance of this gene in vivo during infection of the vertebrate host. I also analyzed transcription of the *angM* gene and showed that this gene is part of an operon that overlaps the ITB operon promoter and operates in the opposite

direction. The existence of a possible overlap also of the Fur box at these two promoters suggests a concerted repression by Fur of both transcriptional units in iron rich conditions. The results obtained with AngM confirmed the role that had been proposed for this protein in the biosynthetic pathway for anguibactin prompting some modifications of the model to better fit the experimental results.

In Chapter 5, I analyzed a second gene identified on the pJM1 plasmid. This gene, *angN*, encodes a predicted protein of 108 kDa that like AngM shows similarity to NRPSs. AngN is an atypical NRPS that possess two free-standing Cy domains in tandem. I showed that this protein is essential for anguibactin biosynthesis with both Cy domains being functional since only mutation in both domains (D133A/D575A and D138A/D580A) resulted in anguibactin-deficient phenotypes. In addition, mutations in the *angN* gene that resulted in the loss of anguibactin production showed a dramatic attenuation in virulence. Even more interesting in the virulence experiments were those mutants that, although affected in anguibactin synthesis, could still produce reduced amounts of the siderophore. The attenuation in virulence of these mutants correlates with the levels of anguibactin produced in the test tube. Analysis of the transcriptional start point for the *angN* gene highlighted a similar organization of the *angN* promoter and an overlapping transposase promoter transcribing in the opposite orientation as the one described for the *tnp-angM* and the ITB operon promoters. Expression of the *angN* gene is regulated by Fur, in a negative fashion, and AngR and TAF, as activators. This is the first example of a gene that is not part of the ITB operon to be regulated by AngR. This study of the role of AngN in the biosynthesis of anguibactin further confirms the pathway proposed.

In conclusion, the collection of the chapters in this thesis presents a thorough analysis of the biosynthetic pathway of the siderophore anguibactin and its contributions to the virulence of *V. anguillarum* by the study of mutations in the genes encoding the biosynthetic enzymes.

Figure 1.1. Schematic representation of the mechanisms of bacterial iron acquisition systems. Hemophores and siderophores are synthesized within the bacterial cell and secreted to the extracellular environment where they bind their ligands. The complex is transported to the periplasm via a specific outer membrane receptor (OMR). Once in the periplasm, it is recognized and bound by the periplasmic binding protein (PBP) that mediates shuttling to the ABC transporter complex in the inner membrane through which it is internalized into the cell cytosol. The iron is then removed from the complex and reduced to ferrous iron or it can be incorporated directly into proteins in the case of heme. Iron can also be acquired by directly binding of the ferric-proteins of the host to the cognate outer membrane receptor. Internalization of the iron source follows the same general pathway as described for the siderophore/hemophore-mediated transport. Transport through the OMR is energized by the TonB-ExbB-ExbD complex.

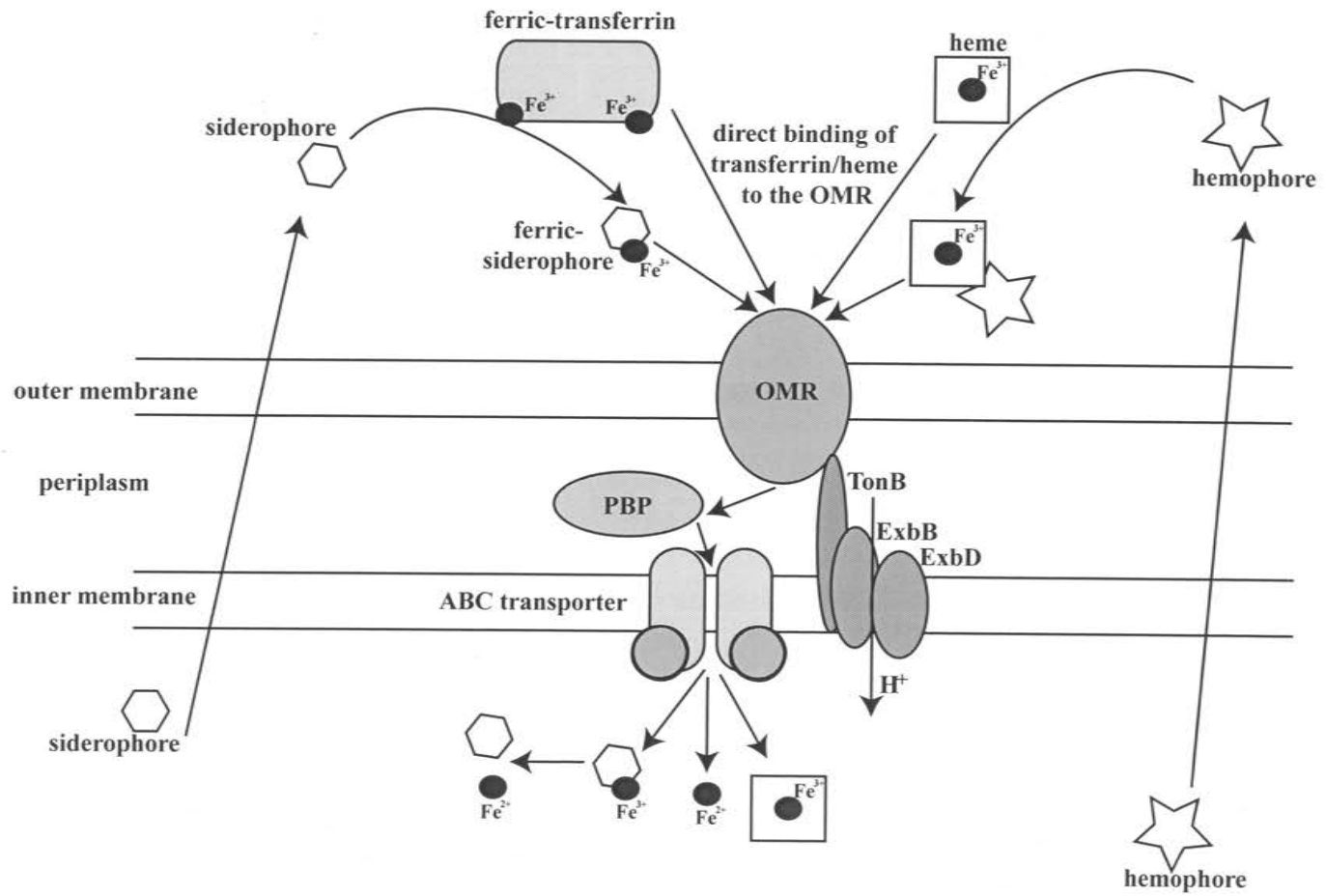


Figure 1.2. Biosynthesis of catechols and phenolates. Chorismic acid is the precursor for catechols and phenolates and it is synthesized from primary metabolites. Chorismic acid is converted to isochorismic acid by isochorismate synthetase enzymes (E1). This intermediary can be converted to either 2,3-dihydro 2,3-dihydroxybenzoic acid or 2-hydroxybenzoic acid (salicylate) by the same class of enzymes, isochorismate lyases (E2). An additional step is required to synthesize 2,3-dihydroxybenzoic acid (DHBA) in a reaction catalyzed by 2,3-dihydro-2,3-DHBA dehydrogenases (E3).

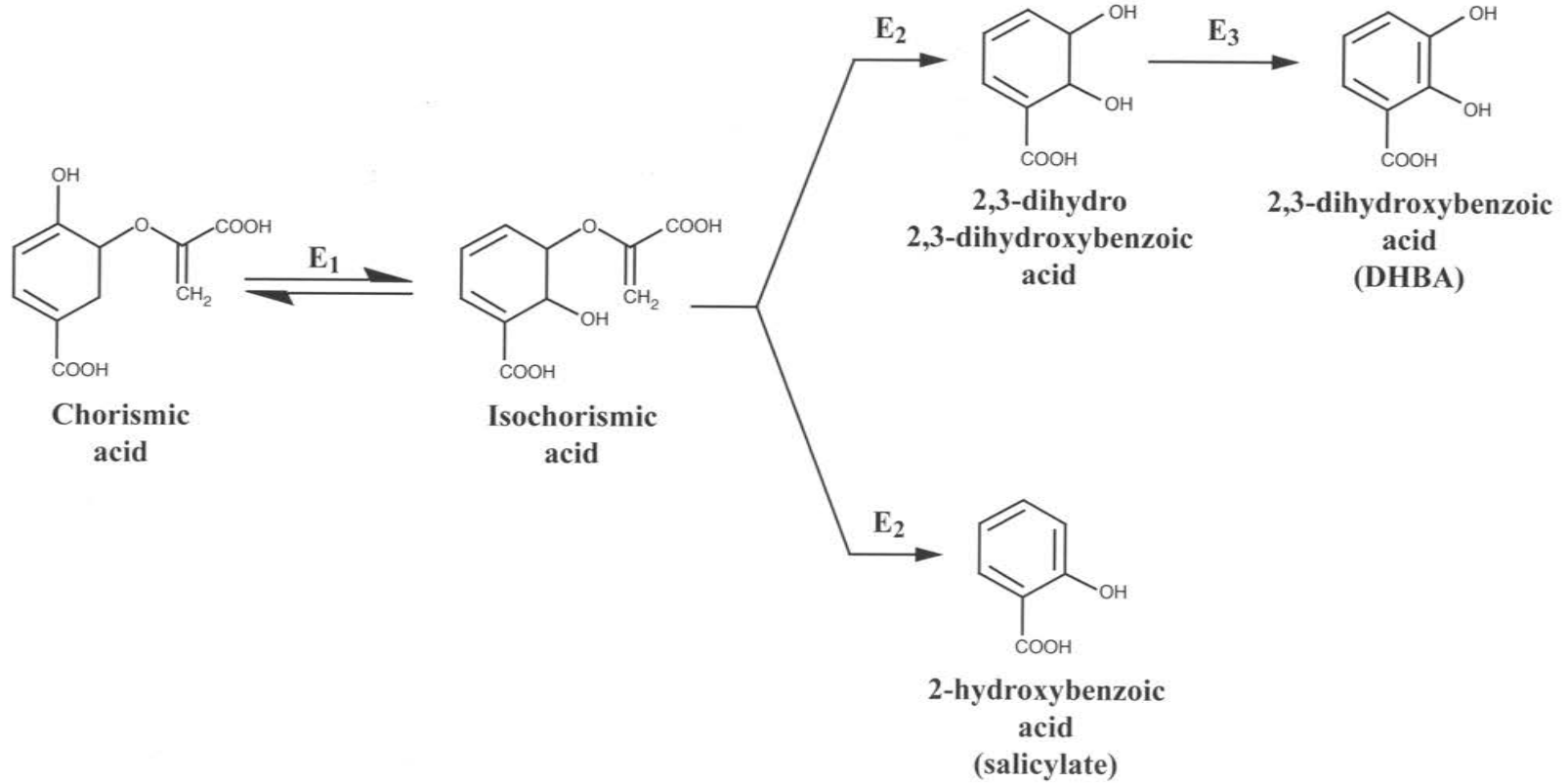


Figure 1.3. Some representatives catechol siderophore structures. Enterobactin (*Escherichia coli*); pyochelin (*Pseudomonas aeruginosa*); yersiniabactin (*Yersinia* species); vibriobactin (*Vibrio cholerae*); vulnibactin (*Vibrio vulnificus*).

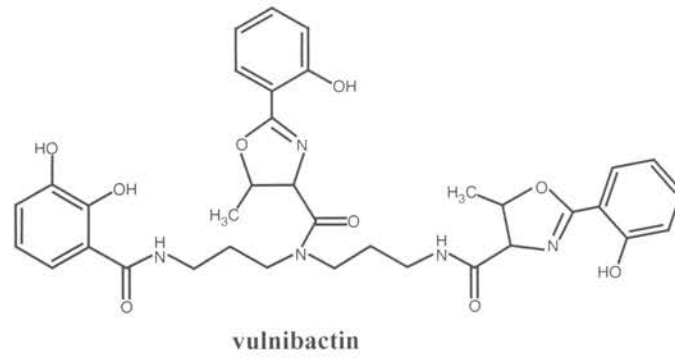
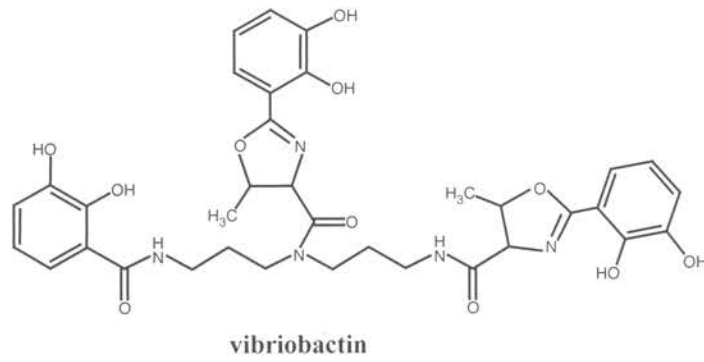
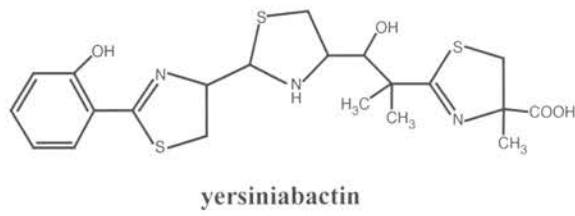
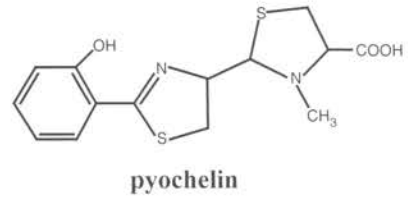
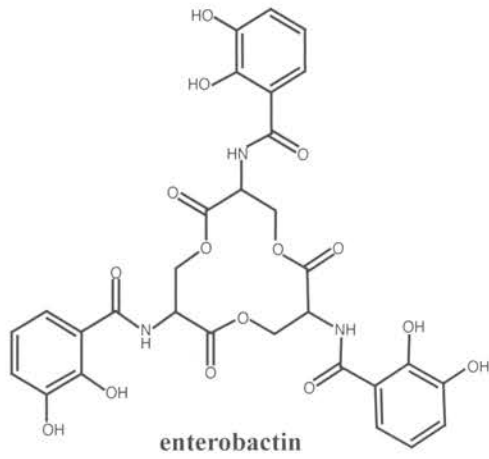


Figure 1.4. Biosynthesis of enterobactin from 2,3-dihydroxybenzoic acid (DHBA) and serine (Ser). Adapted from Walsh, C. T. and Marshall, C. G. (182).

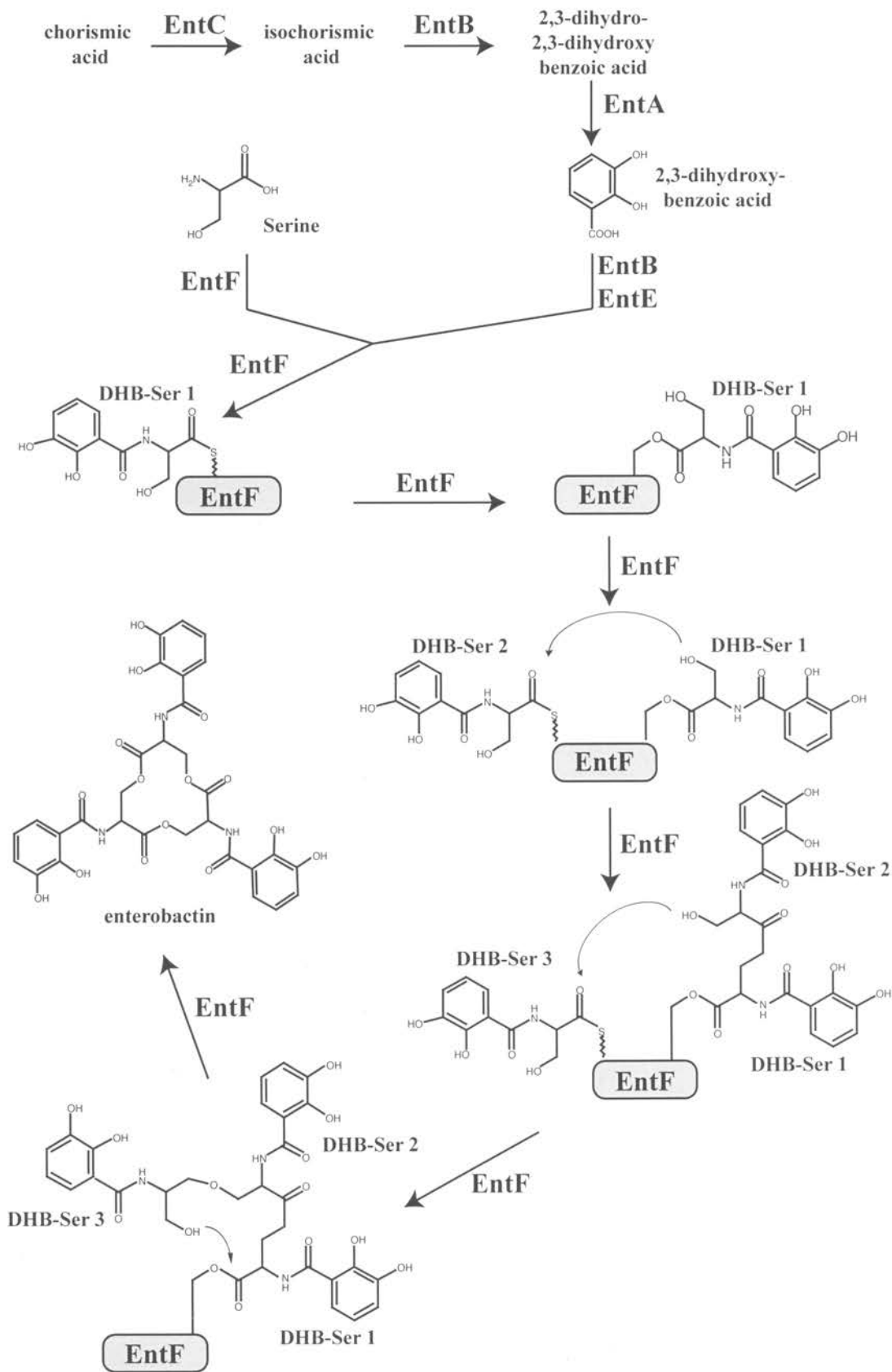
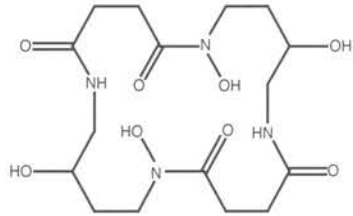
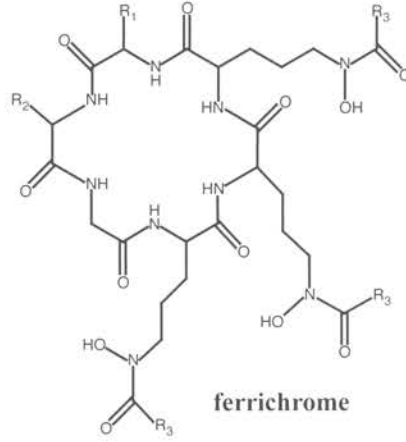


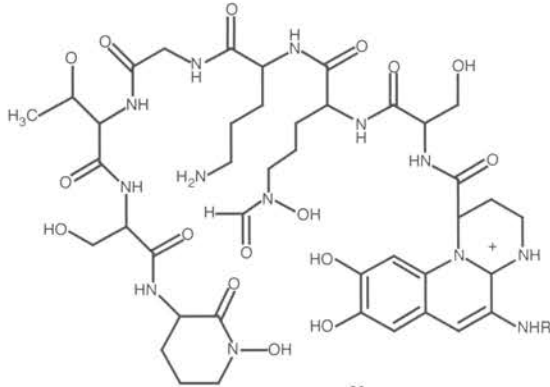
Figure 1.5. Some representatives of hydroxamate siderophore structures. Alcaligin (*Bordetella* species); ferrichrome (*Ustilago sphaerogena*); pyoverdine (*Pseudomonas aeruginosa*); aerobactin (*Escherichia coli*); ornibactin from (*Burkholderia cepacia*); mycobactin (*Mycobacterium tuberculosis*).



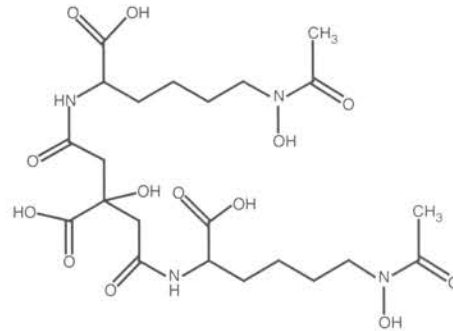
alcaligin



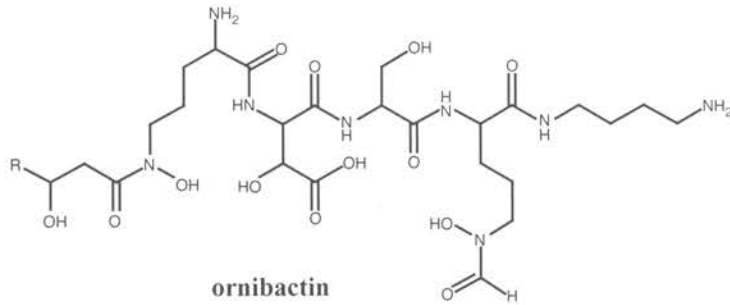
ferrichrome



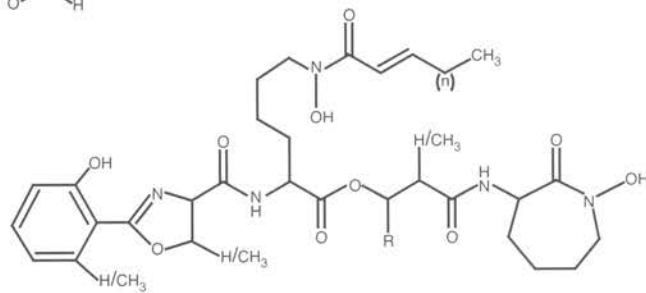
pyoverdine



aerobactin



ornibactin



mycobactin

Figure 1.6. Biosynthesis of aerobactin from lysine, citrate, acetyl-CoA (AcCoA) and O₂. Adapted from Walsh, C. T. and Marshall, C. G. (182).

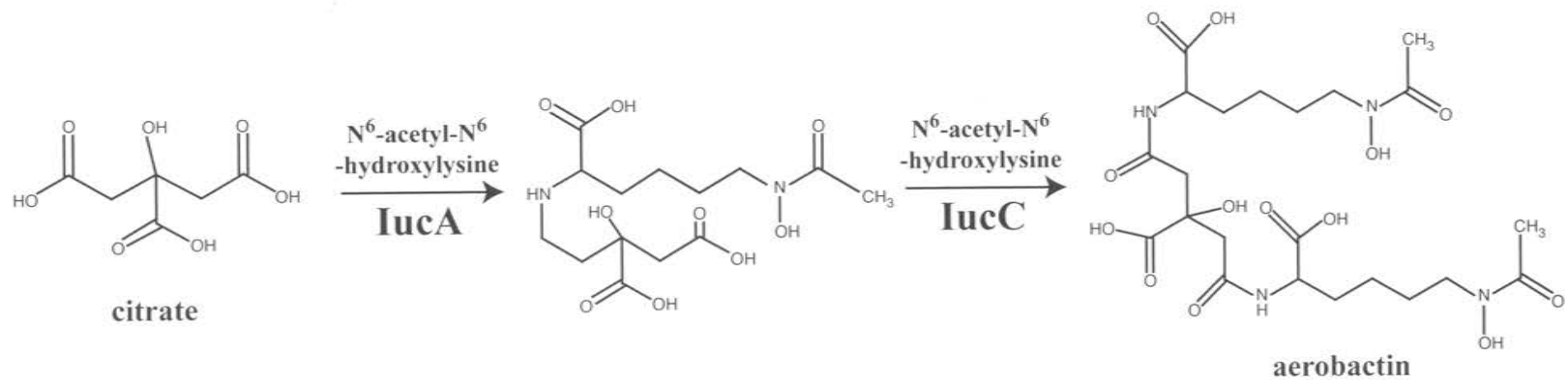
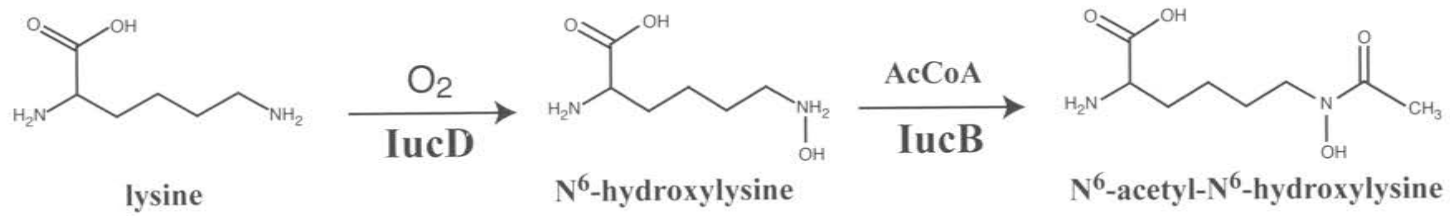


Figure 1.7. Required activities in NRPS modules. The amino acid substrate is activated by the adenylation (A) domain through ATP hydrolysis. The unstable aminoacyl adenylate is transferred and bound as a thioester to 4'-phosphopantetheinyl cofactor tethered on the peptidyl carrier protein (PCP) domain of the same module. The condensation (C) domain catalyzes formation of a peptide bond between an upstream donor and a downstream acceptor amino acids. The thioesterase (TE) domain releases the synthesized peptide from the PCP domain of the last module. Adapted from Walsh, C. T. and Marshall, C. G. (182).

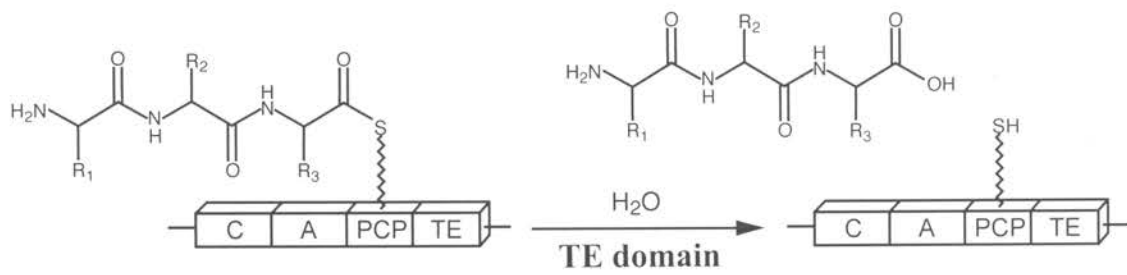
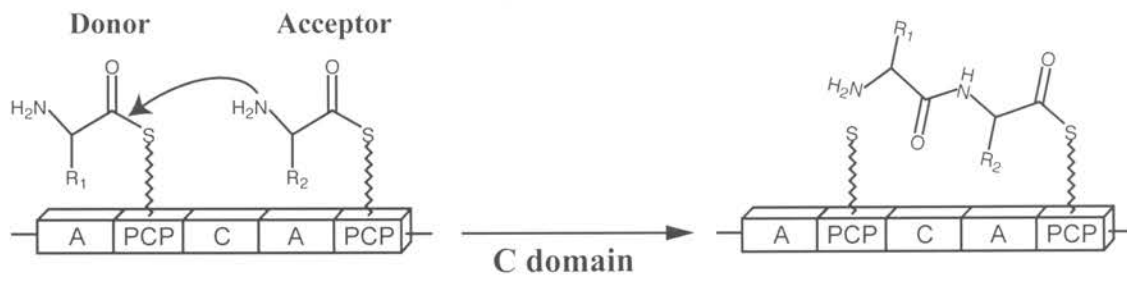
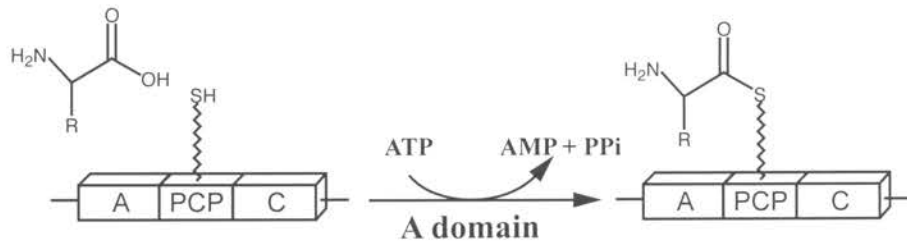


Figure 1.8. Predicted mechanism for the formation of heterocyclic rings by cyclization (Cy) domains. Heterocyclization is achieved in a two-step reaction. In the first step the amide bond is formed between the two substrates as it is proposed for the condensation (C) domains. The amino acid is then cyclized through the nucleophilic attack of the thiol group of cysteine or the β -OH group of serine and threonine to the carbonyl group of the amide. The loss of a water molecule completes cyclization of the amino acid substrate. A: adenylation domain; PCP: peptidyl carrier protein domain. Adapted from Walsh, C. T. and Marshall, C. G. (182).

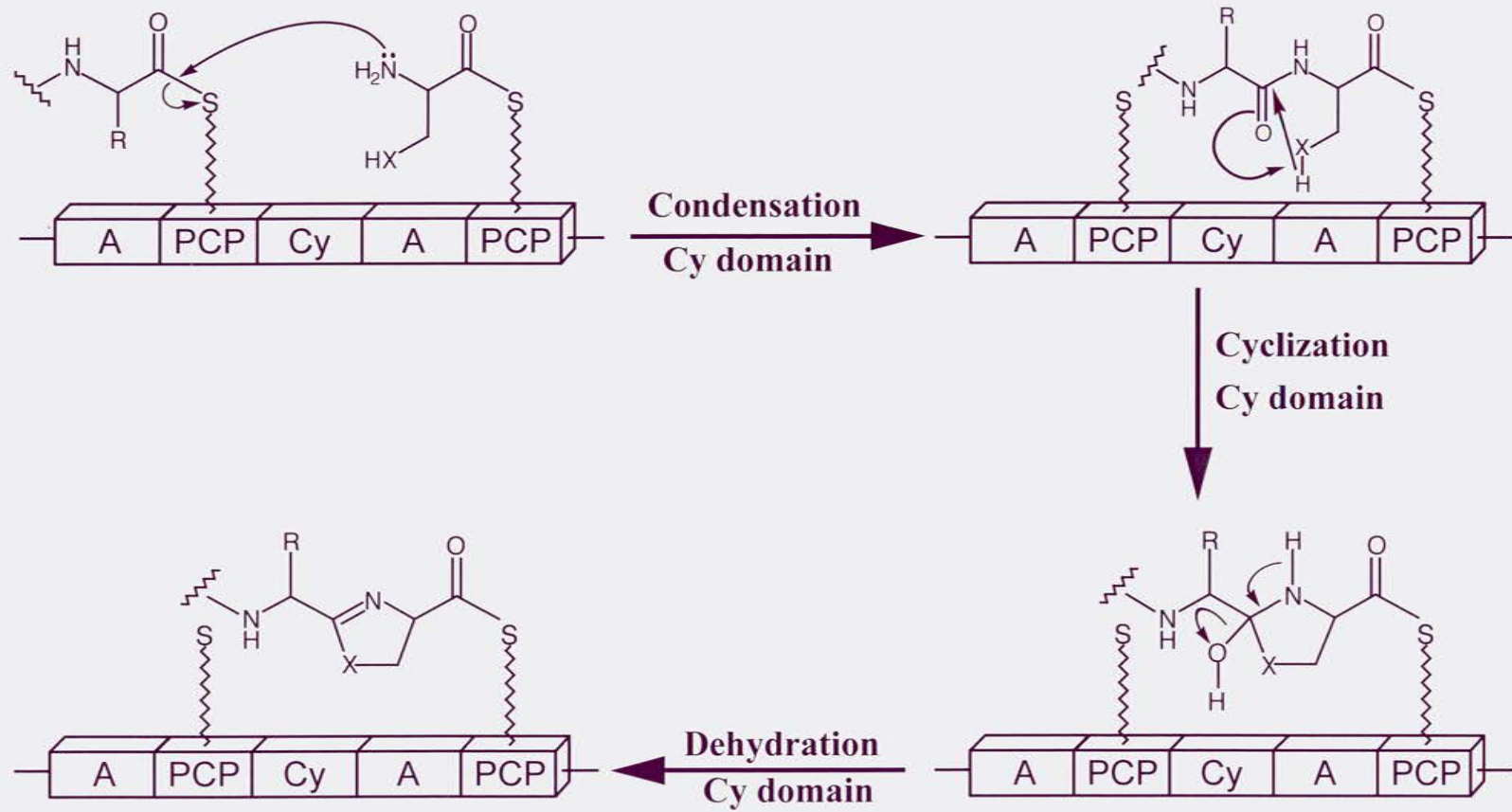


Figure 1.9. Biosynthesis of vibriobactin from 2,3-dihydroxybenzoic acid (DHBA), threonine and norspermidine (NSPD). DHP-mOX: dihydroxyphenyl-methyloxazolinyll. Adapted from Di Lorenzo, M. et al. (46).

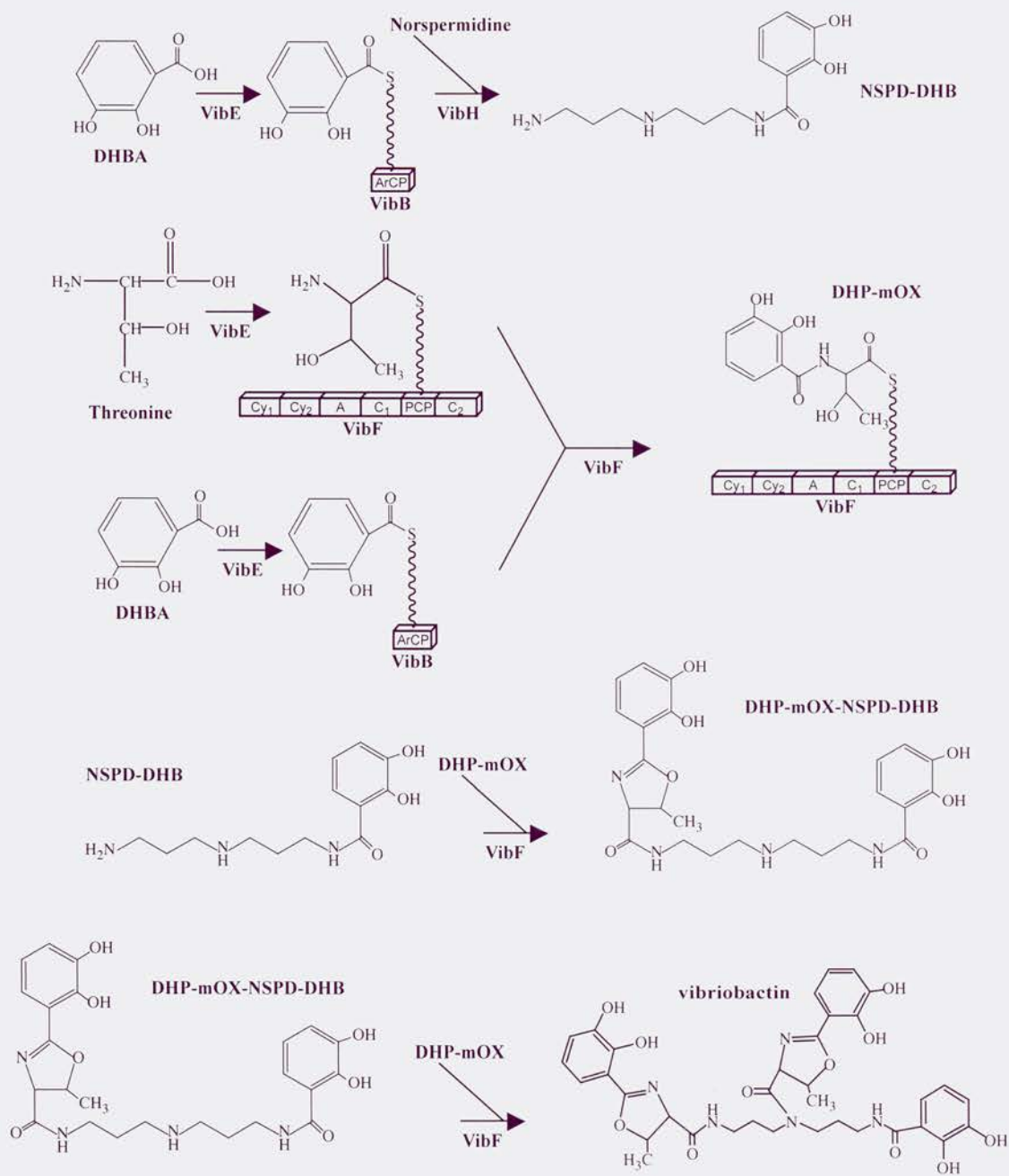


Figure 1.10. Structure of anguibactin and its precursors, dihydroxybenzoic acid (DHBA), cysteine and histidine.

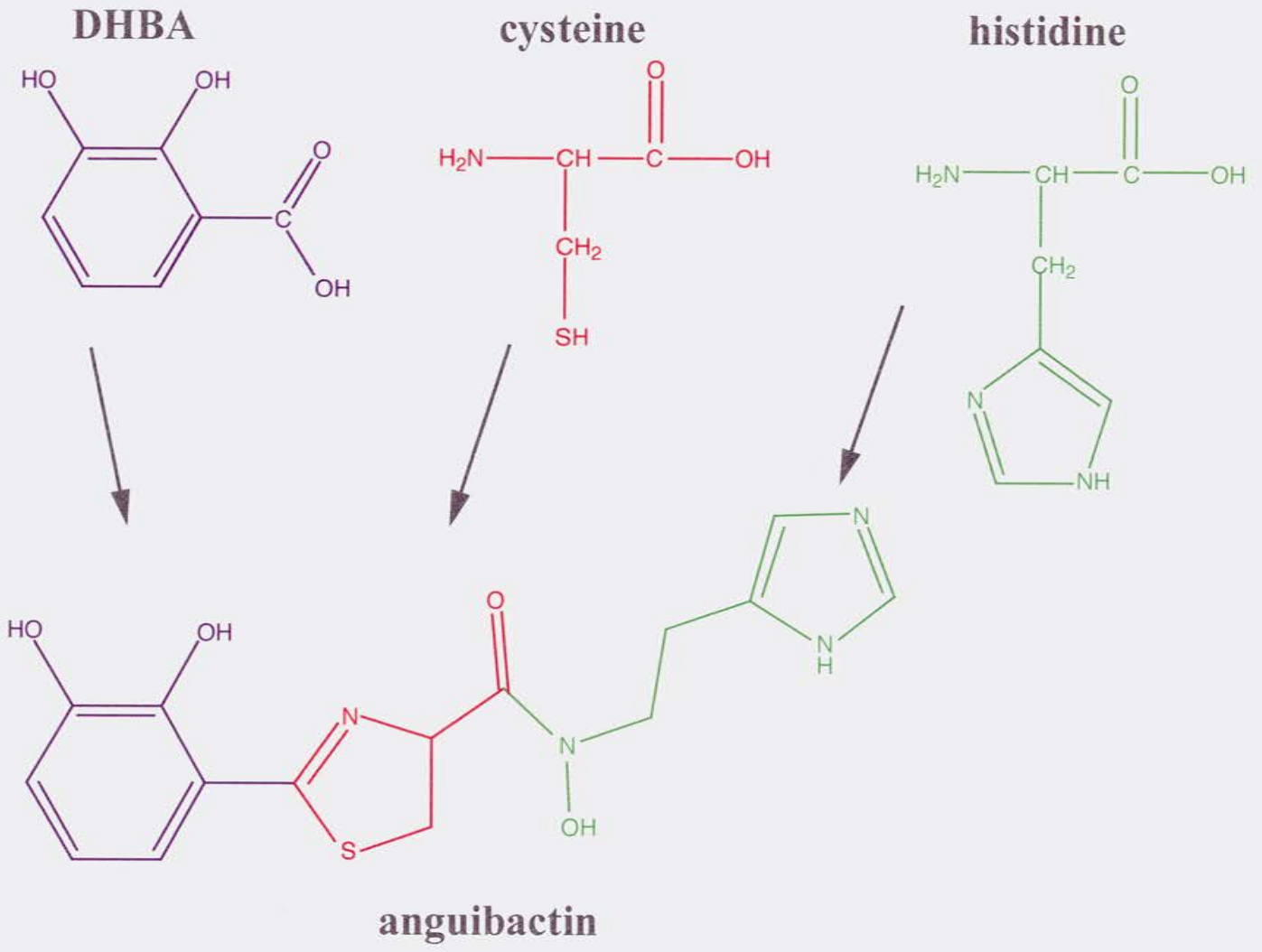


Figure 1.11. Anguibactin in complex with ferric-iron. The color code used in this figure correspond to the one used in Figure 1.10.

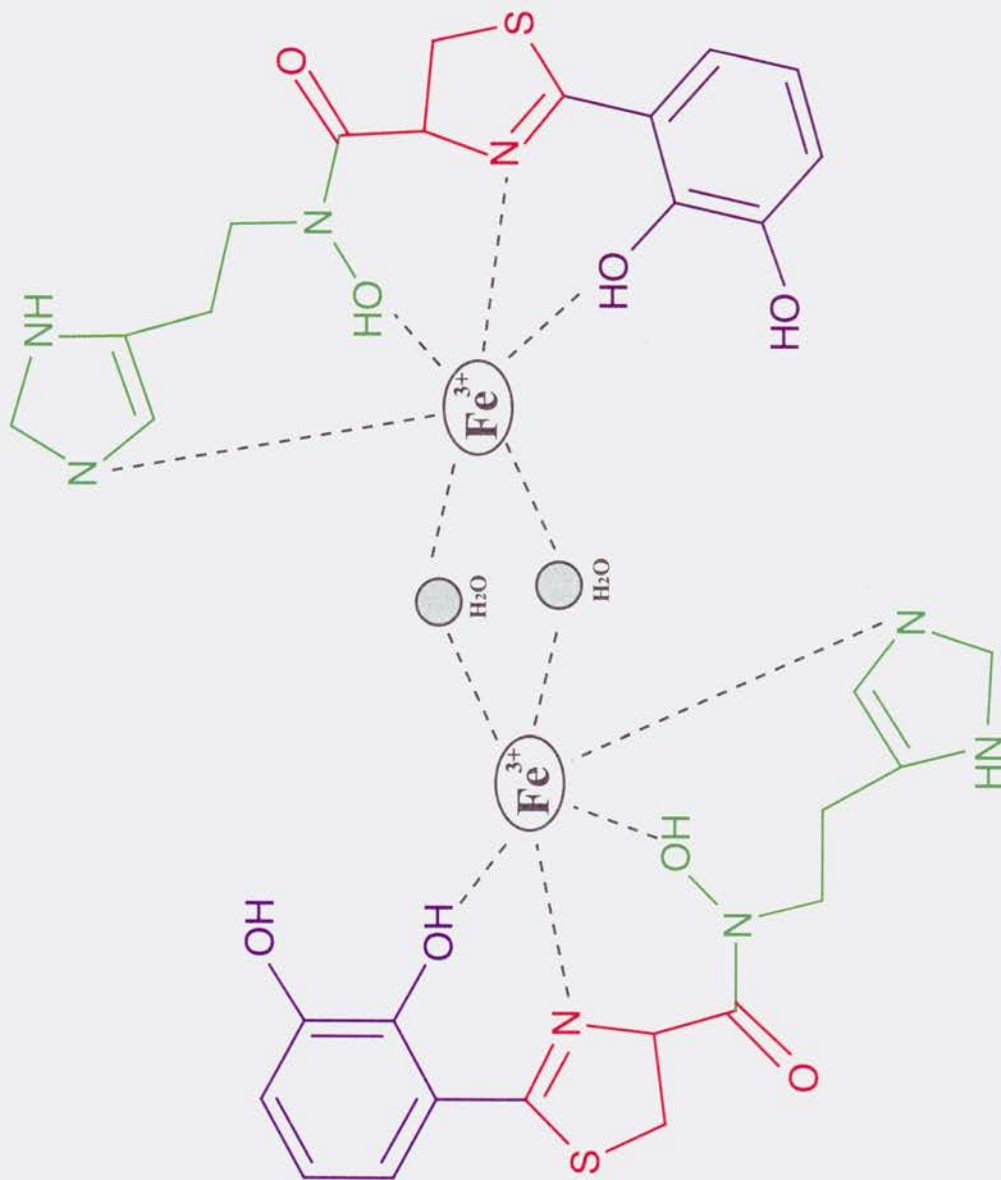
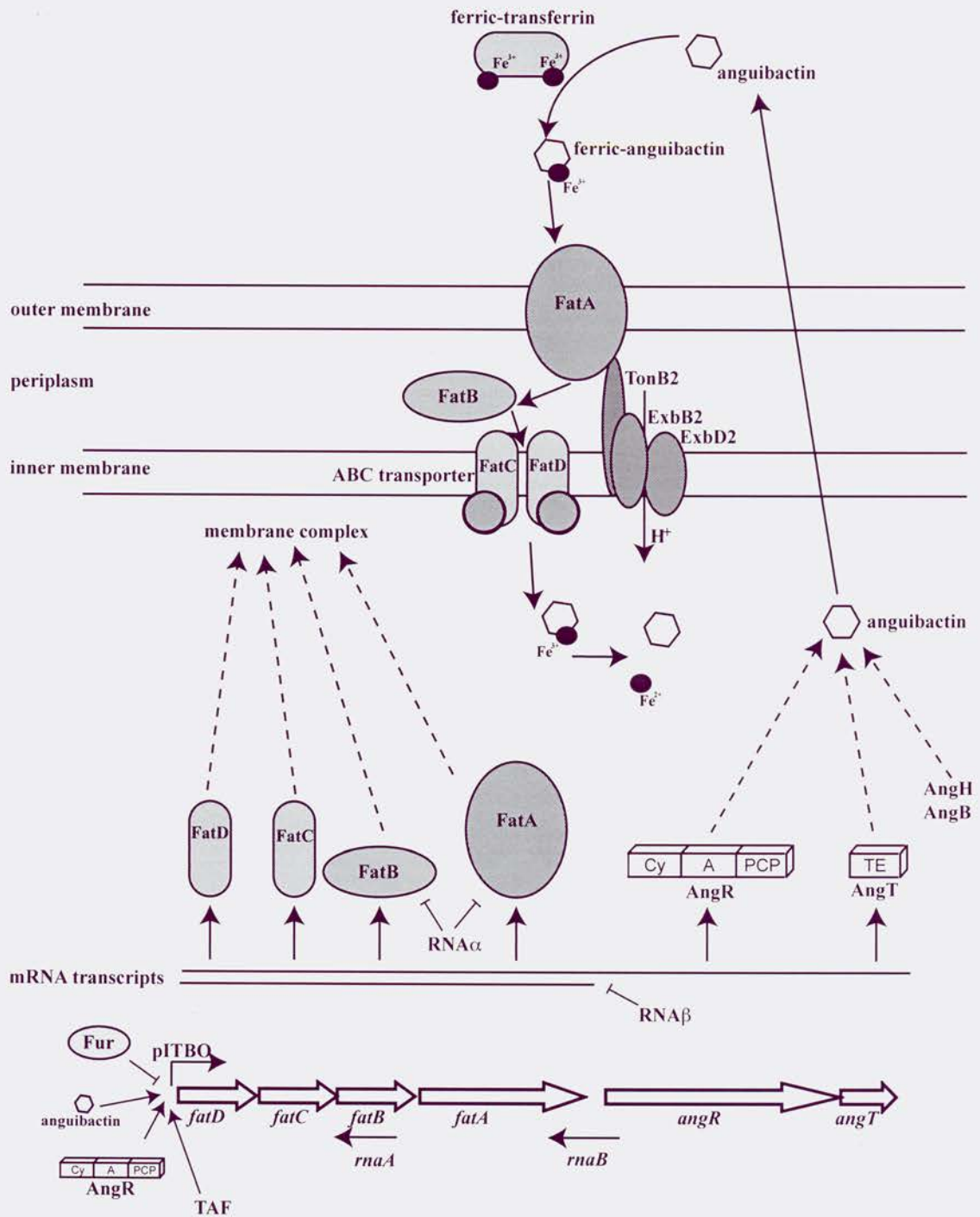


Figure 1.12. Schematic representation of the ITB operon. The functions in anguibactin uptake and the localization within the cell of the products encoded by this operon are shown. The different regulators acting at several levels of ITB operon expression are also included.



CHAPTER 2

The complete sequence of the virulence plasmid pJM1 from the marine fish pathogen *Vibrio anguillarum* strain 775

Manuela Di Lorenzo, Michiel Stork, Marcelo E. Tolmasky, Luis A. Actis, David Farrell, Timothy J. Welch, Lidia M. Crosa, Anne M. Wertheimer, Qian Chen, Patricia Salinas, Lillian Waldbeser, and Jorge H. Crosa

Journal of Bacteriology 185 (19): 5822-5830, 2003

2.0. Abstract

The virulence plasmid pJM1 enables the fish pathogen *Vibrio anguillarum*, a gram-negative polarly flagellated comma-shaped rod bacterium, to cause a highly fatal hemorrhagic septicemic disease in salmonids and other fishes, leading to epizootics throughout the world. The pJM1 plasmid 65,009-nucleotide sequence, with an overall G+C content of 42.6%, revealed genes and open reading frames (ORFs) encoding iron transporters, nonribosomal peptide enzymes, and other proteins essential for the biosynthesis of the siderophore anguibactin. Of the 59 ORFs, approximately 32% were related to iron metabolic functions. The plasmid pJM1 confers on *V. anguillarum* the ability to take up ferric iron as a complex with anguibactin from a medium in which iron is chelated by transferrin, ethylenediamine-di(*o*-hydroxyphenyl-acetic acid), or other iron-chelating compounds. The *fatDCBA-angRT* operon as well as other downstream biosynthetic genes is bracketed by the homologous ISV-A1 and ISV-A2 insertion sequences. Other clusters on the plasmid also show an insertion element-flanked organization, including ORFs homologous to genes involved in the biosynthesis of 2,3-dihydroxybenzoic acid. Homologues of replication and partition genes are also identified on pJM1 adjacent to this region. ORFs with no known function represent approximately 30% of the pJM1 sequence. The insertion sequence elements in the composite transposon-like structures, corroborated by the G+C content of the pJM1 sequence, suggest a modular composition of plasmid pJM1, biased towards acquisition of modules containing genes related to iron metabolic functions. We also show that there is considerable microheterogeneity in pJM1-like plasmids from virulent strains of *V. anguillarum* isolated from different geographical sources.

2.1. Introduction

The fish pathogen *Vibrio anguillarum* strain 775 is the causative agent of vibriosis, a highly fatal hemorrhagic septicemic disease (4). This bacterium disseminates in the vertebrate host by using the otherwise unavailable iron bound by high-affinity iron binding proteins, such as transferrin and lactoferrin. Furthermore, *V. anguillarum* 775 has the ability to grow in vitro in media in which iron is chelated by transferrin, ethylenediamine-di(*o*-hydroxyphenyl-acetic acid), and other iron chelators (37, 169). The metabolic pathway supporting the ability of this bacterium to grow under iron-limiting conditions is linked to the presence in the bacterial cells of the virulence plasmid pJM1 (37).

Iron metabolic plasmids are rare; in addition to the pJM1-like plasmids only the pColV-K30 family of plasmids, identified in human clinical strains of *Escherichia coli* and other enteric bacteria, have been associated with iron metabolism. However, the pJM1 and pColV-K30 plasmid-mediated iron uptake systems are unrelated (40, 185). pJM1-like-plasmids, usually around 65 to 67 kb, have been reported by us and others in different virulent *V. anguillarum* strains isolated from many epizootics throughout the world (121, 126, 175). In this family of plasmids the best characterized is the 65-kb pJM1 plasmid that has been isolated from the *V. anguillarum* strain 775 and is the one that we chose to sequence. The diverse biochemical features of the pJM1 gene products and the possibility of horizontal evolution provided by the existence of insertion elements surrounding some of these genes make this fascinating plasmid also of interest for the study of evolutionary ecology.

Here we report the nucleotide sequence and annotation of the entire pJM1 virulence plasmid from *V. anguillarum* strain 775.

2.2. Materials and methods

2.2.1. Bacterial strains, plasmids, and growth conditions. *V. anguillarum* strain 775 harboring the virulence plasmid pJM1 was grown in M9 minimal medium supplemented with mineral salts and Casamino Acids (Difco) as previously described (190). Plasmids carrying subclones from pJM1 were propagated in *E. coli* HB101 in Luria-Bertani medium in the presence of chloramphenicol (30 µg/ml). Plasmid DNA was extracted using the Qiagen Midi kit.

2.2.2. Determination of the pJM1 sequence. Sequencing primers were designed using Oligo 6.8 primer analysis software and purchased from the Oregon Health and Science University-Molecular Microbiology and Immunology (OHSUMMI) Research Core Facility (<http://www.ohsu.edu/core>) and Invitrogen. The DNA template used for sequencing reactions was either the complete pJM1 plasmid or fragments cloned using pBR325 as cloning vehicle. DNA sequencing reactions were carried out manually by the chain-termination method and by the OHSU-MMI Research Core Facility using a model 377 Applied Biosystems Inc. automated fluorescence sequencer. Base calling was performed on a Macintosh computer with the ABI base-calling program. Cycle sequencing was performed with AmpliTaq FS DNA polymerase with “Big-Dye” labeled terminators, both from Applied Biosystems Inc. The Sequencher software (Gene Code Corporation) was used for sequence assembly and editing. Codon usage tables were generated by the GCG Wisconsin Package. Coding regions were identified with BLAST (8). Coding sequences with associated ribosome binding sites were predicted with GENEMARK (20) and GLIMMER (<http://www.tigr.org/software/glimmer/>) and compared to the BLAST alignments to establish the coding sequence start. Regions

lacking identified open reading frames (ORFs) and giving no BLAST results but revealing, on visual inspection, coding sequences with ribosomal binding sites were included in the annotation. G+C content analyses were performed with Oligo 6.8 primer analysis software.

2.2.3. Nucleotide sequences accession number. The complete circular nucleotide sequence of pJM1 from *V. anguillarum* strain 775 has been deposited in the GenBank sequence library and assigned the accession number AY312585.

2.3. Results

2.3.1. Nucleotide composition. The circular plasmid is comprised of 65,009 bp, and the overall G+C content is 42.6%, which is slightly lower than the average G+C content of the two *V. anguillarum* 775 chromosomes (44%) (146). The G+C content is also reflected by the lack of restriction sites for *AscI* (GGCGCGCC), *NotI* (GCGGCCGC), and *SrfI* (GCCCCGGC) and the presence of only one site for *FseI* (GGCCGGCC). The bias towards A and T in the third codon position is also a consequence of this structural feature (data not shown).

With no demonstrated origin of replication (see below), position 1 of the sequence was arbitrarily assigned to 290 nucleotides upstream of a *Bam*HI site, which corresponds to the last base of the *angM* gene (ORF1). A total of 86.6% of the plasmid genome appears to have a coding function, and 41 of the 59 ORFs either correspond to biochemically characterized proteins or can be correlated with assigned or described functions by high degrees of similarity to sequences in the databases. Additionally, 18 ORFs predicted by GENEMARK, GLIMMER, or visual inspection but having no significant similarity to sequences in the databases may be functionally relevant (Table 2.1). Two additional genes, *rnaA* and *rnaB*, were found on the pJM1 plasmid and were shown to encode two antisense RNAs. The ORFs and the two antisense RNA genes are distributed between the strands in a ratio of 36 on one and 25 on the other strand.

2.3.2. ORF analysis. A graphical representation of the 59 known or predicted ORFs, and the two antisense RNA genes, appears in Figure 2.1. Their relationships to representative homologues in databases are detailed in Table 2.1. Two ORFs, identified by using GLIMMER software, are not included in Table 2.1 because they are encoded

within ORF54 in the opposite strand, they show no homology with any known proteins or ORFs in GenBank, and no obvious Shine-Dalgarno sequence was identified upstream of the AUG of these ORFs.

Based on gene similarity search results, functions associated with ORFs may be classified into the following categories: utilization of iron, transposition, and replication-partition (Table 2.1).

In Figure 2.2 the G+C content of each ORF is shown, including the relative position of insertion sequence (IS) elements.

2.3.3. Utilization of iron. The predicted metabolic abilities linked to pJM1 center on iron uptake and utilization (Figure 2.1). We have demonstrated that the genes *fatDCBA* (ORF3 to ORF6) confer on pJM1-carrying bacteria the ability to utilize ferric-anguibactin and so are part of the pathway of iron utilization (3, 5, 6, 88). We also demonstrated that the genes *angM* (ORF1), *angR* (ORF7), *angT* (ORF8), *angN* (ORF10), and *angBG* (ORF41) encode nonribosomal peptide synthetases while *angU* (ORF9) and *angH* (ORF13) encode tailoring enzymes for the biosynthesis of anguibactin, since transposon insertions in each of these genes resulted in no siderophore production (40, 169-171). Other ORFs encoded on pJM1 (ORF39 to ORF43 and ORF59) show high similarity to siderophore biosynthetic genes found in other bacteria, and some of them could intervene in anguibactin biosynthesis. The homologies in Table 2.1 suggest that the predicted polypeptides of these ORFs could play a role in the early stages of anguibactin biosynthesis: ORF39 (AngD) is a phosphopantetheinyl transferase; ORF41 (AngBG) possesses the isochorismate lyase and aryl carrier protein (ArCP) domains; ORF42 (AngE) is the 2,3-dihydroxybenzoic acid (DHBA) AMP ligase; and ORF43 (AngC) is an

isochorismate synthetase. ORF40 may have a function in the transport of ferric-anguibactin into the cell cytosol. Upstream of *angM* (ORF1) there is another ORF (ORF59) with similarity to a stretch of 159 amino acids within the amino acid sequence of the 2,3-dihydro-DHBA dehydrogenase of *Vibrio cholerae*, the last enzyme in the DHBA biosynthetic pathway (194). Further upstream of ORF59 is a small (23-amino-acid) ORF that corresponds to the amino-terminal end of the 2,3-dihydro-DHBA dehydrogenase. It is thus possible that ORF59 could have been generated by a frameshift of the original full-length gene, resulting in a shorter ORF truncated at the amino-terminal end. The small ORF upstream of ORF59 has not been included in Table 2.1.

Retrobiosynthesis of anguibactin indicates that it is composed of one molecule of DHBA, one of cysteine, and one of *N*-hydroxyhistamine (2, 77). Cysteine is converted to a thiazoline ring, through cyclization, in the process of synthesis, and *N*-hydroxyhistamine is obtained from the modification of histidine.

In *V. anguillarum* strain 775, the anguibactin precursor DHBA is synthesized by chromosome-encoded proteins, as shown by the ability of the plasmidless strain to produce DHBA (29), although some virulent strains of *V. anguillarum*, such as 531A, rely on the pJHC1 (a pJM1-like plasmid)-encoded AngBG protein for the synthesis of this precursor (188). The amino terminus of the pJHC1-encoded AngBG possesses the isochorismate lyase activity, thereby explaining the need for this protein for the synthesis of DHBA in this strain (188). Analysis of mutations in the *angB* ORF of pJHC1 provided evidence that, in addition to *angB*, an overlapping gene, *angG*, exists at this locus and that it encodes polypeptides, which are in frame to the carboxy-terminal end of the isochorismate lyase. The carboxy terminus of AngBG encodes an ArCP domain that

is also present in the internal AngG polypeptides and is where phosphopantetheinylation occurs at a conserved serine residue, the phosphopantetheinylate moiety acting as an acceptor of an activated aryl or amino acid group (188). In strain 775 the *angBG* gene is also found on the pJM1 plasmid (ORF41); however, we do not know at present if the product of this gene is essential for anguibactin biosynthesis, as is the case for strain 531A.

The enzymology of anguibactin biosynthesis is still under investigation; however, predictions can be made based on our knowledge of the structure of this siderophore, genetic evidence, and functions of potential biosynthetic proteins inferred by homology studies (40, 164). The results of this combined genetic and in silico analysis are shown in the model in Figure 2.3. In the biosynthesis of other phenolic siderophores, activation of DHBA, before loading on the specific ArCP domain, occurs by the action of a 2,3-dihydroxybenzoate-AMP ligase, VibE in vibriobactin biosynthesis in *V. cholerae*, and EntE in enterobactin biosynthesis in *E. coli*. ORF42 in pJM1 shows homology with VibE and EntE adenylation domains (Table 2.1), suggesting that it could act as the 2,3-dihydroxybenzoate-AMP ligase in anguibactin biosynthesis. The activated DHBA is then ligated to the phosphopantetheinyl moiety in AngBG. Phosphopantetheinylation of this protein might have occurred by the action of the pJM1-encoded AngD (ORF39), showing homology to phosphopantetheinyl transferases. The pJM1 plasmid-encoded proteins AngR (ORF7), AngM (ORF1), and AngN (ORF10) must play a role in subsequent biosynthetic steps, although AngR, in addition to its biosynthetic function, is also essential for regulation of iron transport gene expression (31, 38, 40, 55, 142, 164, 171, 190). Cysteine, one of the anguibactin precursors, is likely activated by the A

domain of AngR. Activated cysteine is then loaded onto the peptidyl carrier protein (PCP) domain of AngM. Although the AngR amino acid sequence also contains a PCP domain, this may not be functional because an essential serine is replaced by alanine in this domain. The condensation (C) domain of AngM then catalyzes the formation of a peptide bond between DHBA and cysteine, resulting in the DHBA-cysteine dipeptide bound to the PCP domain of AngM. Another plasmid-encoded protein, AngN, contains two tandem cyclization (Cy) domains that are involved in the cyclization of the cysteine moiety to form the thiazoline ring. Another Cy domain is found in the AngR protein; however, the essential first aspartic acid is replaced by asparagine in the highly conserved Cy motif, suggesting that also this domain of AngR is not functional. Anguibactin is released from the PCP domain of AngM by nucleophilic attack of *N*-hydroxyhistamine to the phosphopantetheinyl arm of the PCP domain of AngM. *N*-Hydroxyhistamine is produced by modification of histidine catalyzed by the histidine decarboxylase AngH (ORF13) (170) and a monooxygenase homologue, AngU (ORF9). AngT (ORF8), the thioesterase identified in this system, is not included in this model because it does not appear to be strictly necessary for anguibactin production, since an *angT* mutant results in only a 17-fold-lower yield of anguibactin (40, 190).

After anguibactin is synthesized, it is secreted to the extracellular space. Two ORFs (ORF14 and ORF15), downstream of *angH*, related to the ABC-type transporter, are perhaps involved in secretion as part of the complex that exports anguibactin to the extracellular space. After the siderophore is secreted and bound to iron, the ferric-siderophore complex is transported to the cytosol via a highly specific transport system (3, 5, 6, 88, 169, 173, 174). In *V. anguillarum* 775 this system includes the outer

membrane receptor FatA (ORF6), which binds ferric-anguibactin and shuttles it to the periplasm (3, 5). The energy necessary for this transport is mediated by a chromosomally encoded TonB-ExbB-ExbD complex, which interacts with the FatA protein (163).

The next step in internalizing the ferric-siderophore complex involves the periplasmic binding protein FatB (ORF5). FatB is a lipoprotein (5) that is anchored to the inner membrane, unlike the *E. coli* homologues FhuD and FepB, which are free in the periplasm (87, 161).

We believe that the last step in internalization of ferric-anguibactin involves the inner membrane proteins FatD (ORF3) and FatC (ORF4) and that these catalyze the transport of ferric-anguibactin from the periplasm to the cytosol (6, 88). In other systems, such as the ferrichrome and enterobactin systems, the energy for this transport through the inner membrane is provided by an ATP-binding protein (14, 87, 122). ORF40 shows homology with many of these iron(III) ATP-binding proteins and could provide the missing ATP-binding domain of the permease complex, although the activity of chromosomally encoded ATP-binding proteins cannot be ruled out.

The genes *fatDCBA* together with the genes *angR* and *angT* are located in the iron transport-biosynthesis (ITB) operon (Figure 2.1) (190). Regulation of this operon is carried out at the transcriptional level by the positive regulator AngR and the chromosomally encoded negative regulator Fur and at the posttranscriptional level by two antisense RNAs, RNA α and RNA β , encoded within this operon by the *rnaA* and *rnaB* genes, respectively (Figure 2.1) (30, 143, 179, 180). These two genes have been shown to encode RNAs that are not translated. Another positive regulator of the ITB operon, the *trans*-acting factor (TAF), is encoded in a region noncontiguous to this operon

encompassing ORF29 to ORF53 (169, 174, 188). The TAF determinants have not been identified as yet, and no ORF included in the TAF region shows homology with regulatory proteins, with the exception of ORF51, which shows very low homology (24% identity) to an *E. coli* arylsulfatase regulatory protein.

2.3.4. Insertion elements and transposons. The ITB operon and the biosynthetic genes *angU* (ORF9) and *angN* (ORF10) are located within a structure that resembles a transposon, flanked by the almost identical ISV-A1 and ISV-A2 elements (173). There is a second putative composite transposon on pJM1 that contains homologues of genes (ORF39 to ORF43) involved in the synthesis of DHBA, one of the anguibactin precursors (Table 2.1). These genes are also organized as a cluster that is flanked by identical ISV-A2 sequences. Figure 2.2 shows very clearly that the ISV-A2-flanked DNA has an average G+C content of 39.3%, significantly lower than the average G+C content of the pJM1 plasmid, suggesting a horizontal acquisition of this composite gene region. A third set of ORFs, ORF1 (*angM*) and ORF59, is flanked by ISV-A1 and ISV-A2 sequences, although the ISV-A2 element is interrupted at the 5'-end of the putative transposase gene by an insertion of a sequence containing four ORFs (ORF54 to ORF57). It is of interest that one of these ORFs (ORF54) shows homology to a transposase gene, while another, ORF55, shows high similarity to a resolvase. ORF56 shows similarity to *spnT*, a *Serratia marcescens* gene encoding a protein with no homologues, although when overexpressed it affected both sliding motility and prodigiosin production in this bacterium (76). The other ORF in this cluster, ORF57, encodes a predicted protein with homology to RecX, a *recA* regulator (162). Furthermore this cluster is flanked by 5-bp direct repeats, suggesting that the interruption of the ISV-A2 transposase gene (ORF58) could have

resulted from insertion of a transposon containing these four ORFs.

Besides ISV-A1 and ISV-A2, pJM1 carries several hypothetical IS elements (Table 2.1). Two of them show homology to a *Vibrio metschnikovii* ISVme insertion sequence, and they both contain all three ORFs found in this IS element. These two identical ISVme-like sequences flank a region of 24,085 bp containing 27 ORFs (from ORF19 to ORF45), almost half of the coding capacity of pJM1. Another IS element, RS1 carrying ORF21, which shows homology to a transposase, is found as a single copy in pJM1. Two other ORFs, ORF12 and ORF50, show similarity to transposases; however, no other components of ISs were identified.

2.3.5. Replication and partition. The pJM1 plasmid replicates at a copy number of 1 to 2 in *V. anguillarum* cells (28). ORF19 to ORF28, encoding hypothetical proteins that could be involved in replication and partition, are clustered adjacent to the TAF region. ORF19 shows homology with the RepA protein of *Aeromonas salmonicida* plasmid pRAS3 (91). The presence of four 21-bp direct repeats in the proximity of ORF19, spanning bp 29013 to 29136, and the relatively low G+C content of 33.7% are consistent with the existence of a possible *oriV* in this region. The predicted amino acid sequences of ORF27 and ORF28 show similarity to those of ParB and ParA, respectively. In other systems, the plasmid-encoded ParA and ParB proteins form one operon autoregulated by the Par proteins. The ParA protein is an ATPase that assembles with ParB subunits and forms a nucleoprotein complex that binds to a *cis*-acting centromere-like site, *parS* (90). As predicted for ParA proteins, ORF28 exhibits at its N terminus an ATP-GTP binding consensus sequence (63). In other bacteria, homologues of *parA* and *parB* map adjacent to the chromosomal and plasmid origin regions of replication (95, 128), and this is the

case for pJM1. Experiments are being carried out to characterize the functions of the pJM1 replication region.

2.3.6. The microheterogeneity of pJM1-like plasmids in strains of *V. anguillarum*.

Different virulent *V. anguillarum* strains harboring the pJM1-like-plasmids showed microheterogeneity in their restriction endonuclease patterns. A listing of the *Bam*HI restriction fragment length polymorphisms as well as the *Bam*HI profiles for several naturally occurring pJM1-like virulence plasmids that we have examined is given in Figure 2.4.

2.4. Discussion

The presence of genes of a complex biosynthetic pathway for a siderophore and the carriage of the iron transport operon together with its role in virulence of *V. anguillarum* 775 are unique features of plasmid pJM1 (37, 38, 40). The 65,009-nucleotide sequence, with an overall G+C content of 42.6%, revealed 59 genes and ORFs encoding functions associated with utilization of iron, transposition, and partition. Approximately a third of these ORFs and genes are related to iron metabolic functions, including ferric anguibactin transport proteins, nonribosomal peptide enzymes, and other proteins essential for the biosynthesis of the siderophore anguibactin. The majority of the ORFs encoding iron metabolic functions were experimentally demonstrated to be involved in anguibactin mediated iron metabolism (ORF1 to ORF13). Other ORFs with homology to proteins involved in the biosynthesis and activation of the precursor of anguibactin DHBA, such as ORF39 to ORF43, were also identified. Our recent work has demonstrated that one of these, ORF42, named *angE*, encodes a 2,3-dihydroxybenzoate-AMP ligase that could act in activating DHBA. In a previous publication we reported that the *angE* homologue in plasmid pJHC1, a pJM1-like plasmid found in *V. anguillarum* strain 531A, was not essential for anguibactin production (188). A deletion that eliminated a region including the *angB* and *angE* genes was complemented by just the *angB* gene, demonstrating the existence of a chromosomal homologue of the *angE* gene in this strain (188). We have recently identified in the 775 strain chromosome homologues of *angE* and other genes involved in the production, activation, and incorporation of DHBA in the anguibactin biosynthetic pathway; therefore, the pJM1 plasmid-carried *angE* gene in the 775 strain might not be essential for anguibactin

biosynthesis (7). It is of interest that the amino acid sequence of this chromosomally encoded AngE is identical to that reported previously (7, 75). It is also of interest that ORF39 to ORF43 are organized as a cluster that is flanked by ISV-A2 sequences and that the DNA in this cluster shows an average G+C content of 39.3%, significantly lower than the average G+C content of the pJM1 plasmid. It is tempting to speculate that this ISVA2-flanked structure is a transposon that has been horizontally acquired from other bacteria. Furthermore, the existence of chromosome homologues for some of these ORFs suggests the attractive possibility that there could also have been an integration event in one of the two *V. anguillarum* chromosomes. Curiously, the ITB operon, *fatDCBA-angRT* (ORF3 to ORF8, respectively), and other anguibactin biosynthetic genes, *angU* (ORF9) and *angN* (ORF10), located downstream of this operon, are also bracketed by the highly related ISV-A1 and ISV-A2 ISs. Nevertheless, the fact that ORFs and genes on pJM1 are flanked by IS elements does not necessarily imply that the composite structures are transposons, since the relative orientation of the flanking IS elements is not always as found with the IS elements flanking known composite transposons such as Tn5, Tn7, and Tn10 (15, 35, 84). The positions of IS elements forming a composite transposon-like structure, corroborated by the G+C content of the pJM1 sequence, suggest a modular composition of the virulence plasmid pJM1 of *V. anguillarum* strain 775 biased towards acquisition of transposon modules containing genes related to iron metabolic functions.

An important final step is the secretion of the siderophore to the extracellular milieu, a still-unsolved question for siderophore-mediated iron transport systems. In this vein, although not yet proven, ORF14 and ORF15 could function in the export of anguibactin, since these ORFs show homology to ABC transporters involved in efflux.

Elucidation of their function, if any, will have to await current genetic analysis.

Regions that have features consistent with replication and partitioning functions have been identified adjacent to the TAF region. It is possible that the product of ORF19 is a replication protein that interacts with the 21-bp repeats located in proximity.

Whether these sequences are truly involved in these functions await further analysis, which is currently being carried out.

We also report in this work considerable microheterogeneity in pJM1 plasmids isolated from many parts of the world, even from both the east and west coasts of the United States. Previous work has also shown microheterogeneity in many other examples of pJM1-like plasmids (121, 126, 171, 172). For instance the pJM1-like plasmid pJHC1 from strain 531A shows two major changes, two extra insertions of the RS1 sequence and also an *angR* gene that has a single nucleotide change that results in an amino acid substitution in the AngR protein (H267N). This change was associated with an increased anguibactin production not only in the 531A strain but also in other strains in which the AngR protein shows this H-to-N alteration (171). In other cases the existing microheterogeneity has only been characterized by restriction endonuclease analysis without further genetic analysis (121, 126, 172).

Recently a partial sequence of a pJM1-like plasmid (pEIB1) was submitted to GenBank (accession number AY255699). This plasmid is another example of the microheterogeneity of the pJM1-like plasmids: pEIB1 differs from pJM1, in the sequence of at least two anguibactin biosynthesis genes. The *angR* sequence has the H267N substitution found in several pJM1-like plasmids that leads to a higher siderophore production phenotype (171), while the *angN* sequence shows an internal deletion

compared with the *angN* gene present in pJM1. The deletion in this pJM1-like plasmid resulted in a frameshift splitting the *angN* gene (ORF10 in pJM1) into two ORFs, truncating the first Cy domain of AngN while leaving the second Cy domain intact. It would be of interest to know whether the strain harboring the pJM1-like plasmid with this *angN* deletion is still able to produce anguibactin. Since there is no information on the origin of the strain, we cannot identify whether this plasmid is one of the already described pJM1-like plasmids. Furthermore, this partial sequence submission erroneously assigns homology of the ORF JM15, which is 100% homologous to our ORF56, to the TcbA insecticidal toxin from *Photobacterium luminescens* (GenBank accession number AAC38627). By our analysis ORF56, and thus JM15, shows only low homology (20% identity) to a 110-amino-acid stretch of the 2,504-amino-acid-long TcbA protein. Conversely, we found a strikingly high homology (92% identity [Table 2.1]) of the predicted 464-amino-acid product of ORF56, and thus JM15, to the 464-amino-acid-long SpnT (GenBank accession number AAN52497), an *S. marcescens* protein possibly involved in both sliding motility and prodigiosin production in this bacterium (76).

Our complete sequence analysis and annotation of pJM1 present for the first time the entire sequence of an iron metabolic regulon that is in its majority encoded on a plasmid and that is an essential factor of virulence in *V. anguillarum* infections of fish.

2.5. Acknowledgments

This project was supported by National Public Health Service awards from the National Institutes of Health, AI19018-19 and GM60400-01 to J.H.C. We thank Thomas Keller and the excellent technical support provided by the OHSU-MMI Research Core Facility.

Table 2.1. Summary of ORFs identified by significant homology (BLAST search) or prediction or previously experimentally verified

ORF	Length (amino acids)	CDS (start codon-stop codon) ^a	Gene or function of closest relative (source)	Data bank reference	Identity (%)	e value ^b
1	705	1-2118c	NRPS VibF (<i>V. cholerae</i>)	gb AAG00566.1	209/535 (39%)	e-103
2	302	2207-3115c	transposase for ISV-A1 (<i>V. anguillarum</i>)	gb AAA81774.1	301/302 (99%)	e-173
3	314	3578-4522	iron transport protein FatD (<i>V. anguillarum</i>)	gb AAA25641.1	314/314 (100%)	e-141
4	317	4519-5472	iron transport protein FatC (<i>V. anguillarum</i>)	gb AAA25642.1	317/317 (100%)	e-139
5	322	5526-6494	iron transport protein FatB (<i>V. anguillarum</i>)	gb AAA91580.1	322/322 (100%)	e-178
6	726	6598-8778	iron transport protein Fata (<i>V. anguillarum</i>)	gb AAA91581.1	726/726 (100%)	0.0
7	1048	8863-12009	NRPS AngR (<i>V. anguillarum</i>)	gb AAA79860.1	1048/1048 (100%)	0.0
8	252	12006-12764	NRPS AngT (<i>V. anguillarum</i>)	gb AAA79861.1	252/252 (100%)	e-150
9	442	12862-14190c	rhizobactin biosynthesis protein RhbE (<i>Sinorhizobium meliloti</i>)	gb AAK65920.1	237/435 (54%)	e-143
10	956	14314-17184c	NRPS VibF (<i>V. cholerae</i>)	gb AAG00566.1	332/931 (35%)	e-157
11	306	17396-18316	transposase for ISV-A2 (<i>V. anguillarum</i>)	gb AAA81776.1	305/306 (99%)	6-174
12	322	18437-19405	transposase (<i>V. vulnificus</i>)	gb AAO10886.1	301/322 (93%)	e-152
13	386	19652-20854	histidine decarboxylase AngH (<i>V. anguillarum</i>)	emb CAA83945.1	386/386 (100%)	0.0
14	536	20970-22580	ABC transporter homologue (<i>E. coli</i>)	gb AAN79727.1	37/548 (25%)	3e-27
15	560	22577-24259	putative ABC transporter (<i>Streptomyces coelicolor</i>)	emb CAC17507.1	132/461 (28%)	2e-40
16	105	24444-24761	Orf1 ISVme (<i>V. metschnikovii</i>)	gb AAN33020.1	24/96 (25%)	1.4
17	117	24758-25111	Orf2 ISVme (<i>V. metschnikovii</i>)	gb AAN33021.1	41/103 (39%)	e-15
18	513	25171-26712	Orf3 ISVme (<i>V. metschnikovii</i>)	gb AAN33022.1	217/526 (41%)	2e-99
19	304	26817-27731c	RepA (<i>Aeromonas salmonicida</i>)	gb AAK97757.1	52/205 (25%)	e-07
20	343	27728-28759c	related to DNA mismatch repair protein (<i>Streptococcus mutans</i>)	gb AAN59686.1	28/93 (30%)	0.67
21	362	29673-30761c	transposase for IS801 (<i>Pseudomonas syringae</i>)	emb CAA40540.1	171/341 (50%)	8e-92
22	128	31031-31417	Unknown (<i>V. vulnificus</i>)	gb AAO07608.1	34/99 (34%)	0.014
23	99	31555-31854	conserved hypothetical protein (<i>Pseudomonas putida</i>)	emb CAC86752.1	54/92 (58%)	e-22
24	96	31878-32168	hypothetical protein (<i>P. putida</i>)	emb CAC86751.1	48/83 (57%)	2e-21
25	409	32297-33526c	GLIMMER, GENEMARK prediction; no homology			
26	127	33513-33896c	GLIMMER prediction; no homology			
27	323	33902-34873c	ParB (<i>Xylella fastidiosa</i>)	gb AAF85627.1	64/218 (29%)	5e-16
28	273	34870-35691c	ParA (<i>Leptospira interrogans</i>)	gb AAN51545.1	74/247 (29%)	3e-22
29	514	35892-37436	putative bacteriophage protein (<i>Salmonella enterica</i>)	gb AAO69541.1	101/307 (32%)	5e-32
30	115	37505-37852	GLIMMER prediction; no homology			
31	103	37883-38194	GLIMMER prediction; no homology			
32	264	38616-39410	GLIMMER, GENEMARK prediction; no homology			
33	104	39738-40052	GLIMMER, GENEMARK prediction; no homology			
34	116	40152-40451	GLIMMER prediction; no homology			
35	93	40396-40677	GLIMMER prediction; no homology			
36	136	40727-41137	GLIMMER prediction; no homology			
37	176	41246-41776	GLIMMER prediction; no homology			
38	306	41945-42865c	transposase for ISV-A2 (<i>V. anguillarum</i>)	gb AAG33855.1	306/306 (100%)	e-174
39	239	43053-43772	NrgA (<i>Photobacterium luminescens</i>) similar to EntD (<i>E. coli</i>)	gb AAO17175.1	91/227 (40%)	3e-40
40	251	43873-44628	iron(III) ABC transporter (<i>V. parahaemolyticus</i>)	dbj BAC62003.1	183/250 (73%)	e-101
41	287	44827-45690	AngB/G (<i>V. anguillarum</i>)	gb AAG33854.1	287/287 (100%)	0.0
42	546	45741-47381c	DHBA-AMP ligase (<i>V. cholerae</i>)	gb AAF93937.1	307/536 (57%)	e-151
43	393	47362-48543c	isochlorismate synthase (<i>V. vulnificus</i>)	gb AAO07758.1	252/392 (64%)	e-149
44	306	48880-49800	transposase for ISV-A2 (<i>V. anguillarum</i>)	gb AAG33856.1	306/306 (100%)	e-174
45	277	49943-50776c	DHAP synthase (<i>V. vulnificus</i>)	gb AAO07756.1	149/268 (55%)	2e-82
46	513	50796-52337c	Orf3 ISVme (<i>V. metschnikovii</i>)	gb AAN33022.1	217/526 (41%)	2e-99
47	117	52397-52750c	Orf2 ISVme (<i>V. metschnikovii</i>)	gb AAN33021.1	41/103 (39%)	e-15
48	105	52747-53064c	Orf1 ISVme (<i>V. metschnikovii</i>)	gb AAN33020.1	24/96 (25%)	1.4
49	115	53664-54011	GLIMMER prediction; no homology			
50	153	55181-55561c	putative transposase (<i>Klebsiella pneumoniae</i>)	emb CAA09339.1	98/151 (64%)	4e-55
51	112	55679-55951c	putative arylsulfatase regulatory protein (<i>E. coli</i>)	gb AAN83151.1	24/97 (24%)	0.73
52	140	55971-56393c	GLIMMER prediction; no homology			
53	389	56383-57552c	hypothetical protein (<i>P. putida</i>)	gb AAN662271.1	34/101 (33%)	0.002
54	980	57830-60772	transposase (<i>Mesorhizobium loti</i>)	dbj BAB54451.1	431/965 (44%)	0.0
55	194	60891-61475	putative resolvase (<i>Serratia marcescens</i>)	gb AAN52496.1	183/194 (94%)	8e-88
56	464	61553-62947	SpiT (<i>S. marcescens</i>)	gb AAN52497.1	430/464 (92%)	0.0
57	144	62944-63378	RecX (<i>E. coli</i>)	dbj BAA16560.1	54/146 (36%)	e-18
58	299	63430-64329	transposase for ISV-A2 (<i>V. anguillarum</i>), partial	gb AAG33855.1	293/293 (100%)	e-166
59	175	64326-64853c	VibA (<i>V. cholerae</i>), partial	gb AAF93939.1	91/159 (57%)	2e-42

^a CDS, coding sequence; c, complementary strand.

^b An E value of >0.4 indicates no homology.

Figure 2.1. Schematic representation of the ORFs on the two strands of pJM1 DNA.

Red, ORFs related to biosynthesis of the siderophore; blue, ORFs related to transport of the siderophore; green, ORFs related to IS elements and composite transposon; cyan, ORFs related to replication and partitioning; yellow, conserved hypothetical ORFs and ORFs with no known functions; black, ORFs with functions that do not fall in any of the above categories. The black blocks represent genes encoding antisense RNAs: *rnaA*, antisense RNA α and *rnaB*, antisense RNA β .

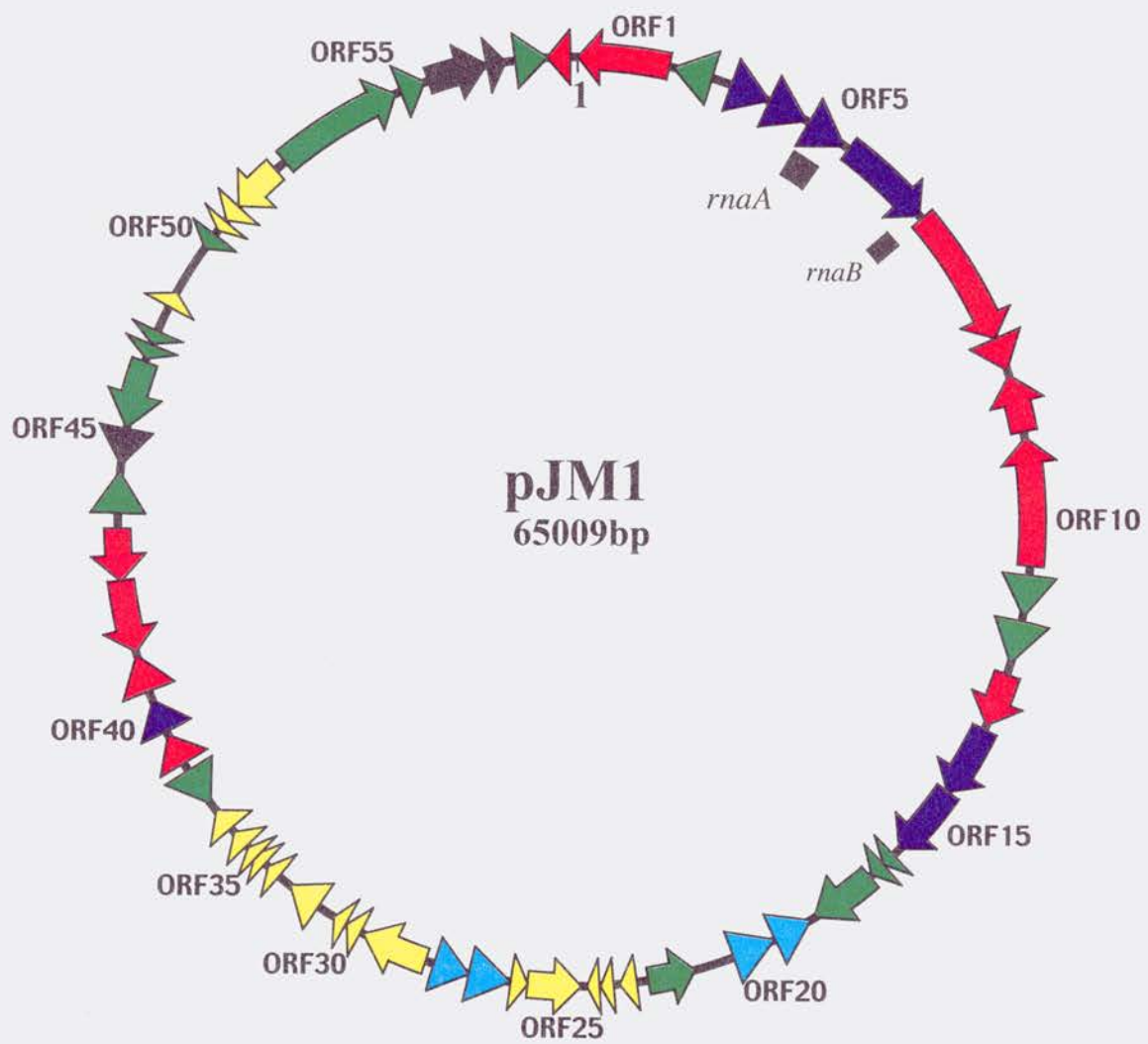


Figure 2.2. G+C contents of the ORFs of pJM1. Dashed line, mean G+C content of pJM1 DNA (42.6%). Asterisks indicate the highly related ISV-A1 and ISV-A2.

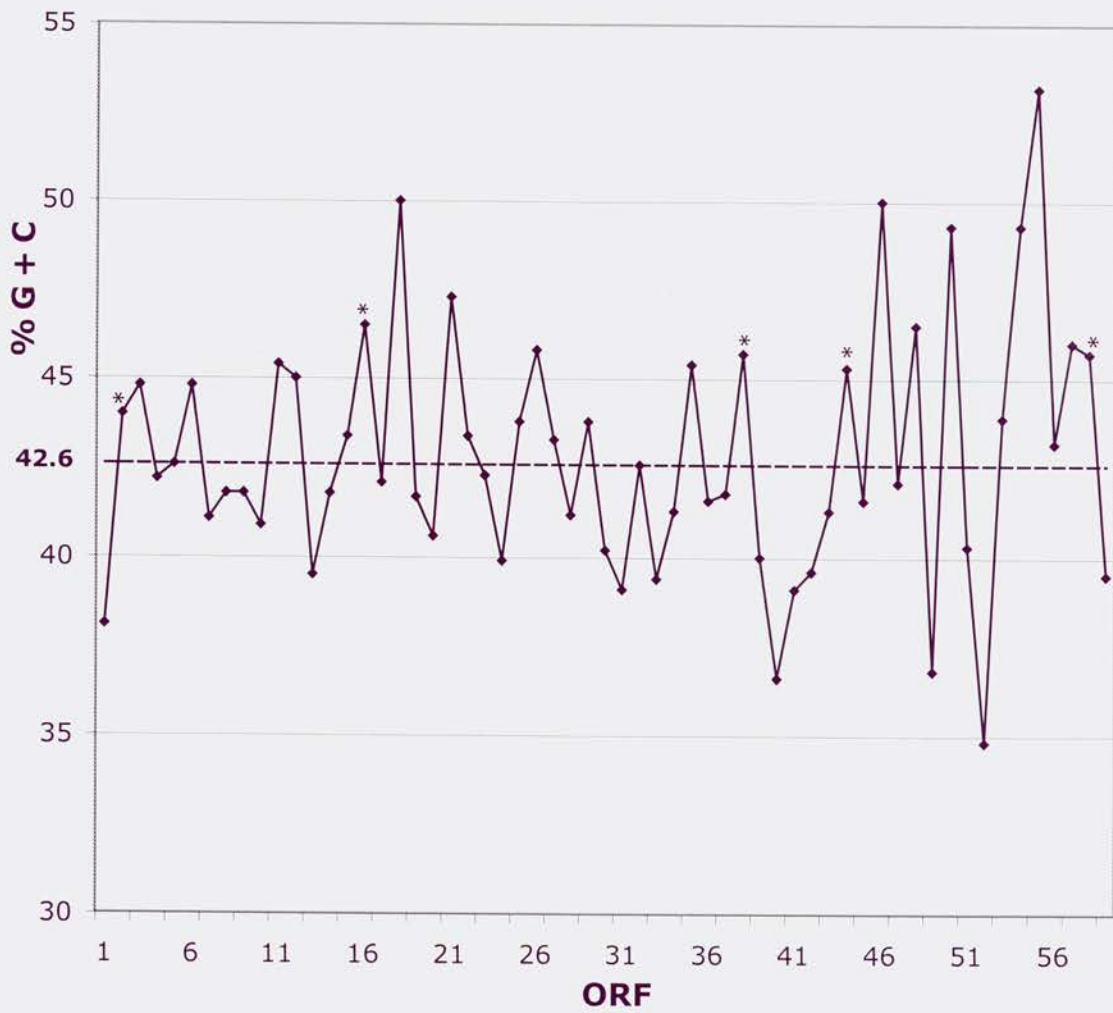


Figure 2.3. Model of anguibactin biosynthesis. The predicted ORF numbers from Table 2.1 are given under the protein designations. Abbreviations: DHB, corresponds to DHBA and radicals thereof such as a diphenolic ring; Cyst, cysteine; Thiaz, thiazoline ring; PPant, phosphopantetheinyl moiety; isochor.,isochorismate.

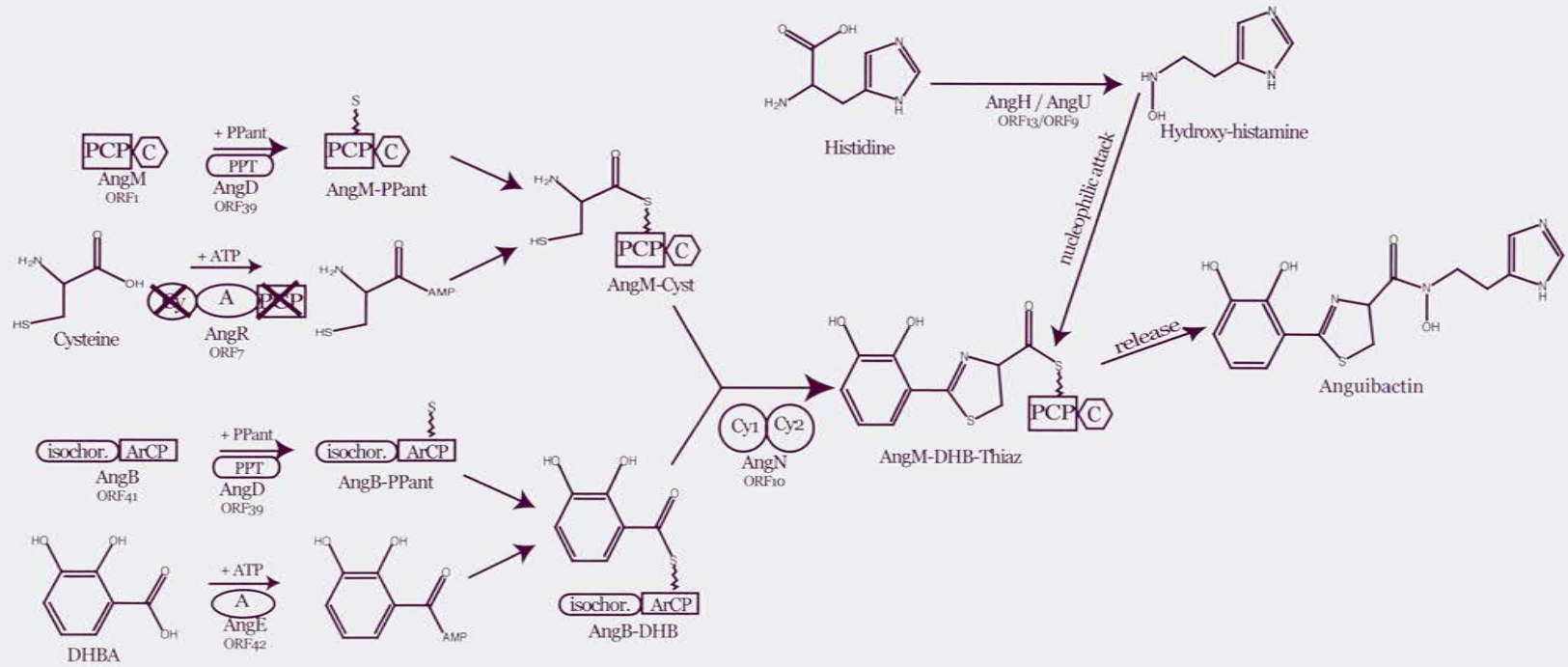
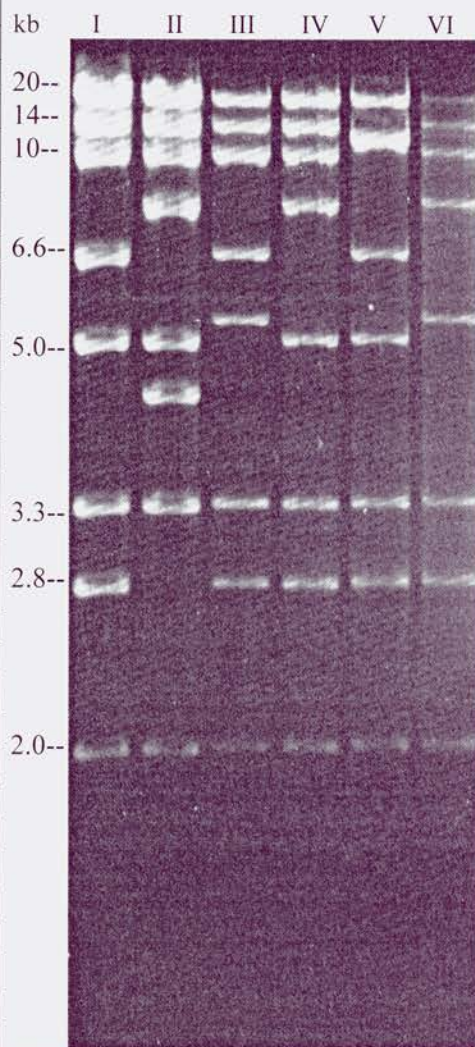


Figure 2.4. Microheterogeneity of pJM1-like plasmids from *V. anguillarum* strains.

*, “kb” indicates sizes in kilobase pairs of each of the pJM1 *Bam*HI restriction endonuclease fragments.

Strain	Geographic source	<i>Bam</i> HI restriction pattern*					
775	Washington	I					
133-S	Washington	I					
V15	Washington	V					
PB1	Tukushima, Japan	I					
PT77022	Tukushima, Japan	IV					
PT77052	Tukushima, Japan	I					
PT77082	Tukushima, Japan	IV					
PT77097	Tukushima, Japan	I					
PT223	Tukushima, Japan	I					
LS-173	Oregon	I					
LS-174	Oregon	I					
507	Maine	III					
521	Maine	II					
521A	Maine	III					
522A	Maine	II					
522C	Maine	II					
523B	Maine	II					
527	Maine	III					
528	Maine	III					
531A	Maine	II					
531B	Maine	II					
532	Maine	III					
533	Maine	II					
535	Maine	II					
540A	Maine	II					
543A	Maine	III					
547B	Maine	III					
500	New Hampshire	III					
509	New Hampshire	III					
R61	Galicia, Spain	VI					
R72	Galicia, Spain	VI					



CHAPTER 3

**Genetic and biochemical analyses of chromosome and plasmid
angB homologues encoding ICL and ArCP domains
and their functions in anguibactin biosynthesis
in *Vibrio anguillarum* strain 775**

Manuela Di Lorenzo, Michiel Stork, and Jorge H. Crosa

Submitted to Journal of Bacteriology

3.0. Abstract

Anguibactin, the siderophore produced by *Vibrio anguillarum* 775 is synthesized from 2,3-dihydroxybenzoic acid (DHBA), cysteine and hydroxyhistamine via a nonribosomal peptide synthetase (NRPS) mechanism. Most of the genes encoding anguibactin biosynthetic proteins are harbored by the pJM1 plasmid. In this work we report the identification of a homologue of the plasmid-encoded *angB* on the chromosome of strain 775. The products of both genes harbor an isochorismate lyase (ICL) domain that converts isochorismic acid to 2,3-dihydro-2,3-dihydroxybenzoic acid, one of the steps of DHBA synthesis. We show in this work that both ICL domains are functional in the production of DHBA in *V. anguillarum* as well as in *E. coli*. Substitution by alanine of the aspartic acid residue in the active site of both ICL domains completely abolishes their isochorismate lyase activity in vivo. The two AngB proteins carry also an aryl carrier protein (ArCP) domain but in contrast with the ICL domain only the plasmid encoded ArCP can participate in anguibactin production as determined by complementation analysis and site-directed mutagenesis, S248A, in the active site. The site-directed mutants, D37A in the ICL domain and S248A in the ArCP domain of the plasmid encoded AngB were also tested in in vitro reactions clearly showing the importance of each residue for the domain function and that each domain operates independently.

3.1. Introduction

Vibrio anguillarum is a marine bacterium responsible for both marine and freshwater fish epizootics throughout the world (4). Certain strains of *V. anguillarum* possess the 65-kb virulence plasmid pJM1 encoding an iron-scavenging system, which is essential for virulence in this bacterium (37, 39, 45, 183). This system includes a low-molecular-weight iron-binding compound, anguibactin, which once secreted, competes for bound iron within the host fish (6, 192). The iron-anguibactin complex is then internalized by a transport system that includes the FatA, -B, -C, and -D proteins and requires the TonB2 complex as the energy-transducing system (2, 5, 163). Anguibactin possesses both a catechol and a hydroxamate group and it has been characterized as ω -*N*-hydroxy- ω -*N*((2'-(2",3"-dihydroxyphenyl)thiazolin-4'-yl)carboxy)histamine by crystal X-ray diffraction studies and chemical analysis (2, 77). Retrobiosynthesis and experimental data showed that anguibactin is synthesized from 2,3-dihydroxybenzoic acid (DHBA), cysteine, and hydroxyhistamine (7, 29, 170, 188).

The genes encoding proteins involved in the biosynthesis and transport of anguibactin lie on a 25-kb contiguous region of the virulence plasmid (169). An additional gene cluster was identified in a non-contiguous region of pJM1 and the products encoded by the genes in this cluster are homologues to enzymes involved in the biosynthesis and activation of DHBA (47). We have also reported the presence of this cluster in the pJM1-like plasmid pJHC-1 of strain 531A including the gene encoding the bifunctional AngB protein: its amino end conferring an isochorismate lyase activity required for the production of DHBA and its carboxyl end provides an aryl carrier protein functioning in anguibactin assembly (188). Furthermore, the carboxy-terminal end of

AngB can be synthesized from the 3' region of *angB*, as an independent polypeptide which, like the carboxy terminal portion of AngB, also functions as an aryl carrier protein involved in anguibactin assembly (188). This pJHC1 plasmid-mediated *angB* gene is essential not only for anguibactin biosynthesis but also for the production of DHBA in the 531A strain since when this strain was cured of the pJM1-like plasmid pJHC1, resulting in strain S531A-1, it could no longer produce DHBA (188). Previous work in our laboratory had shown that the prototypic strain 775 when cured of the pJM1 plasmid, generating plasmidless strain H775-3, still produced DHBA (29). Recently a partial sequence of an open reading frame (*orf*) with homology to the plasmid-encoded *angB* gene was identified in the chromosomal DNA of *V. anguillarum* 775 (7). We report in this work the complete sequence of this chromosomal *angB* gene from strain 775 and an analysis of its activities as compared to the plasmid-encoded version. Our results also explain the phenotypic differences in DHBA production between the 531A and 775 strains of *V. anguillarum*.

3.2. Materials and methods

3.2.1. Bacterial strains, plasmids and growth conditions. Bacterial strains and plasmids used in this study are described in Table 3.1. *V. anguillarum* was cultured at 25°C in either trypticase soy broth or agar supplemented with 1% NaCl (TSBS and TSAS respectively). For experiments determining iron uptake characteristics, the strains were first grown on TSAS supplemented with the appropriate antibiotics and passed to M9 minimal medium (144) supplemented with 0.2% Casamino acids, 5% NaCl, the appropriate antibiotics and either ethylenediamine-di-(*o*-hydroxyphenyl acetic acid) (EDDA) for iron-limiting condition or ferric ammonium citrate for iron-rich conditions. Antibiotic concentrations used for *V. anguillarum* were ampicillin (Ap) 500 to 800 µg/ml, rifampicin (Rif) 100 µg/ml, spectinomycin (Sp) 100 µg/ml, chloramphenicol (Cm) 10 to 15 µg/ml and kanamycin (Km) 100 to 200 µg/ml.

E. coli strains were grown in Luria-Bertani (LB) medium in the presence of the appropriate antibiotics. Antibiotic concentrations used for *E. coli* were Ap 100 µg/ml, Sp 100 µg/ml, Cm 30 µg/ml, Km 50 µg/ml and trimethopim (Tp) 10 µg/ml.

3.2.2. General methods. Plasmid DNA preparations were performed using the alkaline lysis method (17). Sequence quality plasmid DNA was generated using Wizard® Plus SV Minipreps (Promega). Restriction endonuclease digestion of DNA was performed under the conditions recommended by the supplier (Invitrogen, Roche, NEB). Transformations in the *E. coli* strains HB101, XL1 Blue and BLR(DE3) and other cloning strategies were performed according to standard protocols (144). DNA sequencing reactions were carried by the OHSU-MMI Research Core Facility (<http://www.ohsu.edu/core>) using a model 377 Applied Biosystems Inc. automated

fluorescence sequencer. Sequencing primers were designed using Oligo 6.8® primer analysis software and purchased from the OHSU-MMI Research Core Facility (<http://www.ohsu.edu/core>) and Invitrogen. DNA and protein sequence analysis were carried out at the NCBI using the BLAST network service (8). The web server Tcoffee (http://igs-server.cnrs-mrs.fr/Tcoffee/tcoffee_cgi/index.cgi) was used for multiple sequence alignment (129, 130).

Plasmids were transferred from *E. coli* to *V. anguillarum* by triparental conjugation as previously described (169).

3.2.3. Construction of the complementing clone. The fragment containing the *angB* gene from the pJM1 plasmid was amplified by PCR and cloned into the pBR322 derivative pTW99 as previously described for the *angB* gene of plasmid pJHC1 (188). The generated construct, pAngBp, was sequenced to confirm that the *angB* gene sequence was not mutated during the PCR amplification or the cloning. A 1.1 kb fragment containing the chromosomal copy of the *angB* gene of strain 775 was amplified by PCR using the AngBc-*Clal*F (5'-CAATCGATTTTTATGCGTAGAC-3') and the AngBc-*Bam*HIR (5'-AGTGGATCCGGTATACTCAAA-3') primers and pJM1 as a template. The forward and the reverse primer were modified to contain restriction endonuclease sites (underlined in the sequence) suitable for cloning downstream of the promoter of the tetracycline resistance gene of pBR322. Reactions consisted of 3 minutes at 95°C followed by 30 cycles of 45 seconds at 94°C, 1 minute at 55°C, and 2 minutes at 72°C followed by a single cycle at 72°C for 10 minutes. The PCR product was cloned in the pCR®2.1-TOPO® vector using the TOPO TA PCR Cloning Kit (Invitrogen). The 1.1 kb *Clal*-*Bam*HI fragment was subcloned into the *Clal*-*Bam*HI sites

of pBR322 to generate the pAngBc plasmid carrying the *angBc* gene. After recloning in pBR322 the entire *angBc* gene was sequenced to verify that no mutation was generated in the gene during amplification or cloning.

3.2.4. Site-directed mutagenesis. Site-directed mutants were generated using the Quickchange™ site-directed mutagenesis kit (Stratagene). Plasmids pAngBp and pAngBc as template and the primer pairs D37A-U (5'-TCGGTTGTTCTAGTTCACGCTTTACAGGCTTATTTTCTCA-3')/ D37A-L (5'-TGAGAAAATAAGCCTGTAAAGCGTGAAGTACTAGAACCAACCGA-3') and D71A-U (5'-GCGGTACTGCTCATTACGCTATGCAAAAGTACTTTATCA-3')/ D71A-L (5'-TGATAAAGTACTTTTGCATAGCGTGAATGAGCAGTACCGC-3') were used for the mutation in the ICL domain of the plasmid (pAngBpD37A) and chromosomal (pAngBcD71A) copy respectively. For the mutant in the ArCP of the plasmid copy primers S248A-U (5'-TGATTTTCCTTGGACTTGATGCGATACGCATAATGACACT-3') and S248A-L (5'-AGTGTCATTATGCGTATCGCATCAAGTCCAAGGAAAATCA-3') were used with plasmid pAngBp as template to generate pAngBpS248A. The whole procedure was performed according to the manufacturer recommendations, with 16 cycles consisting of: 30 seconds at 95°C followed by 1 minute at 55°C and 12 minutes at 68°C. For the amplification, *Pfu* polymerase was used and after the PCR, the mixture was treated with *DpnI* to cleave the parental DNA. Then 1 µl of the mixture was transformed in the XL1 Blue chemically competent cells provided with the Quickchange™ kit. Site-specific mutations were confirmed by DNA sequencing with the appropriate primers and the entire *angB* mutant genes were sequenced to verify that no other region was affected during mutagenesis.

3.2.5. Construction of *V. anguillarum* mutant strains by allelic-exchange. Mutants 775(pJM1:: Ω) and 775(pJM1::K) were generated as previously described by Welch et al (188), employing the suicide vector pTW-MEV harboring either the *angBp*:: Ω or the *angBp*::K mutant

To construct mutant 775*angBc*::Cm, the *angBc* gene was replaced with the chloramphenicol resistance cassette in the cosmid vector SuperCos harboring a 15 kb of insert containing the *angBc* gene (Cos #2) using the λ red system (41). Cos #2 was obtained as part of a cosmid library by Dr. Hiroaki Naka in the laboratory. The chloramphenicol acetyl transferase (*cat*) gene was amplified from plasmid pKD3 with primers *angBc*-P1 (5'-GGCTTTAAGGCATCACGAACGAGAAAAGCCTCTTTTAACAGTGTAGGCTGGAGCTGCTTC-3') and *angBc*-P2 (5'-AACTGGTTGCTCTTCAGTAGAACGCGTGTCCGTTACTTGACATATGAATATCCTCCTTAG-3') that have 40 bases of homology to the *angBc* sequence at their 5'-end and 20 bases of homology with pKD3 at the 3'-end. The PCR product was transferred by electroporation in HB101 cells harboring Cos #2 and pKD46. Cells were made electro-competent by washing the cells grown in the presence of arabinose (0.2%) four times with ice-cold sterile water at 0°C. Transformants were plated on LB plates containing Cm at 37°C. At this temperature the pKD46 plasmid is lost and only cells containing Cos #2 where the *angBc* sequence is replaced with the *cat* gene are able to grow. Plasmid isolation and restriction digest was performed to assure no rearrangements occurred during the mutagenesis. The *NotI* fragment containing the entire insert from the cosmid was cloned in vector pTW-MEV using the Cm resistance cassette replacing the *angBc* gene as a selection in the transformation. The *angBc* null-mutant was obtained using the mutation-containing

suicide vector as described for the plasmid mutants. The same procedure was repeated for the 775(pJM1::Ω) and 775(pJM1::K) strains to obtain the double mutants.

3.2.6. Determination of DHBA and anguibactin production. DHBA was assayed by employing the Arnow reaction for catechols (9). In addition, a bioassay with *Salmonella* strains that require DHBA to synthesize enterobactin and grow was used to confirm the presence of this catechol (131).

The siderophore anguibactin was detected by three methods. Chrome azurol S (CAS) plates were used to test production of iron-binding compounds by each strain (152). The results obtained on CAS plates were confirmed by a bioassay using strains CC9-16 and CC9-8 that detect specifically anguibactin synthesis, as previously described (169, 183). Furthermore, strains were tested for sensitivity to the iron-chelating compound EDDA via growth assay in liquid minimal medium.

3.2.7. AngBp protein expression and purification. The complete *angBp* gene was cloned in the expression vector pQE60 under the control of the T5 promoter (pQEAngBp). Cloning into the *Bgl*II site of pQE60 adds a C-terminal histidine tag and two extra amino acids to the overexpressed protein (GSHHHHHH). Site-directed mutants in the overexpression clone were generated using primer pairs D37A-U/D37A-L (pQEAngBpD37A) and S248A-U/S248A-L (pQEAngBpS248A), the *angBp* gene cloned in pQE60 as template and the same procedure used for the mutants in the complementing clone. The AngBp proteins were purified from *E. coli* XL1 Blue containing the expression vector. Cultures were grown in LB broth supplemented with Ap at 37°C to an OD₆₀₀ of 0.3 and then cooled to room temperature. Gene expression was induced with 100 μM isopropyl-β-D-thiogalactopyranoside (IPTG) at 25°C for 4 h. The harvested

cells were resuspended in 25 mM Tris-HCl, pH 8.0, 300 mM NaCl and 2 mM MgCl₂, lysed by sonication and the lysate clarified by centrifugation. The supernatant was incubated with Qiagen Ni-NTA Superflow resin for 16 h at 4°C. Proteins were eluted with a step gradient of 5 column volumes of lysis buffer containing 25-200 mM imidazole in 25 mM increments. Fractions containing purified AngBp proteins (as determined by 12% SDS-PAGE analysis) were pooled and dialyzed against 20 mM Tris, pH 8.0, 50 mM NaCl, 2 mM MgCl₂, 1 mM DTT and 10% glycerol. Samples were concentrated using a Centricon YM-3 (Amicon) and quantified from absorbance at 280 nm using the predicted molar extinction coefficient, $\epsilon = 48,790$ as determined using <http://au.expasy.org/tools/protparam.html>.

3.2.8. Expression and purification of EntC, Sfp and VibE. The *entC* gene was amplified from *E. coli* HB101 genomic DNA using primers EntC-*NdeI* (5'-TGTGGAGGATCATATGGATA-3') and EntC-*XhoI* (5'-CTCGCTCGAGATGCAATCCA-3') and cloned in the corresponding sites of the expression vector pET29b. The resulting plasmid pEntC expressed the EntC protein as a translational fusion of a C-terminal hexahistidine tag. The construct was transferred to strain BLR(DE3) for expression. For overproduction of EntC a procedure as the one used for the AngBp proteins was followed with few modification. Cultures were grown in LB broth supplemented with kanamycin at 37°C to an OD₆₀₀ of 0.5 prior induction with 500 μ M IPTG. Harvested cells were resuspended in 50 mM Tris-HCl, pH 8.0, 300 mM NaCl and 20 mM β -mercaptoethanol and then disrupted by sonication.

The construct overexpressing the Sfp and the VibE proteins as translational fusions to C-terminal hexahistidine tags were received from the laboratory of Professor

Christopher T. Walsh (Harvard Medical School). VibE was expressed and purified as previously described (79). Sfp was expressed and purified following the same procedure of the AngBp proteins with minor modification. Strain BLR(DE3)pSfp was cultured in LB broth supplemented with kanamycin at 37°C to an OD₆₀₀ of 0.6 prior to induction with 1 mM IPTG for 5 h at 25°C.

3.2.9. Assay for isochorismate lyase activity. Isochorismate lyase activity of the ICL domain of the AngBp protein was determined by a coupled assay with L-lactate dehydrogenase, LDH (140, 154). In this assay the concentration of pyruvate in the reaction mixture was calculated from the decrease of absorbance at 340 nm due to NADH oxidation. Pyruvate and 2,3-dihydro-2,3-dihydroxybenzoic acid are formed from isochorismic acid in equimolar amounts in the reaction catalyzed by isochorismate lyases. Reaction mixtures contained 100 mM Tris-HCl, pH 7.5, 6 mM MgCl₂, 1.3 mM chorismic acid, 76 nM EntC, 80 nM AngBp (wild type and mutant proteins), 0.2 mM NADH and 7 units of LDH. The reaction mixtures were incubated at 25°C for 40 minutes and the OD₃₄₀ measured every 5 minutes. After 40 minutes, virtually all the NADH was oxidized in the reaction mixtures containing an active ICL domain.

3.2.10. Analysis of covalent [¹⁴C] salicylation of the ArCP domain. Reaction mixtures contained 75 mM Tris-HCl, pH 7.5, 10 mM MgCl₂, 2 mM tris(carboxyethyl)phosphine (TCEP), 200 μM Coenzyme A, 1 μM Sfp (the phosphopantetheinyl transferase) and 10 μM AngBp (wild type and mutant proteins). After 1 h incubation at 25°C to obtain holo-AngB, 10 mM ATP, 100 μM [¹⁴C] salicylate and 1 μM VibE (adenylation enzyme) were added to the mixtures and the samples were incubated at 25°C for additional 60 minutes before precipitation with 10% trichloroacetic

acid (TCA) and 60 µg of BSA. Pellet were washed twice with 10% TCA, redissolved in 88% formic acid and submitted for liquid scintillation counting. The percentage of label protein was calculated from the cpm, the specific activity of [¹⁴C] salicylate and the moles of AngB protein present in the reaction (105).

The accessory proteins Sfp and VibE used in this assay are not the proteins specific for the AngBp protein and the anguibactin system. It was previously shown that Sfp and VibE work to high efficiency in the phosphopantetheinylation of AngB and activation of the substrate to be loaded on AngB (105). Salicylate is not the actual substrate for VibE or AngB but it was shown to work in this system and the natural substrate DHBA is not available in radioactive-labeled form (105).

3.2.11. Nucleotide sequences accession number. The GenBank accession numbers for the sequences were as follows: for *angBp*, AY312585 for strain 775 and AF311973 for strain 531A; for *entC*, M36700.

The sequences of the *angBc* genes of 775 and 531A strains were deposited with GenBank and assigned the accession numbers XXXXX and XXXXX (pending). The previously deposited sequence (AY738106) contains several errors in the partial sequence of the 775 *angBc* gene.

3.3. Results

3.3.1. Identification of a chromosomal *angB* gene in strain 775. Previous work in our laboratory had shown that strain 775 of *V. anguillarum*, when cured of the pJM1 plasmid (H775-3) still produced 2,3-dihydroxybenzoic acid, DHBA (29). In contrast, the plasmid-less strain derivative of 531A (S531A-1) could no longer produce DHBA (188). Furthermore, it was also shown that in the 531A strain only one of the genes of the DHBA biosynthetic pathway, *angB*, encoded on the pJM1-like plasmid pJHC1, was required to complement strain S531A-1 (188). Recently a partial sequence of an open reading frame (*orf*) with homology to the plasmid-encoded *angB* gene was identified in the chromosomal DNA of *V. anguillarum* 775 (7). Completion of the nucleotide sequence of the chromosomal gene revealed an *orf* of 1038 bp that encodes a predicted protein with 64% identity and 78% similarity to the plasmid-encoded AngB (Fig. 3.1A). The chromosomally encoded AngB (AngBc) of 775 possesses the isochorismate lyase (ICL) and the aryl carrier protein (ArCP) domains that are also found in the plasmid-encoded AngB, AngBp (Fig. 3.1B). ICL domains are involved in DHBA biosynthesis and catalyze the conversion of isochorismic acid to 2,3-dihydro 2,3-dihydroxybenzoic acid (61, 140). The ArCP domain is the domain required for tethering of activated DHBA and thus required for siderophore biosynthesis (61, 188).

Sequencing of the same locus of *V. anguillarum* 531A showed that the same *orf* is present in this strain but a deletion of a base at the 5'-end of the gene resulted in premature termination of translation. As shown in Figure 3.1C, in 531A the predicted product of the *angBc* gene is only 94 amino acids long. Welch et al (188) previously showed that in 531A the *angBp* gene is required for DHBA and anguibactin production,

thus the frame-shift generated by the base deletion in the chromosomal *angB* copy of 531A resulted in the plasmid-encoded copy becoming essential for DHBA production.

3.3.2. Mutational analysis of the *angBp* gene in strain 775. To test the functionality of the chromosomal-encoded *angB* we generated a mutant, 775(pJM1:: Ω), consisting of the insertion of the Ω transcriptional-translational terminator (58) at the *Bgl*III site in the 5'-end of the *angBp* gene (Fig. 3.2A). This mutant was tested for its ability to produce DHBA by the Arnow test, specific for catechols, and the results were confirmed by bioassay using *Salmonella* strains *enb-1* and *enb-7* that require DHBA and/or enterobactin to grow in iron limiting conditions. Anguibactin production was determined by CAS agar and growth in iron limiting conditions. To confirm that the iron-binding compound detected on CAS agar is actually anguibactin, bioassays employing strains CC9-8(pJHC9-8) and CC9-16(pJHC9-16) as explained in the Materials and Methods section were performed. As shown in Figure 3.2A, strain 775(pJM1:: Ω) did not produce anguibactin but it was still able to produce DHBA. We then constructed a second mutant in the *angBp* gene of 775 that should affect only the ICL domain and not the ArCP domain. Mutant 775(pJM1::K) is a 4-bp insertion at the *Bgl*III site in *angB*, generated by cleaving the *Bgl*III site and filling in the ends with the Klenow fragment of DNA polymerase I prior to re-ligation. This mutant could still produce anguibactin as determined by CAS and bioassay without any DHBA exogenously added to the media since it was able to produce DHBA endogenously (Fig. 3.2A). In conclusion, the ICL domain of the chromosomally encoded AngB in 775 must be functional although not essential while the ArCP of AngBp is essential for anguibactin biosynthesis.

Furthermore, the results obtained with mutant 775(pJM1::K) indicate that also in 775 the

plasmid-encoded ArCP domain can be translated and function independently of the ICL domain.

3.3.3. Mutational analysis of the *angBc* gene and generation of a double *angB*

mutant in strain 775. To confirm that the chromosomally encoded *angB* is only functional in DHBA production and that the AngBp protein possesses the only ArCP domain involved in anguibactin biosynthesis, we generated a mutation in the *angBc* gene by replacing almost the complete gene with a chloramphenicol resistance gene as explained in the Materials and Methods section. The *angBc* gene was replaced by the *angBc::Cm* construct in 775, 775(pJM1:: Ω) and 775(pJM1::K) at its chromosomal location in each strain and the resulting derivatives analyzed for DHBA and anguibactin production. Anguibactin was determined by CAS agar, bioassay and growth of the strains in minimal media supplemented with 2 μ M ethylenediamine-di-(*o*-hydroxyphenyl acetic acid), EDDA. The presence of DHBA in the supernatant was determined with the Arnow test and verified by a bioassay with *Salmonella* strains that require DHBA to synthesize enterobactin. Strain 775(pJM1:: Ω) although not able to synthesize anguibactin can still produce DHBA (Fig. 3.2). Strain 775*angBc::Cm* and strain 775(pJM1::K) are not affected in DHBA and in anguibactin production, while both double mutants, 775*angBc::Cm*(pJM1:: Ω) and 775*angBc::Cm*(pJM1::K), are unable to produce either compound (Fig. 3.2B). As expected, addition of DHBA to the growth media restored siderophore production in strain 775*angBc::Cm*(pJM1::K), data not shown. Clearly both ICL domains function in the synthesis of DHBA and they are the only two ICL domains present in strain 775. Therefore, the chromosomal and plasmid versions of the AngB protein can intervene in DHBA production, an essential precursor

of anguibactin. This product can then be incorporated in the siderophore only by the plasmid-encoded ArCP domain.

3.3.4. Characterization of the AngB functions in vivo. Each *angB* gene from *V. anguillarum* was cloned in vector pBR322 under the control of the tetracycline resistance gene promoter generating pAngBp and pAngBc, respectively. To analyze the functionality of both AngB domains, we mutated conserved residues in the ICL and ArCP domain by site-directed mutagenesis. In the ICL domain the residue to be mutated was chosen based on an alignment of this domain with several other ICL domains. In the isochorismate lyase PhzD from *Pseudomonas aeruginosa*, an aspartic acid residue in the active site is essential for 2,3-dihydro-3-hydroxyanthranilic acid production from 2-amino-2-deoxyisochorismate (123). The PhzD protein possesses only an ICL domain and it is involved in the biosynthesis of phenazine (123). The same aspartic acid and several surrounding residues are conserved in AngB as well as in the ICL domain of several enzymes involved in DHBA production (Fig. 3.3). This conserved aspartic acid residue was mutated to an alanine in the construct harboring either the *angBp* or the *angBc* gene generating the constructs pAngBpD37A and pAngBcD71A, respectively. In the ArCP domain of AngBp, the residue mutated to an alanine was the conserved serine (S248) that has been shown for the AngBp protein of strain 531A to be essential for the attachment of the phosphopantetheinyl arm (188). Since we have shown that the ArCP domain of AngBc is not functional in anguibactin production, we did not mutate this domain, although it is worthy to notice that a conserved serine (S283) in the chromosomally encoded AngB corresponds to the serine residue 248 of AngBp and to the conserved serine residue of other ArCP domains (Fig. 3.3).

The wild type and mutant constructs were used to complement strain AN192 (an *E. coli entB* mutant) as well as the plasmid terminator mutant 775(pJM1:: Ω) and the double *angB* mutant of *V. anguillarum*.

The *E. coli* strain AN192 can be complemented for DHBA production by both wild type *angB* genes of *V. anguillarum* (Fig. 3.4A). Strain AN192 complemented with pAngBp or pAngBc were demonstrated to produce enterobactin as determined by growth in iron-limiting conditions and by bioassay with the *Salmonella* strains (Fig. 3.4A). Enterobactin production in strain AN192 does not require the ArCP domain of AngB since the mutation in *entB* in this strain affects the functionality of the ICL domain of EntB but not the ArCP domain (156). The ICL D to A mutants in either of the pAngBp or pAngBc constructs were not able to complement strain AN192, clearly showing that the aspartic acid residue is indeed essential for the activity of the ICL domain of both proteins (Fig. 3.4A).

Complementation of both *V. anguillarum* mutants with pAngBp restores anguibactin production while strains containing pAngBc still cannot produce the siderophore; nevertheless both constructs in the double mutant restored DHBA production (Fig. 3.4B). As it was the case in *E. coli*, the ICL mutant constructs could not complement the double *V. anguillarum* mutant for DHBA (Fig. 3.4B). Furthermore, the ArCP mutant in AngBp (pAngBpS248A) could not complement strain 775(pJM1:: Ω) for anguibactin production although it was able to restore DHBA production in strain 775*angBc*::Cm(pJM1:: Ω) (Fig. 3.4B and data not shown). These results further confirm that the ArCP domain of AngBp is the only one that can tether DHBA to be utilized in

anguibactin production while either version of the ICL domain can intervene in DHBA production.

3.3.5. ICL and ArCP domain activities in vitro. To assess the functionality in vitro of the AngBp domains, we overexpressed the wild type and the mutant proteins as C-terminal His-tagged proteins in *E. coli* as described in the Material and Methods section.

To determine ICL activity, we used an L-lactate dehydrogenase-coupled assay in which pyruvate concentration in the reaction mixture was calculated from the amount of NADH oxidized, measured by the decrease of absorbance at 340 nm (140, 154). In the reaction that converts isochorismate to 2,3-dihydro-2,3-dihydroxybenzoic acid catalyzed by ICL domains, pyruvate is produced in equimolar amounts with 2,3-dihydro-2,3-dihydroxybenzoic acid (Fig. 3.5A). As shown in Figure 3.5B, NADH was completely oxidized to NAD^+ in the reaction containing wild type AngBp or the ArCP mutant protein. On the contrary the ICL mutant protein behaved as the no-ICL sample in the oxidation of NADH confirming the results obtained in vivo for this mutant protein (Fig. 3.5B).

Functionality of the ArCP domain was determined by in vitro salicylation with ^{14}C labeled salicylate of the purified proteins (105). Although the wild type AngB protein purified from *E. coli* is obtained partially in its holo form, i.e., with the phosphopantetheine arm already tethered to the ArCP domain (data not shown), holo-ArCP was formed in vitro prior of the salicylation reaction by incubation with the phosphopantetheinyl transferase of *Bacillus subtilis*, Sfp (135) and coenzyme A (CoA). Figure 3.6 shows that the wild type AngBp protein as well as the ICL mutant can be salicylated in vitro to similar extent while the percentage of the ArCP S248A mutant

labeled with [¹⁴C] salicylate is similar to that of the sample in which no adenylation domain (VibE) was added. These results are in agreement with the results obtained for the AngB-S248A mutant in anguibactin production *in vivo*.

3.4. Discussion

The iron uptake system mediated by the plasmid pJM1 is composed of a small molecular weight compound, the 348-Da siderophore anguibactin that is synthesized from DHBA, cysteine and hydroxyhistamine, and a membrane receptor complex specific for ferric-anguibactin. This system is an important virulence factor for the fish pathogen *V. anguillarum* (192).

The sequence of the pJM1 plasmid of strain 775 revealed a gene cluster (*orf39* to *43*) that encodes products that share homology with proteins involved in synthesis and activation of DHBA (47). A similar cluster was identified on the pJM1-like plasmid pJHC1 of strain 531A and it was shown that the *angB* gene (*orf41*) in this cluster is essential for DHBA and anguibactin production in this strain (188). One interesting difference between the two *V. anguillarum* strains 775 and 531A can be assessed by studying their plasmidless derivatives. H775-3, the 775 derivative, is proficient in DHBA production while S531A-1, the 531A derivative, is not. Therefore, an additional copy of the *angB* gene must be present on the chromosome of strain 775. We identified an *orf* with homology to the plasmid-encoded *angB* gene in the chromosomal DNA of *V. anguillarum* 775. Sequencing of this *orf* revealed that it encoded a protein 78% similar and 64% identical to the plasmid-encoded AngB, although 57 amino acids longer. The predicted amino acid sequence of the chromosomal copy includes the ICL and ArCP domains as it is the case for the plasmid copy. Surprisingly, the same sequence was found on the 531A chromosomal DNA but deletion of a base at the 5'-end resulted in a non-functional truncated protein as the truncation occurs in the ICL domain before the conserved residues of the active site.

Furthermore, in this work we also characterized the two *angB* gene copies of 775 and assessed by a combination of knock-out and site-directed mutation and determined that the ArCP domain of the plasmid-encoded copy is essential for anguibactin biosynthesis, while the ICL domain of either the chromosomal copy or the plasmid copy can be used in DHBA production. The two ICL domains can also complement an *E. coli entB* mutant for DHBA production.

Site-directed mutagenesis of the ICL domain of the two AngB proteins of 775 confirmed that the active site of this domain corresponds to the active site of PhzD an isochorismate lyase that is not an enzyme of the DHBA biosynthetic pathway and is not associated with an ArCP domain (123). In vitro experiments with the purified plasmid-encoded AngB protein demonstrated that the site-directed mutant in the ICL domain was affected in the isochorismate lyase activity but its ArCP domain could still be loaded with [¹⁴C]-salicylate as is the case for the wild type protein. The same was true for the ArCP domain mutant (S248A), whose ability to convert isochorismate to 2,3-dihydro-dihydroxybenzoic acid was not altered while the loading of [¹⁴C]-salicylate was completely abolished. Thus the in vitro results confirmed those obtained in vivo in *V. anguillarum* and *E. coli*. Furthermore, the in vitro experiments with the site-directed mutants (D37A and S248A) clearly showed the importance of each residue for the domain function and that each domain operates independently.

The identification of a chromosomal-encoded copy of the *angB* gene leads us to speculate the evolution of the iron-uptake systems of *V. anguillarum* species. The chromosomal-encoded gene lies within a cluster of other genes dedicated to DHBA biosynthesis and activation (7). Therefore, it is possible that the genes in this cluster

were part of a chromosomal encoded iron uptake system that became not essential once the plasmid-encoded cluster was acquired. Serotype O1 strains without a pJM1-like plasmid and serotype O2 strains of *V. anguillarum*, produce a chromosomal-encoded siderophore that contains DHBA (94). The fact that an apparently functional ArCP domain, the chromosomally encoded one, is not able to participate in anguibactin production may also suggest a system specificity of the NRPS domains in which interaction occurs only amongst the proteins of the same system. A recent publication points to the involvement of short N-terminal and C-terminal sequences in protein-protein interactions in the NRPS family (70). Taking in account these recent findings in other systems and the fact that the chromosomal encoded AngB presents amino acid extensions at both ends of the protein when compared with the other homologues including the *V. anguillarum* plasmid copy, the lack of functionality of the AngBc ArCP domain in siderophore production could be explained by an impairment of this protein to interact with the other proteins of the anguibactin system, AngE, AngM, AngN and AngR (7, 45, 47, 190). The system specificity of the anguibactin pathway may not apply to DHBA biosynthesis since the ICL domain activity seems to be independent of the other enzymes and strain background.

3.5. Acknowledgements

This project was supported by Grants from the National Institute of Health, AI19018 and GM64600, to J.H.C. We are grateful to Christopher T. Walsh for his insightful discussions and the VibE and Sfp expression constructs. We also wish to thank Hiroaki Naka for the Cos #2 construct.

Table 3.1. Strains and plasmids used in this study.

Strain and plasmids	Relevant characteristics	Source or reference
<i>Vibrio anguillarum</i>		
775(pJM1)	Wild type; Pacific Ocean prototype	(39)
531A(pJHC1)	Wild type; Atlantic Ocean prototype	(175)
775(pJM1::Ω)	775 carrying pJM1 with Ω transcription-translation terminator at the <i>Bgl</i> I site in <i>angB</i>	This study
775(pJM1::K)	775 carrying pJM1 with a Klenow modification at the <i>Bgl</i> I site in <i>angB</i>	This study
775 <i>angBc</i> ::Cm	775 with the <i>angBc</i> gene replaced by the chloramphenicol resistance cassette gene	This study
775 <i>angBc</i> ::Cm(pJM1::Ω)	775 with the <i>angBc</i> gene replaced by the chloramphenicol resistance cassette gene, carrying pJM1 with Ω transcription-translation terminator at the <i>Bgl</i> I site in <i>angB</i>	This study
775 <i>angBc</i> ::Cm(pJM1::K)	775 with the <i>angBc</i> gene replaced by the chloramphenicol resistance cassette gene, carrying pJM1 with a Klenow modification at the <i>Bgl</i> I site in <i>angB</i>	This study
CC9-16(pJHC9-16)	Anguibactin-deficient, iron transport-proficient	(183)
CC9-8(pJHC9-8)	Anguibactin-deficient, iron transport-deficient	(183)
<i>Escherichia coli</i>		
XL1 Blue	<i>recA1, endA1, gyrA46, thi, hsdR17, supE44, relA, lacF^r [proAB^r, lacP^r, lacZΔM15 Tn10(tet^r)]</i>	Stratagene
HB101	<i>supE44 hsd20 (r^h m^h) recA13 ara-14 proA2 lacY1 galK2 rpsL20 xyl-5 mtl-1</i>	(21)
BLR(DE3)	F ⁻ <i>ompT hsdS^r (r^h m^h) gal dcmΔ(srl-recA)306::Tn10(tet^r)</i> (DE3)	Novagen
AN192	<i>proC14 leu-6 trpE38 thi-1 fhuA23 lacY1 mtl-1 xyl-5 rpsL109 azi-6 tsx-67 entB402</i>	(156)
<i>Salmonella typhimurium</i>		
<i>enb-1</i>	LT2 derivative, enterobactin ⁻ , Sm ^r	(131)
<i>enb-7</i>	LT2 derivative, enterobactin ⁻ , DHBA ⁻ , Sm ^r	(131)
Plasmids		
pJM1	Indigenous plasmid in strain 775	(39)
pJHC1	Indigenous plasmid in strain 531A	(175)
pJHC9-16	pJM1 derivative carrying TAF and transport genes,	(169, 183)
pJHC9-8	pJM1 derivative carrying only the TAF region	(169, 183)
pRK2073	Helper plasmid for conjugation, Tp ^r , Tra ^r	(56)
pCR*2.1-TOPO*	Cloning vector, Ap ^r , Km ^r	Invitrogen
SuperCos 1	Cosmid vector, Ap ^r	Stratagene
pTW-MEV	Suicide vector, R6K ori, <i>sacB</i> , Ap ^r	(188)
pTW99	pBR322 with kanamycin resistance gene from pUC4K cloned in <i>Sal</i> I site	(188)
pBR322	Cloning vector, Tc ^r , Ap ^r	(19)
pKD46	pSC101 ori ^T S, P _{araB} γ β <i>exo</i> , Ap ^r	(41)
pKD3	R6K ori, Cm ^r , Ap ^r	(41)
pQE60	T5 phage promoter expression vector, Ap ^r	Qiagen
pET29b	T7 phage promoter expression vector, Km ^r	Novagen
Cos #2	SuperCos 1 harboring a 15 kb fragment from 775 genomic DNA	H. Naka
pAngBp	<i>angBp</i> gene of plasmid pJM1 cloned by PCR in pTW99	This study
pCR- <i>angBc</i>	1.1 kb PCR fragment from 775 genomic DNA containing the <i>angBc</i> gene cloned in pCR*2.1-TOPO*	This study
pAngBc	<i>Cla</i> I- <i>Bam</i> HI fragment from pCR- <i>angBc</i> cloned in pBR322	This study
pAngBpD37A	pAngBp with mutation D37A in ICL domain	This study
pAngBcD71A	pAngBc with mutation D71A in ICL domain	This study
pAngBpS248A	pAngBp with mutation S248A in ArCP domain	This study
pQEAngBp	<i>angBp</i> cloned as a <i>Nco</i> I- <i>Bgl</i> II fragment in pQE60	This study
pQEAngBpD37A	pQEAngBp with mutation D37A in ICL domain	This study
pQEAngBpS248A	pQEAngBp with mutation S248A in ArCP domain	This study
pEntC	<i>entC</i> cloned in pET29b	This study
pVibE	<i>vibE</i> cloned in pET29b	(80)
pSfp	<i>sfp</i> cloned in pET29b	C. T. Walsh

Figure 3.1. Chromosomal and plasmid-encoded AngB proteins and their domain organization. Panel A. Amino acid sequence alignment of the AngBc and AngBp proteins from 775. The plusses show conserved amino acid substitutions, while the identical residues are shown between the two protein sequences. Panel B. The ICL and ArCP domain organization common to the two AngB proteins of *V. anguillarum* 775 and their function in DHBA and anguibactin production, respectively, are shown. Panel C. Schematic representation of the predicted chromosomal *angB* products from *V. anguillarum* 775 and 531A. The 531A AngB possesses only a truncated ICL domain.

A

```

AngBc: 1 MWRLSTNTSLLFLKSLALRHHHEREKPLLTRITFMAIPKIASYSIPLAETFPKKNKVHWHV 60
                                     MAIPKIASY + E+FP NKV W +
AngBp: 1                                     MAIPKIASYQVLPLESFPTNKVDWVI 26

AngBc: 61 QADRAVLLIHDMQKYFINFFDHSQAPVPELLANISELKSLARQANIPVVYTAQPPNQDPI 120
          ++V+L+HD+Q YF+NFFD + +PVPELL N++++ AR A IPVVYTAQP NQDP
AngBp: 27 DPKKSVVLVHDLQAYFLNFFDKTSLSPVPELLLRNVNKVTESARSAGIPVVYTAQPANQDPN 86

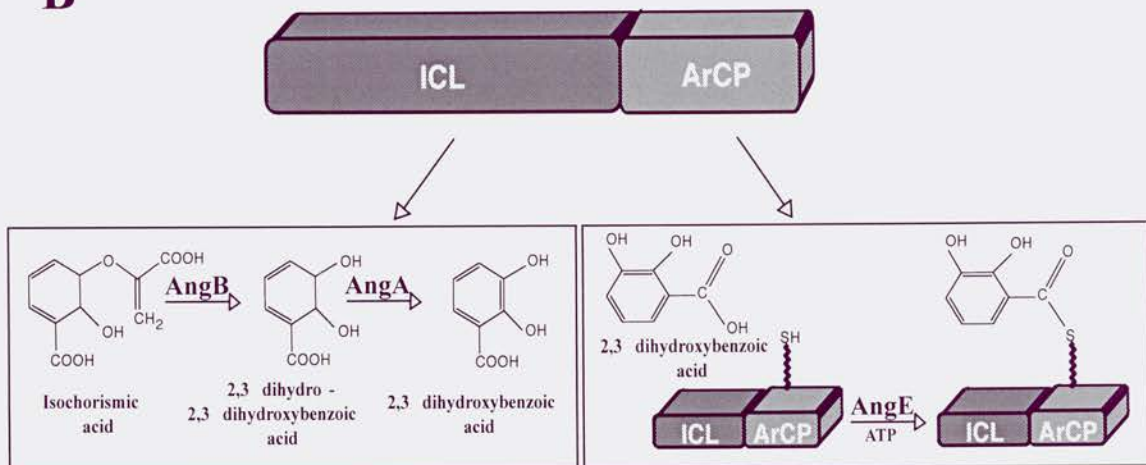
AngBc: 121 ERALLTDFWGTGLTKDTEIVSELSPEGDQIYTKWRYSAPKKTPLLERMKETQRDQLIIV 180
          ERALLTDFWG GLT+DTEIV E+SP+ DIYTKWRYSAPKKTPLLE MKE QRDQL+IV
AngBp: 87 ERALLTDFWGVGLTQDTEIVPEVSPQPEDIQYTKWRYSAPKKTPLLEWMKEEQRDQLVIV 146

AngBc: 181 GVYAHIGILSTALDAFMLDIQPFVVGDAVADFSLEDHHTLKYITERVGCVTSLEALKPQ 240
          GVY HIGILSTALDAFMLDI+PFV+GDA+ADFS EDH +TLKY+ R G V S ++ +
AngBp: 147 GVYGHIGILSTALDAFMLDIKPFVIGDAIADFSKEDHMNTLKYVASRSGSVKSVD----E 202

AngBc: 241 MIHSQETRL---LSLEQMRQQVAELLDLDEVDVDEKLTFLGLDSIRAVTLFESWRKMG 397
          I S TR LSLE MRQ VA +LD+DLDEVDVDE L FLGLDSIR +TL W+K+G
AngBp: 203 FIDSVTTRSFGELSLESMRQDVANILDVLDLDEVDVDENLIFLGLDSIRIMTLHSRWKKG 262

AngBc: 398 IECASFSEMIKYSTLREWWH-VMEPSVVAQSSHQVTDTRSTEEQPV 441
          I+ +EM+ +T+++WW V
AngBp: 263 IDIELAEMVGKNTIKDWWDVSVQVAA 287
    
```

B



C

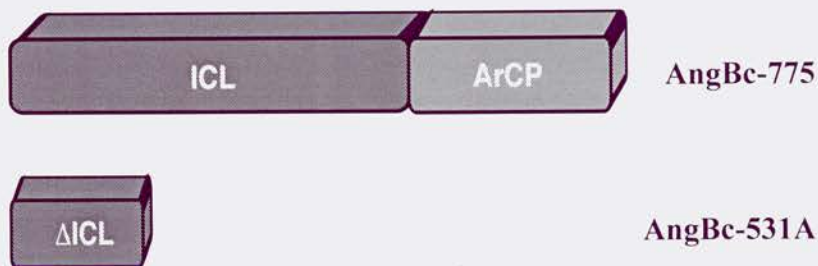


Figure 3.2. DHBA and anguibactin production of mutants of the *V. anguillarum* *angB* genes. Panel A. The *angBp* mutants with their DHBA and anguibactin production phenotypes are shown and compared to the wild type strain. Presence of DHBA in the supernatant of cultures grown in iron-limiting conditions was analyzed by using the Arnow reaction and confirmed by bioassays with *Salmonella* strain *enb-1* and *enb-7*. Anguibactin production by the different strains was detected by CAS agar, bioassays and growth in iron limiting conditions. The results obtained on CAS agar plates are shown where a lighter halo around the colony indicates production of an iron-binding compound by the bacterial cells. Panel B. The *angBp*, *angBc* and the double mutants with their phenotype in DHBA and anguibactin production are shown and compared to the wild type strain. DHBA and anguibactin production was analyzed by the same methods in Panel A. Anguibactin production is shown as the ability of each strain to grow in iron-limiting conditions achieved by supplementing minimal media with 2 μ M EDDA.

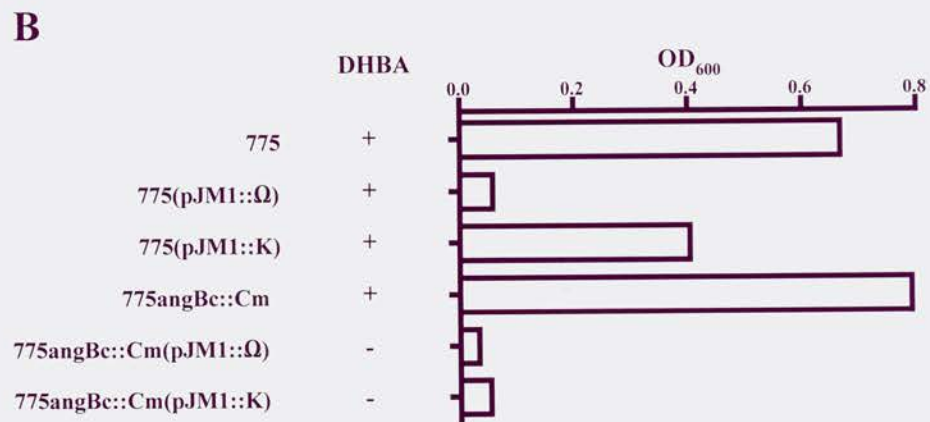
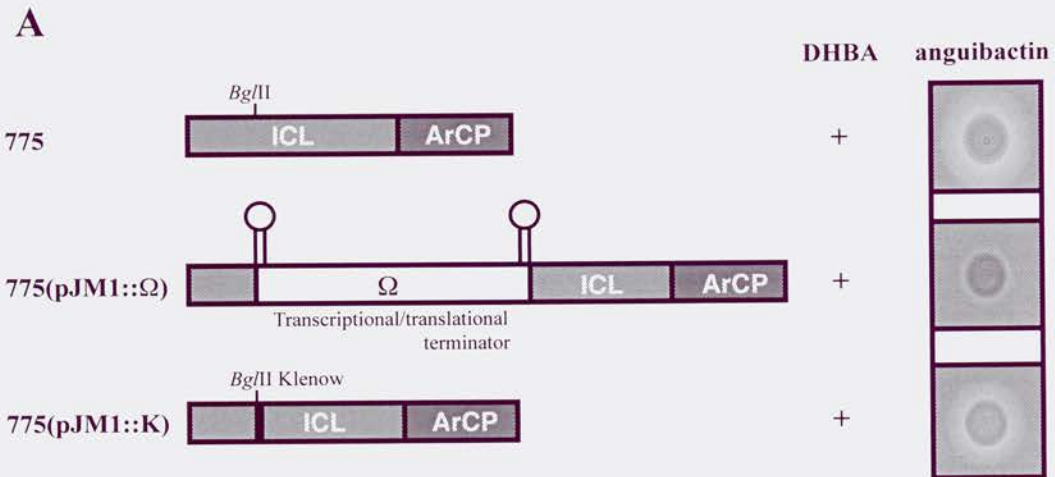


Figure 3.3. Multiple sequence alignment of isochorismate lyase enzymes. All the proteins in this alignment except PhzD participate in DHBA biosynthesis as well as in siderophore biosynthesis. PhzD possesses only the ICL domain and it is involved in the biosynthesis of phenazine. The identical residues are shown shaded in darker grey while the conserved amino acids are shaded in lighter grey. The two conserved residues in the ICL and ArCP domains that were mutated to an alanine in the AngB proteins are boxed and indicated with an asterisk.

```

1      10      20      30      40      50      60      70
AngBp .....MAIPKIASYQVLPLESFPPTNKVDWVIDPKKSVVLVH
AngBc MWRLSTNTSLLFLKSLALRHHHEREKPLLTRITFMAIPKIASYSIPLAETFPKNKVHWHVQADRAVLLIH
VibB .....MAIPKIASYPLPV..SLPTNKVDWRIDASRAVLLIH
EntB .....MAIPKLQAYALPESHDI PQNKVDWAFEPQRAALLIH
PhzD .....MSGIPEITAYPLPTAQQLPANLARWSLEPRRAVLLVH

```

```

80      90      100     110     120     130
AngBp DLQAYFLNFFDKT LSPVPELLRNVNKVTESARSAGIPVVYTAQ PANQDPNERALLTDFWGVGLTQDTE..
AngBc DMQKYFINFFDHSQAPVPELLANISELKSRLARQANIPVVYTAQPNQDPIERALLTDFWGTGLTKDTE..
VibB  DMQEYFVHYFDSQAEPIPSLIKHIQQLKAHAKQAGIPVVYTAQ PANQDPAERALLSDFWGPGLSEETA..
EntB  DMQDYFVSFWGENCPMMEQVIANIAALRDYCKQHNIPVVYTAQ KEQSDERALLNDMWGPGLTRSPEQQ
PhzD  DMQRYFLRPLPESLRA..GLVANAARLRRCVVEQGVQIAYTAQ GMSMTEEQRGLLKDFWGP GMRASPADR
*
```

```

140     150     160     170     180     190     200
AngBp .IVPEVSPQEDIQYTKWRYSAFKKTPLLEWMKKEQRDQLVIVGVYGHIGILSTALDAFMLDIKPFVIGD
AngBc .IVSELSPEDGDIQYTKWRYSAFKKTPLLERMKETORDQLIIVGVYAHIGILSTALDAFMLDIQPFVVG
VibB  .IIAPLAPESGDVQLTKWRYSAFKKSPLLDWLRRETGRDQLIITGVYAHIGILSTALDAFMFDIOPFVIG
EntB  KVVDRLTPDADDTVLVKWRYSAFHRSPLLEQMLKESGRNQLIITGVYAHIGCMTTATDAFMRDIKPFMVAD
PhzD  EVVEELARGPDDWLLTKWRYSAFHSDLLQRMRAAGRDQLVLCGVYAHVGVLISTVDAYSNDIQPELVAD

```

```

210     220     230     240     250     260     270
AngBp AIADFSKEDHMNTLKYVASRSGSVKSVDEFIDS.VTTR..SFGELSLESMRQDVANILDVDLDEVVDEN
AngBc AVADFSLEDHHTLKYITERVGCVTSLKALKPQMIHSQ..ETRLLSLEQMRQQVAELLDLDDLDEVVDDEK
VibB  GVADFSLSDEHFSRLYISGRGTGAVKSTQOACLE.IAAQHSKLTGLSLRTMQHDVAALNLSVDEVVDQEN
EntB  ALADFSRDEHLSLKYVAGRSGRVVMTEELLPAPIPAS..KA...AL...REVILPLLD.ESDEPFDDDN
PhzD  AIADFSSEAHHERMALEYAASRCAMVVTTDEVLE.....REVILPLLD.ESDEPFDDDN

```

```

280     290     300     310     320     330     340
AngBp LIFLGLDSIRIMTLHSRWKKIGIDIELAEMVGKNTIKDWWDVSVQVAA.....
AngBc LTFLGLDSIRAVTLFESWRKMGIECAFSEMIKYSTLREWWHVMEPSVVAQSSHQVTDTRSTEEQPV
VibB  LLFLGLDSIRAIQLLEKWKKAQGADISFAQLMEHVTLQQWWTIQANLHQPCSA.....
EntB  LIDYGLDSVRMMALAAARWRKVHGDIDFVMLAKNPTIDAWKLLSREVK.....
PhzD  .....
*
```

Figure 3.4. Complementation of the *entB* mutant of *E. coli* and the *angB* mutants of *V. anguillarum* 775. Panel A. Complementation of the *E. coli entB* mutant AN92 with the wild type and mutant constructs of the two *angB* genes of *V. anguillarum*. The ability to produce DHBA and enterobactin of each strain is measured as the ability to grow in iron-limiting conditions and by bioassay with the *Salmonella* strains *enb1* and *enb7*. Panel B. The phenotypes in DHBA and anguibactin production of the complemented *angB* mutants are shown and compared to the wild type strain. DHBA production was measured by the Arnow test on supernatant of cultures grown in iron-limiting conditions. Growth in iron-limiting conditions (minimal media supplemented with 2 μ M EDDA) is used to determine the ability of each strain to produce anguibactin.

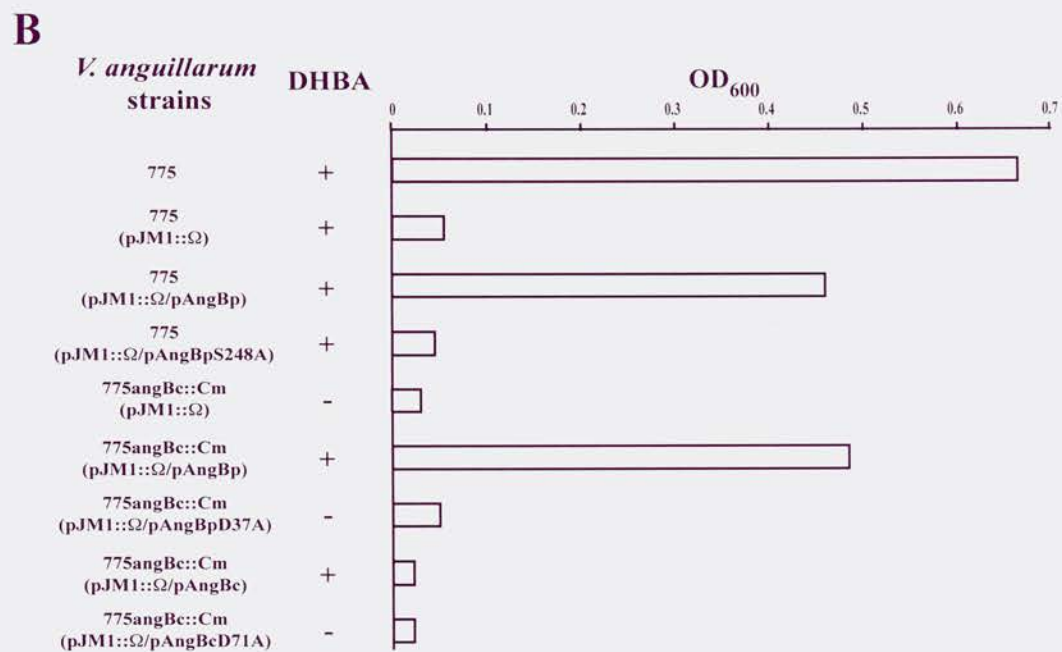
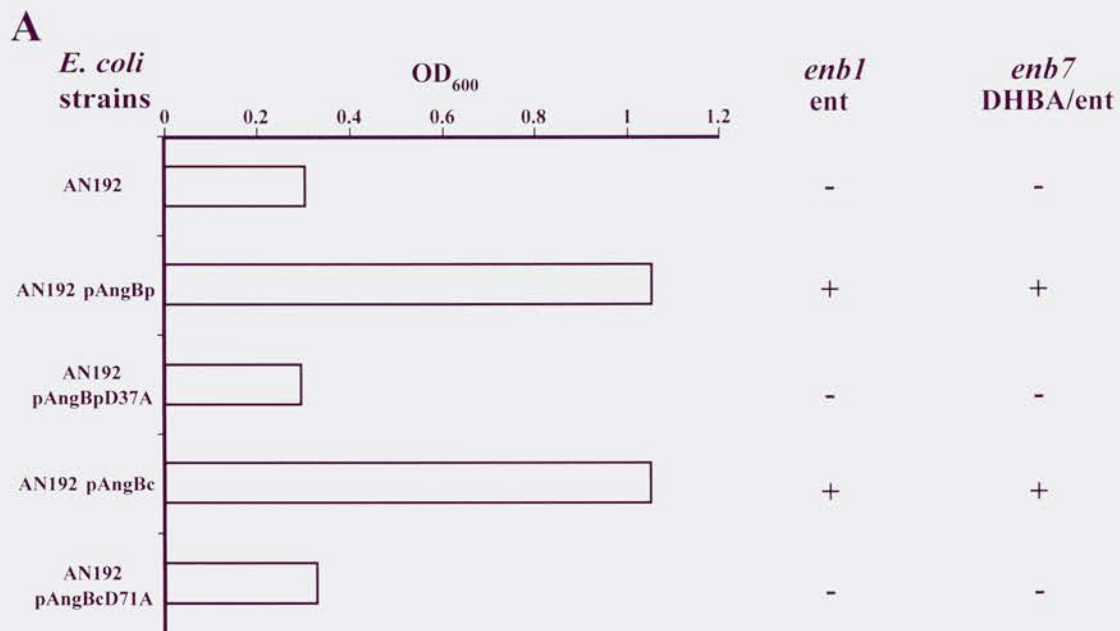


Figure 3.5. In vitro ICL reaction with purified wild type and mutant AngBp

proteins. Panel A. Scheme of the in vitro ICL reaction. Isochorismic acid, the substrate for AngB is obtained from chorismic acid by addition of purified EntC protein.

Production of pyruvate from isochorismic acid is measured as the oxidation of NADH by L-lactate dehydrogenase in the reaction mix. Panel B. Production of pyruvate expressed as nanomoles is plotted over time for each AngB protein. Each point is calculated as the mean of three independent experiments in which the same amount of proteins and substrate were used. The error bars indicate the standard error of the mean (SEM) of the results from replicate samples.

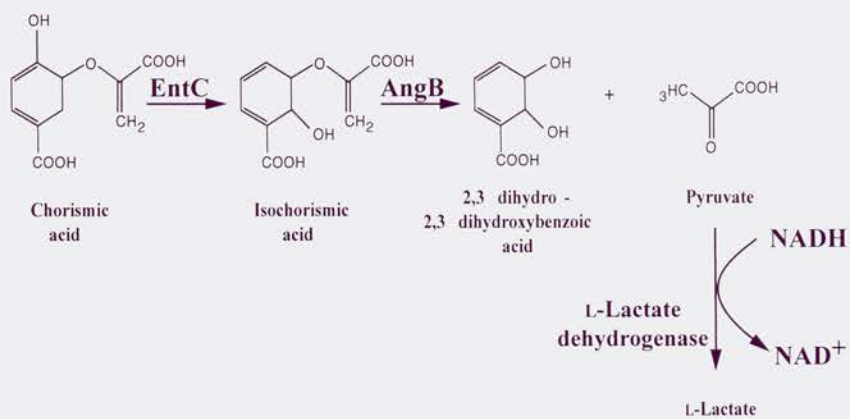
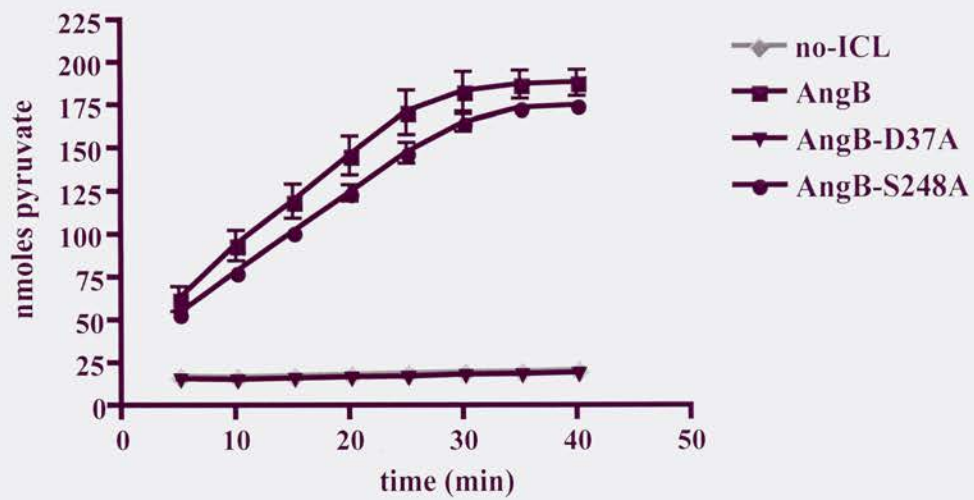
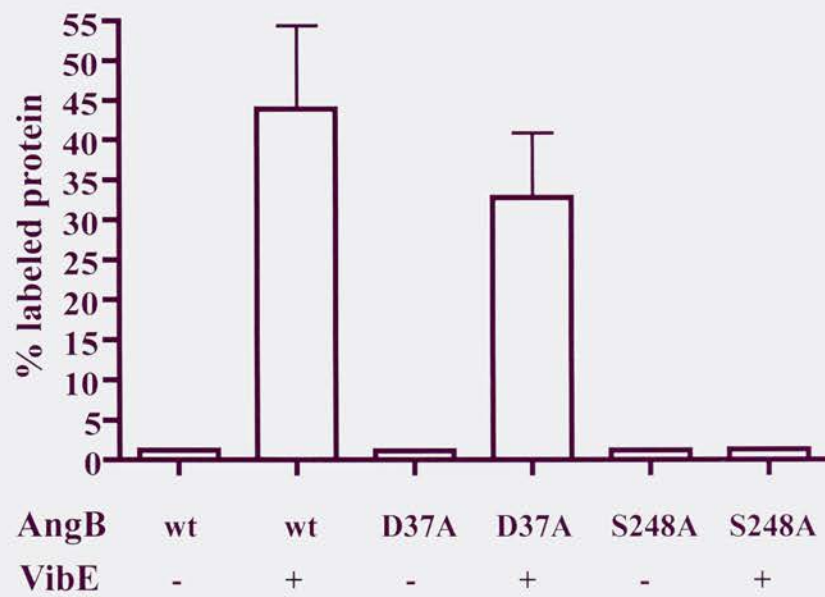
A**B**

Figure 3.6. In vitro salicylation reaction with purified wild type and mutant AngBp proteins. The percentage of ArCP domain labeled with [¹⁴C]-salicylate is shown with each bar calculated from the mean of three independent experiments in which the same amount of proteins and substrate were used. As controls each AngB protein was incubated without the adenylating enzyme VibE. The means for the wild type and the D37A mutant AngBp proteins are not significantly different when compared by the t test at $P \leq 0.05$ ($P = 0.45$). The error bars indicate the standard error of the mean of the results from replicate samples. wt, wild type AngBp; D37A, D37A mutant of AngBp; S248A, S248A mutant of AngBp.



CHAPTER 4

**A nonribosomal peptide synthetase with a novel domain
organization is essential for siderophore biosynthesis
in *Vibrio anguillarum* strain**

Manuela Di Lorenzo, Sophie W. Poppelaars, Michiel Stork, Maho Nagasawa,

Marcelo E. Tolmasky, and Jorge H. Crosa

Journal of Bacteriology 186 (21): 7327-7336, 2004

4.0. Abstract

Anguibactin, a siderophore produced by *Vibrio anguillarum*, is synthesized via a nonribosomal peptide synthetase (NRPS) mechanism. We have identified a gene from the *V. anguillarum* plasmid pJM1 that encodes a 78-kDa NRPS protein termed AngM, which is essential in the biosynthesis of anguibactin. The predicted AngM amino acid sequence shows regions of homology to the consensus sequence for the peptidyl carrier protein (PCP) and the condensation (C) domains of NRPSs, and curiously, these two domains are not associated with an adenylation (A) domain. Substitution by alanine of the serine 215 in the PCP domain and of histidine 406 in the C domain of AngM results in an anguibactin-deficient phenotype, underscoring the importance of these two domains in the function of this protein. The mutations in *angM* that affected anguibactin production also resulted in a dramatic attenuation of the virulence of *V. anguillarum* 775, highlighting the importance of this gene in the establishment of a septicemic infection in the vertebrate host. Transcription of the *angM* gene is initiated at an upstream transposase gene promoter that is repressed by the Fur protein in the presence of iron. Analysis of the sequence at this promoter showed that it overlaps the iron transport-biosynthesis promoter and operates in the opposite direction.

4.1. Introduction

Iron is an essential element for nearly all microorganisms, and bacteria have evolved systems, such as siderophores, to scavenge ferric iron from the environment and in particular from the iron-binding proteins of their hosts (23, 24, 136). Siderophores are low-molecular-weight iron chelators (36, 67, 136), and the systems include the biosynthetic machinery to assemble the siderophores and the specific membrane receptors and transport protein complexes that recognize the ferric siderophore (23, 54). These systems are tightly regulated in their expression by the concentration of free iron in the environment. Thus, once synthesized under conditions of iron limitation, secreted siderophores act as extracellular solubilizing agents for organic compounds or minerals.

Vibrio anguillarum is the causative agent of vibriosis (4), a terminal hemorrhagic septicemia in salmonid fishes, and many isolates of this bacterium possess a plasmid-mediated iron uptake system that has been shown to be essential for virulence (37, 192). Our laboratory has recently reported the complete sequence of the 65-kb virulence plasmid pJM1 of *V. anguillarum* strain 775 (37). This plasmid harbors most of the genes encoding the proteins for the biosynthesis of the 348-Da siderophore anguibactin as well as those involved in recognition of the ferric-anguibactin complex and transport of iron into the cell cytosol (3, 6, 47, 169). Anguibactin belongs to a unique structural class of siderophores that possess both a catechol and a hydroxamate group, and it has been characterized as a ω -*N*-hydroxy- ω -*N*[(2'-[2'',3''-dihydroxyphenyl]thiazolin-4'-yl)carboxyl]histamine by crystal X-ray diffraction studies and chemical analysis (2, 77). We predict that anguibactin is synthesized from 2,3-dihydroxybenzoic acid, cysteine, and histamine. Indeed, recent investigations demonstrated that both 2,3-

dihydroxybenzoic acid and histamine are required for the biosynthesis of this siderophore (29, 170, 188).

Proteins belonging to the nonribosomal peptide synthetase (NRPS) family are a hallmark in the biosynthesis of peptide siderophores (40, 52, 106, 110). NRPSs synthesize peptide siderophores or antibiotics in the absence of an RNA template via a multistep process (83, 115, 177). Diverse peptide structures are derived from a limited number of catalytic domains of NRPSs. Sets of catalytic domains constitute a functional module containing the information needed to complete an elongation step in peptide biosynthesis. Each module combines the catalytic functions for activation by ATP hydrolysis of a substrate amino acid, for transfer of the corresponding adenylate to the enzyme-bound 4'-phosphopantetheinyl cofactor, and for peptide bond formation. A classic module thus consists of an adenylation (A) domain, a peptidyl carrier protein (PCP) domain, and a condensation (C) domain, with additional domains that could lead to modification of the substrates if required in the synthesis of the peptide (103, 159, 178). In *V. anguillarum*, we have already characterized two of the anguibactin biosynthetic proteins, AngR and AngB, as NRPSs (188, 190).

A mutant was isolated from a transposon insertion collection that did not produce anguibactin. In this work, we characterized the mutated gene, designated *angM*, revealing that it encodes a novel NRPS that harbors only PCP and C domains. Mutagenesis and complementation studies demonstrated that AngM is essential for the biosynthesis of anguibactin and for the virulence of *V. anguillarum* in the fish host.

4.2. Materials and methods

4.2.1. Bacterial strains, plasmids, and growth conditions. The bacterial strains and plasmids used in this study are described in Table 4.1. *V. anguillarum* was cultured at 25°C in either Trypticase soy broth or agar supplemented with 1% NaCl (TSBS and TSAS, respectively). For experiments determining iron uptake characteristics, the strains were first grown on TSAS supplemented with the appropriate antibiotics and passaged to M9 minimal medium (144) supplemented with 0.2% Casamino Acids, 5% NaCl, appropriate antibiotics, and either various concentrations of ethylenediamine-di-(*o*-hydroxyphenyl acetic acid) (EDDA) for iron-limiting condition or 2 µg of ferric ammonium citrate per ml for iron-rich conditions. The antibiotic concentrations used for *V. anguillarum* were ampicillin at 1 mg/ml, tetracycline at 5 µg/ml, rifampin at 100 µg/ml, chloramphenicol at 10 to 15 µg/ml, and gentamycin at 10 µg/ml.

Escherichia coli strains were grown in Luria-Bertani (LB) medium in the presence of the appropriate antibiotics. The antibiotic concentrations used for *E. coli* were ampicillin at 100 µg/ml, tetracycline at 10 µg/ml, chloramphenicol at 30 µg/ml, gentamycin at 10 µg/ml, and trimethopim at 10 µg/ml.

4.2.2. General methods. Plasmid DNA was prepared with the alkaline lysis method (17). Sequence-quality plasmid DNA was generated with the Qiaprep Spin miniprep kit (Qiagen) and Wizard Plus SV minipreps (Promega). Restriction endonuclease digestion of DNA was performed under the conditions recommended by the supplier (Invitrogen, Roche, and New England Biolabs). Transformations in *E. coli* strains HB101 and XL1 Blue and other cloning strategies were performed according to standard protocols (144). DNA sequencing reactions were carried by the OHSU-MMI Research Core Facility

(<http://www.ohsu.edu/core>) with an Applied Biosystems Inc. model 377 automated fluorescence sequencer. Manual sequencing was performed by the dideoxy chain termination method with the Sequenase version 2.0 DNA sequencing kit (U.S. Biochemicals) with appropriate primers. Sequencing primers were designed with Oligo 6.8 primer analysis software and purchased from the OHSU-MMI Research Core Facility (<http://www.ohsu.edu/core>) and Invitrogen. DNA and protein sequence analyses were carried out at the NCBI with the BLAST network service and also with the Sequence Analysis Software Package of the University of Wisconsin Genetics Computer Group (GCG). The GCG programs Pileup and Bestfit were used for comparisons of amino acid sequences.

4.2.3. Construction of the complementing clone. A 2.5-kb fragment containing the *angM* gene was amplified by PCR with the AngM-F (5'-TAACGGAGTGGAAATCT GAGTC-3') and AngM-*Nhe*IR (5'-GACTCAATGCCACATGCAACT GTAC-3') primers and pJM1 as a template. Reactions consisted of 4 min at 94°C, followed by 30 cycles of 30 s at 94°C, 30 s at 60°C, and 3 min at 72°C, followed by a single cycle at 72°C for 7 min. The PCR product was cloned in the pCR-BluntII-TOPO vector with the Zero Blunt TOPO PCR cloning kit (Invitrogen), resulting in plasmid pMDL4. A *Bst*EII (blunt)-*Nhe*I fragment from pMDL4 was subcloned into the *Cla*I (blunt) and *Nhe*I sites of pBR325-M200 to generate plasmid pMDL21 carrying the *angM* gene. After recloning in pBR325-M200, the entire *angM* gene was sequenced to verify that no mutation was generated in the *angM* gene during amplification or cloning. The pBR325-M200 cloning vector was derived from pBR325 by digestion with *Pst*I, blunting of the ends with T4 DNA polymerase (Gibco), and religation, resulting in inactivation of the ampicillin

resistance gene.

4.2.4. Site-directed mutagenesis. Plasmids pMDL4-S215A and pMDL4-H406A were generated with the Quickchange site-directed mutagenesis kit (Stratagene). The template used in this experiment was pMDL4, which contains the *angM* gene. Primers S215A-F (5'-GATTCTTGTGCTAATAACGCGTGACCACCCATTTC-3') and S215A-R (5'-GAAATGGGTGGTCACGCGTTATTAGCAACAA GAATC-3') were used for the mutation in the PCP domain, and primers H406A-F (5'-AGTTTTATCTTTCCTAATCC ATGCAATGATTATTGATGAATG-3') and H406A-R (5'-CATTCATCAATAATCAT GCATGGATTAGGAAAGATAAAACT-3') were used for the mutation in the C domain. The whole procedure was performed according to the manufacturer's recommendations, with 16 cycles that consisted of 30 s at 95°C, followed by 1 min at 55°C and 12 min at 68°C. For the amplification, *Pfu* polymerase was used, and after the PCR, the mixture was treated with *DpnI* to cleave the parental DNA. Then 1 l of the mixture was transformed into the XL1 Blue chemically competent cells provided with the Quickchange kit. Site-specific mutations were confirmed by DNA sequencing with the appropriate primers. Once mutated, a *BstEII* (blunt)-*NheI* fragment from each derivative was subcloned into the *ClaI* (blunt) and *NheI* sites of pBR325-M200 to generate plasmids carrying *angM* derivatives with mutations in the PCP and C domain listed in Table 4.1. After recloning in pBR325-M200, the entire *angM* mutant genes were sequenced to verify that no other region of *angM* was affected during mutagenesis or cloning.

4.2.5. Construction of promoter fusions in pKK232-8. The 1.9-kb *EcoRI* fragment from pJM1 harboring the transposase (*tnpA1*) gene of the ISV-A1 sequence and the beginning of the *angM* gene was cloned in the *EcoRI* site of pBluescript SK, generating

plasmid pECO13. Plasmid pECO13 was used to generate nested deletions, and the full-length *EcoRI* fragment as well as each deletion were subcloned from pECO13 and derivatives by *Bam*HI-*Hind*III digestion and ligation in the corresponding sites in pKK232-8. Each construct in pKK232-8 was sequenced to verify the sequence of the insertion.

4.2.6. Construction of *V. anguillarum* strains by conjugation and allelic exchange.

Plasmids were transferred from *E. coli* to *V. anguillarum* by triparental conjugation as previously described (169).

To generate strain 775(pJM1::63), plasmid pJHC-T7::63 was transferred to *V. anguillarum* 775 by conjugation. In a second conjugation, plasmid pPH1JI, whose origin of replication is incompatible with the replicon of pJHC-T7::63, was transferred to the strain obtained from the first conjugation. By plating in the presence of gentamycin (the resistance marker of pPH1JI) and ampicillin (the resistance gene harbored by Tn3::HoHo1), it was possible to select cells in which the *angM* gene with the Tn3::HoHo1 insertion had replaced the wild-type gene on plasmid pJM1. The loss of pJHC-T7 was confirmed by Southern blot hybridization with the pVK102 vector sequence for probing (data not shown).

4.2.7. Growth in iron-limiting conditions and detection of anguibactin.

For mutant and wild-type strains, we determined the MIC of EDDA with liquid cultures at increasing concentrations of EDDA (1, 2, 5, and 10 μ M) in M9 minimal medium at 25°C. From these analyses, we chose a concentration of 2 μ M EDDA to assay for the ability of all the strains to grow in iron-limited conditions.

The siderophore anguibactin was detected by the chrome azurol S (CAS) assay

and by bioassays with strains CC9-16 and CC9-8 as previously described (188, 190).

4.2.8. Fish infectivity assays. Virulence tests were carried out on juvenile rainbow trout (*Oncorhynchus mykiss*) weighing ca. 2.5 to 3 g which were anesthetized with tricaine methane sulfonate (0.1 g/liter). A total of 50 anesthetized fish were inoculated intraperitoneally with 0.05 ml of each bacterial dilution, i.e., 50 fish per bacterial dilution. The dilutions were prepared with saline solution from 16-h cultures grown at 25°C in TSBS containing antibiotics for selection of the plasmids harbored by the strains. The dilutions were prepared to test a range of cell concentrations from 10^2 to 10^8 cells/ml per strain. Therefore, 350 fish were tested per strain. After bacterial challenge, test fish were maintained in fresh water at 13°C for 1 month, and mortality was checked daily. Virulence was quantified as the 50% lethal dose (LD_{50}) (mean lethal dose; the number of microorganisms that will kill 50% of the animals tested) as determined by the method of Reed and Muench (138).

4.2.9. CAT assay. *V. anguillarum* strains were cultured into either minimal medium supplemented with 0.5 μ M EDDA (iron-limiting conditions) or minimal medium supplemented with 2 μ g of ferric ammonium citrate (iron-rich conditions) per ml with the appropriate antibiotics and grown to an optical density of 0.3 to 0.5 at 600 nm (OD_{600}). A commercial chloramphenicol acetyltransferase (CAT) enzyme-linked immunosorbent assay kit (Roche) was used, and 1-ml samples of total proteins were prepared from each culture following the supplier's instructions. All samples were normalized for total protein levels prior to assay. All assays were repeated at least three times.

4.2.10. RNA isolation. A 1:100 inoculum from an overnight culture was grown in minimal medium with appropriate antibiotics. Cultures were grown with 2 μ g of ferric

ammonium citrate (iron-rich) per ml or with EDDA (iron-limiting) added to achieve similar levels of iron-limiting stress for each strain tested (see the figure legends). Total RNA was prepared when the culture reached an OD₆₀₀ of 0.3 to 0.5 with the RNAwiz (Ambion) isolation kit, following the manufacturer's recommendation.

4.2.11. Primer extension. The primer extension experiment was carried out with the synthetic primer PEX-*tnp* (5'-CATCTATGGCTGAATCATCTATCC-3'), which is complementary to the 5'-end region of the *tnpA1* gene. The primer was end labeled with T4 polynucleotide kinase (Life Technologies, Inc.) in the presence of [γ -³²P]ATP and annealed to *V. anguillarum* 775 total RNA (50 μ g). Reverse transcription from the primer with avian myeloblastosis virus reverse transcriptase (Promega) and electrophoresis on a urea-polyacrylamide (6%) gel were carried out as previously described (26). Manual sequencing was performed by the dideoxy chain termination method with the Sequenase version 2.0 DNA sequencing kit (U.S. Biochemicals), plasmid pSC25 as the template, and primer Seq1762 (5'-GTGTA CTATTGGT GCGAGC-3').

4.2.12. RNase protection assays. Labeled riboprobes were generated by in vitro transcription of 1 μ g of the linearized DNA with T7 or T3 RNA polymerase (Maxiscript by Ambion) in the presence of [α -³²P]UTP with pMN5 (linearized with *Xho*I) as a template for *angM* and QSH6 (linearized with *Rsa*I) as a template for *aroC*. The probes were gel purified on a 6% polyacrylamide gel. For each probe, the amount corresponding to 4 x 10⁵ cpm was mixed with each RNA sample (20 μ g). RNase protection assays were performed with the RPA III (Ambion) kit following the supplier's instructions. The *aroC* riboprobe was used in each reaction as an internal control for the amount and quality of

RNA.

4.3. Results

4.3.1. Sequencing and analysis of a transposon insertion in the *angM* gene. A

collection of biosynthetic and transport mutants were generated by insertional mutagenesis with transposon Tn3::HoHo1 in the recombinant clone pJHC-T7 (169), which contains a stretch of DNA from plasmid pJM1 with iron uptake genes involved in anguibactin biosynthesis and transport. We sequenced one of these transposon mutants, pJHC-T7::63, that is deficient in anguibactin production and found that the site of Tn3::HoHo1 insertion is within the 2,145-bp open reading frame (ORF) that we named *angM*. The insertion occurred 438 bp from the 3'-end of *angM*, which is predicted to encode a polypeptide of 715 amino acid residues, with a calculated molecular mass of about 78 kDa (GenBank accession number AAA81775) (47).

Homology searches of the DNA and the protein databases with the BLAST search engine (8) produced significant matches with other polypeptides involved in the biosynthesis of siderophores, such as VibF of *Vibrio cholerae*, PhbH of *Photobacterium luminescens*, and DhbF of *Bacillus subtilis*. As shown in Figure 4.1A, AngM shows 58% similarity and 39% identity with a stretch of 209 amino acids within the sequence of the *V. cholerae* six-domain NRPS VibF, which is required for vibriobactin biosynthesis (25). The AngM protein sequence possesses domains highly homologous to the PCP and C domains of NRPSs. However, no sequence corresponding to the A domain, which is usually found adjacent to the PCP domain, was identified in AngM (Fig. 4.1B). The PCP and C domains in AngM are located at positions 196 to 248 and 279 to 569, respectively.

4.3.2. Construction of an *angM* mutant in plasmid pJM1 and complementation with the cloned *angM* gene.

To discard any possible effect of the copy number of the

recombinant clone pJHC-T7 (8 to 10 copies per cells) originally used to generate mutant 63, the 63 insertion mutant was integrated by allelic exchange onto the *angM* gene on plasmid pJM1, resulting in *V. anguillarum* 775(pJM1::63). The site of Tn3::HoHo1 insertion in pJM1::63 was confirmed to correspond to the same site of insertion in pJHC-T7::63 by sequencing. Strain 775(pJM1::63), harboring the insertion in the *angM* gene on plasmid pJM1, was tested for its ability to grow in iron-limiting conditions. The results shown in Figure 4.2 demonstrated that this strain was indeed impaired in its growth under iron-limiting conditions, behaving like the plasmidless strain derivative of *V. anguillarum* 775, H775-3 (37).

For complementation analyses, expression of the *angM* gene was placed under the control of the tetracycline resistance gene promoter of the pBR325 vector by cloning a PCR product encompassing the complete *angM* gene as a *Bst*EII (blunt)-*Nhe*I fragment in the *Cla*I (blunt) and *Nhe*I restriction sites in pBR325-M200 to generate plasmid pMDL21. Plasmid pMDL21 was introduced by triparental mating into *V. anguillarum* 775(pJM1::63), and growth of the mutant strain and its complemented derivative was determined in the presence of the iron chelator EDDA at a concentration of 2 μ M with the wild-type strain harboring pJM1 and the empty vector (pBR325) as a positive control.

Figure 4.2 shows that the mutant strain, *V. anguillarum* 775(pJM1::63/pR325-M200), did not grow at this EDDA concentration, while the complemented strain, 775(pJM1::63/pMDL21), grew to wild-type levels under these conditions. Therefore, the presence of an intact *angM* gene is required for growth under iron-limiting conditions. Consistent with the results of the growth experiment, the mutant strain did not produce anguibactin, as determined by CAS plate assays (Fig. 4.2) and bioassays (data not

shown), while complementation resulted in a level of anguibactin that was comparable to that of the wild-type strain (Fig. 4.2).

It is clear that the ability conferred by *angM* on *V. anguillarum* to grow under iron-limiting conditions is due to an essential role in anguibactin biosynthesis.

4.3.3. PCP and C domains of AngM are essential for anguibactin biosynthesis.

During siderophore biosynthesis, the PCP domains of NRPSs undergo covalent phosphopantetheinylation prior to attachment of the assembling siderophore.

Phosphopantetheinylation occurs at a specific serine residue within the highly conserved motif (DxFFxLGGDSL) of this domain (147, 157, 186). A homologous motif including the specific serine residue (DDFFEMGGHSL) is present in the PCP domain of AngM.

Therefore, we decided to replace the serine residue with an alanine to assess its influence on anguibactin production. By site-directed mutagenesis, a serine-to-alanine (S215A) mutation was generated in *angM*, resulting in plasmid pMDL21-S215A. This plasmid was conjugated into the 775(pJM1::63) strain. Figure 4.2 shows that the S215A mutation in plasmid pMDL21-S215A completely abolished the ability of this construct to complement insertion mutant 63, as determined by growth ability and CAS plate assays.

The highly conserved motif (HHxxxDGWS) of the C domain of NRPSs possesses two histidine residues, of which the second one has been shown to be essential to catalyze peptide bond formation (16). The C domain of AngM possesses this conserved motif (HHMIIDEWS). Therefore, to determine whether the second histidine residue also played an important role in anguibactin biosynthesis, we mutated it to an alanine (H406A) by site-directed mutagenesis. The mutant *angM* gene in pMDL21-H406A was then tested for its ability to complement the *angM* null mutant *V. anguillarum*

775(pJM1::63). As was the case for the site-directed mutation in the PCP domain, this mutation also affected the ability to complement insertion mutant 63 for anguibactin production and growth in iron-limiting conditions (Fig. 4.2). Analysis, by western blot with an AngM polyclonal antibody, of the proteins synthesized by *V. anguillarum* 775(pJM1::63) harboring the clones containing the wild-type *angM*, the PCP domain S215A mutant, and the C domain H406A mutant identified a 78-kDa protein in all three strains, suggesting that the mutations did not affect the integrity of the AngM protein (data not shown).

4.3.4. Effect of *angM* mutations on the virulence phenotype of *V. anguillarum* 775.

Since *angM* mutations affected anguibactin production and growth under iron limitation, we predicted that they would also affect virulence. To determine whether expression of AngM is correlated with the virulence phenotype of *V. anguillarum* in the fish model of infection (37, 39), we carried out experimental infections of rainbow trout with the 775(pJM1::63) mutant and this mutant complemented by either pMDL21, pMDL21-S215A, or pMDL21-H406A. The results in Table 4.2 show that mutant 63, the AngM PCP domain mutant, and the AngM C domain mutant were all attenuated in virulence compared to the wild type. The LD₅₀s for these mutants are of the same order of magnitude as the LD₅₀ obtained with the plasmidless strain H775-3 (Table 4.2). Plasmid pMDL21 carrying the wild-type *angM* gene could complement the transposition mutant, resulting in an LD₅₀ of the same order of magnitude as that of the *V. anguillarum* strain carrying pJM1.

4.3.5. Transcription and regulation of the *angM* gene. To determine the location of the promoter for the *angM* gene, we constructed several transcriptional fusions with the

chloramphenicol acetyltransferase (*cat*) gene. The *Eco*RI fragment from plasmid pECO13 as well as various deletions (Fig. 4.3) of this fragment were cloned upstream of the promoterless *cat* gene of pKK232-8. Each construct was transferred by conjugation into the plasmidless derivative H775-3, and the amount of CAT protein produced by each construct in *V. anguillarum* was measured in iron-rich and iron-limiting conditions. The results in Figure 4.3 indicate that one main iron-regulated promoter is located upstream of the transposase (*tnpA1*) gene of the ISV-A1 element (173). Other very weak promoters, as assessed by the level of CAT enzyme, could be identified in a region between the *Aat*II restriction endonuclease site within *tnpA1* and the beginning of *angM*, but these weak promoters do not seem to be iron regulated (Fig. 4.3).

To determine the transcription start site of the *tnpA1-angM* mRNA, we performed a primer extension experiment with a primer (PEX-*tnp*) complementary to the beginning of *tnpA1*. The results showed three iron-regulated primer extension products (Fig. 4.4, P1, P2, and P3) initiated within a 121-bp region upstream of *tnpA1*, confirming the existence of an iron-regulated promoter for the *tnpA1-angM* operon. In a primer extension analysis carried out with a primer complementary to the 5'-end of the *angM* gene, numerous primer extension products could be identified (data not shown). These products could originate from processing of the larger mRNA encoding the *tnpA1* and the genes transcribed from the transposase promoter, or they could be the result of initiation of transcription from the putative weak promoters identified in the transcriptional fusion experiments. As shown in Figure 4.5, analysis of the sequence upstream of *tnpA1* and of the P1 primer extension product revealed -10 and -35 sequences adjacent to the iron transport-biosynthesis operon promoter (pITBO) but in the opposite orientation (26).

From the primer extension and *cat* fusion experiments, it was obvious that the transcription of *angM* is negatively regulated by iron at the transposase promoter. To confirm that iron regulates the expression of *angM*, we performed RNase protection assays with total RNA obtained from *V. anguillarum* 775 cultures grown under iron-rich and iron-limiting conditions. To quantify the amount of *angM*-specific mRNA, we used an internal fragment of the *angM* gene as a probe. An *aroC*-specific riboprobe was included in each reaction to provide an internal control for the quality of the RNA and the amount of RNA loaded onto the gel, since the *aroC* housekeeping gene is expressed independently of the iron concentration of the cell (29). The results shown in Figure 4.6, lanes 1 and 2, demonstrated that *angM* gene transcription is indeed dramatically reduced under iron-rich conditions.

To determine whether iron repression of *angM* gene expression is mediated by Fur, we also performed an RNase protection assay with a *V. anguillarum* 775 strain (775MET11) that has a null mutation in the *fur* gene (189). Inspection of Figure 4.6, lanes 3 and 4, indicates that the *angM* gene is constitutively expressed in the Fur-deficient strain under both iron-rich and iron-limiting conditions, although the level of transcription appears to be reduced compared to the wild type under iron limiting conditions (Fig. 4.6, lane 2). As shown in Figure 4.5, the *tnpA1-angM* operon promoter is located within the already identified Fur binding sites that regulate expression of the pITBO (26); therefore, Fur regulates the expression of these two divergent promoters by binding to common sequences.

4.4. Discussion

The iron uptake system mediated by plasmid pJM1 is an important virulence factor for the fish pathogen *V. anguillarum* (37). This system is composed of anguibactin, a 348-Da siderophore, and a membrane receptor complex specific for ferric anguibactin (6, 88). Besides the genes encoding the transport proteins, many genes on the virulence plasmid are part of a biosynthetic circuit in which NRPSs and tailoring enzymes result in the production of anguibactin (47).

In this work we characterized one of these essential genes, *angM*. Knockout of this gene dramatically affected anguibactin production and also resulted in a very significant decrease in virulence. The amino acid sequence deduced from the nucleotide sequence of *angM* revealed a 78-kDa polypeptide harboring the PCP and C domains of NRPSs. Curiously, the A domain that is usually associated with these two domains in other NRPSs (80, 82, 103, 106, 134, 139, 158) was not identified in this protein. The amino-terminal end of the AngM protein shows no similarity with any of the domains of NRPSs or any ATP-binding domain of any protein family (32, 68, 120). Although the possibility that AngM contains an atypical adenylation domain at its amino terminus cannot be discarded, the lack of any homology of the first 162 amino acids with motifs found in proteins that bind ATP strongly suggests otherwise.

Site-directed mutagenesis of S215 in the PCP domain and of H406 in the C domain of AngM resulted in an anguibactin deficient phenotype, underscoring the importance of these two domains in the function of this protein. It is of interest that although the LD₅₀ for mutant 63, the AngM PCP domain mutant, and the AngM C domain mutant were all of the same order of magnitude as the LD₅₀ obtained with the

plasmidless derivative H775-3, the attenuation in virulence resulting from lack of a functional AngM was about half that obtained with the cured derivative (Table 4.2). This difference in attenuation might be explained by considering that the cured derivative H775-3 does not produce any of the intermediaries that are produced by the *angM* mutants and that these products could participate in the pathogenesis of *V. anguillarum*. One of the products that the plasmidless derivative fails to produce is histamine (11, 170), which could play a role in amplifying the inflammatory response of the fish to the bacterial infection and result in septic shock with a smaller number of infecting bacteria.

Several genes, including *angM*, encoding NRPSs, and tailoring enzymes were identified on plasmid pJM1 (47). It is of interest that one of them, AngR, which plays a role in regulation of the expression of iron transport genes as well as in the production of anguibactin, possesses a cyclization (Cy) domain, an A domain, and a PCP domain (190). However, in this PCP domain, the highly conserved serine present in most PCP domains (147) is replaced by an alanine. The serine residue in PCP domains is necessary for the attachment of a phosphopantetheine group for thioester formation during the process of biosynthesis. Therefore, an attractive possibility is that AngM provides an operational PCP domain, while AngR provides the A domain required to activate a substrate amino acid, possibly cysteine, prior to tethering it on the PCP domain of AngM (Fig. 4.7).

We propose that the C domain of AngM catalyzes the formation of the peptide bond between the dihydroxyphenylthiazolinyl group, which is still tethered to AngM, and the secondary amine group of hydroxyhistamine (Fig. 4.7). As in the case of VibH during vibriobactin biosynthesis (80-82), the C domain of AngM does not interact with two carrier protein domains but rather with only one upstream (the PCP domain of

AngM), while the downstream substrate is the soluble nonprotein-bound hydroxyhistamine. The proposed biosynthetic pathway of anguibactin is shown in Figure 4.7 with the additional enzymes required. The expression of *angM* at the level of transcription was repressed by high iron concentrations, and this negative regulation required the Fur protein. In the Fur-deficient strain, the *angM* gene is constitutively expressed, although at a reduced level. We do not know if this is a peculiarity of *angM* mRNA expression in the Fur mutant strain or is a more general phenomenon. Experiments to identify the mechanism responsible for this reduced expression are being carried out.

The main iron-regulated transcript was initiated at the ISV-A1 transposase promoter (173), suggesting the existence of an operon encoding the transposase and *angM* genes, although minor transcripts could also be initiated in a region between the *tnpA1* and *angM* genes. The fact that *angM* is expressed as part of an iron-regulated operon with the upstream gene encoding a transposase is intriguing because there is no clear reason why a transposase-like protein should be expressed with an NRPS involved in siderophore biosynthesis. This operon could just be the result of a modular acquisition by the plasmid of mobile elements containing genes involved in siderophore biosynthesis as well as genes necessary for transfer of the mobile element.

Analysis of the sequence at the *tnpA1-angM* operon promoter shows that it overlaps the iron transport-biosynthesis operon promoter pITBO and operates in the opposite orientation. Our previous work (26) identified the region on the pITBO sequence where the Fur protein binds and determined that this interaction causes a bending of the DNA in that stretch leading to DNase I-hypersensitive sites on the

complementary strand. The region that Fur binds includes the -35 and -10 sequences of the promoter of the *tnpA1-angM* operon, strongly supporting the idea that Fur binding leads to concerted repression of the two divergent operons.

The possibility that *angM* is part of a mobile genetic element and its role in the virulence of *V. anguillarum* 775 not only underscore the importance of this gene in the establishment of a septicemic infection in the host vertebrate but also suggest possible mechanisms for the epizootic spread of this virulence factor.

4.5. Acknowledgments

This project was supported by grants from the National Institutes of Health, AI19018-19 and GM604000-01, to J.H.C.

Table 4.1. Strains and plasmids used in this study.

Strain or plasmid	Relevant characteristics	Source or reference
<i>Vibrio anguillarum</i>		
775(pJM1)	Wild type	(39)
H775-3	Plasmidless derivative of 775	(39)
775MET11(pJM1)	Fur-deficient mutant of 775(pJM1)	(189)
CC9-16(pJHC9-16)	Anguibactin-deficient, iron transport-proficient	(183)
CC9-8(pJHC9-8)	Anguibactin-deficient, iron transport-deficient	(183)
775(pJM1::#63)	775 carrying pJM1 with Tn3::Ho-Ho1 insertion in <i>angM</i>	This study
<i>Escherichia coli</i>		
XL1 Blue	<i>recA1, endA1, gyrA46, thi, hsdR17, supE44, relA, lacF'</i> [<i>proAB</i> , <i>lacF'</i> , <i>lacZΔM15</i> Tn10 (Tet ^r)]	Stratagene
HB101	<i>supE44 hsd20 (r^H m^H) recA13 ara-14 proA2 lacY1 galK2 rpsL20 xyl-5 mtl-1</i>	(21)
Plasmids		
pJM1	Indigenous plasmid in strain 775	(39)
pJHC-T7	Recombinant clone carrying a 17.6 kb region of pJM1 cloned in pVK102, Tc ^r	(169)
pJHC-T7#63	pJHC-T7 with a Tn3::Ho-Ho1 insertion in <i>angM</i> , Tc ^r , Ap ^r	(169)
pJHC9-8	pJM1 derivative carrying only the TAF region	(169)
pJHC9-16	pJM1 derivative carrying TAF and transport genes.	(169)
pPH1J1	Plasmid with RP4 <i>ori</i> , incompatible with pJHC-T7, Gm ^r	(74)
pRK2073	Helper plasmid for conjugation, Tp ^r , Tra ⁺	(56)
pBluescript SK ⁺	Cloning vector, Ap ^r	Stratagene
pCR [®] -BluntII-TOPO [®]	Cloning vector, Km ^r	Invitrogen
pBR325	Cloning vector, Tc ^r , Cm ^r , Ap ^r	(19)
pBR325-M200	Cloning vector derived from pBR325, Tc ^r , Cm ^r , Ap ^r	This study
pKK232-8	Cloning vector carrying a promoterless <i>cat</i> gene, Ap ^r	Pharmacia
pMDL4	2.5 kb PCR fragment from pJM1 cloned in pCR [®] -BluntII-TOPO [®]	This study
pMDL4-S215A	pMDL4 with mutation S215A in PCP domain	This study
pMDL4-H406A	pMDL4 with mutation H406A in C domain	This study
pMDL21	<i>BstEII-NheI</i> fragment from pJM1 cloned in pBR325-M200	This study
pMDL-S215A	<i>BstEII-NheI</i> fragment from pMN4-S215A cloned in pBR325-M200	This study
pMDL-H406A	<i>BstEII-NheI</i> fragment from pMN4-H406A cloned in pBR325-M200	This study
pECO13	1.9 kb <i>EcoRI</i> fragment from pJM1 cloned in pBluescript SK ⁺	This study
pKKE13	<i>BamHI-HindIII</i> fragment from pECO13 cloned in pKK232-8	This study
pKKE13-1	<i>PstI-AatII</i> deletion of pECO13 cloned in pKK232-8	This study
pKKE13-2	<i>PstI-BstEII</i> deletion of pECO13 cloned in pKK232-8	This study
pKKE13-3	<i>PstI-HpaI</i> deletion of pECO13 cloned in pKK232-8	This study
pSC25	421 bp <i>Sall-PvuI</i> fragment of the <i>fatB</i> gene cloned in pBluescript SK ⁺	This study
pMN5	102 bp <i>BamHI-BstXI</i> fragment of the <i>angM</i> gene cloned in pBluescript SK ⁺	This study
pQSH6	415 bp <i>Sall-ClaI</i> fragment of the <i>aroC</i> gene cloned in pBluescript SK ⁺	This study

Table 4.2. Virulence as assessed by LD₅₀ and relative fold attenuation.

<i>V. anguillarum</i> strains	LD ₅₀	Attenuation ^a (fold)
775(pJM1/pBR325)	4.2 x10 ³	1
H775-3(pBR325)	1.9 x10 ⁵	44
775(pJM1::#63/pBR325-M200)	0.5 x10 ⁵	12
775(pJM1::#63/pMDL21)	5.2 x10 ³	1.2
775(pJM1::#63/pMDL21-S215A)	0.8 x10 ⁵	19
775(pJM1::#63/pMDL21-H406A)	1.1 x10 ⁵	26

^a Attenuation is calculated by the LD₅₀ of each strain normalized to the LD₅₀ of the wild-type strain.

Figure 4.1. Amino acid sequence and domain alignment of AngM and VibF. A. Amino acid sequence alignment of AngM from *V. anguillarum* and VibF from *V. cholerae*. The consensus sequence of the highly conserved motifs of the PCP and C domains is underlined. The plusses show conserved amino acid substitutions, while the identical residues are shaded and shown between the two protein sequences. B. Alignment of the AngM domains with the domains of VibF.

A

AngM: 163 NFESKLNPIYLDISKIDNNNNIEQIILSEFRASLDDPEVELGDDFFEMGGHSLLATRII 222
 N + L L++S + N++ +E+ IL+EFR++L E+ DDF+ GGHSL+ATR+I
 VibF: 1841 NAHAALAESELEISAV--NSSAVEECILAEFRSALGVAEMTAEDDFDFGGHSLIATRVI 1898

AngM: 223 GNLMMNHDI EISFNDFKSPSAQALARCVS LTKSSRNKPVDMALPHGSTSIGSKLPLSF 282
 G L++ IE+ ND F P+A+ LA+ L KP + SK PLS
 VibF: 1899 GRLLSEQCIELHINDMFSFPNAKCLAQQAVL----HIKPTSTSFASEVVVSSKAPLSL 1953

AngM: 283 AQSFLWNA--HLA'GQCAIENLPFMRFDAEVD EEFKIAFSL LIRHIGLRTLFNEGT 339
 AQ+ LW A + G IFNLPPA+ F EV+E+ F AF LL+RH GLRT F
 VibF: 1954 AQA SLWKAMSKYAKIGLTHIENLPFAKFLLEVNEQAFGEAFHWLLLRHAGLRTHFGLED 2013

AngM: 340 DGSIQQVIDEKDLI(YSWFWSSAESGTSS---LESEASVYFDLSKELPLRIRFFKDRKT 395
 Q VI ++ Y WFW+S ++ S L EA + FDLS+ELPLR+ F +D +T
 VibF: 2014 GOPYQHVI AASNI EHYQWFWTSKD NAAQSVARLLAQA EHTFDLSQELPLRLNFVRDECT 2073

AngM: 396 NQQVLSFLIHHMIID EWSLNNLMSELS DAYLARSONQEP EWDKSAYS JHDYALAQKNRGP 455
 Q LS L HH++DEWS+N LM EL+ Y Q P+W H++A Q++
 VibF: 2074 GTQYLSLLFH HI VLDEWSINILMDELAQVYQHSVQGRPOWQTEPLPHEFARKQRSSAF 2133

AngM: 456 IAEDINYVWNHLRGSTSG LNLCTE-PDQNGPEVNPIE ANWIEIDLGFSAVHSHSLARE 514
 +NYW+ G L + P N V+ E W+EI L S S++ LA+
 VibF: 2134 NQTHINYWLTKFAGVPWAQHLFAADHPLSNS TGVDLGEGGWVEIKLPKSTMVSLYQLAKA 2193

AngM: 515 YNSSIFSVVYSAIAQALHNAGNLKDLVIGTSASGRDDAKYFDSVGYFTTW AHRVIFEPD 574
 ++S+F+V+Y+AI+ ++H G + L++GT ASGR DA++FD+VGYFTTM V F
 VibF: 2194 RHASLFNVMYAAISASVHCIGAPEKLLVGT PASGRLD AEFDTVGYFTTMGVQLVDFTKV 2253

AngM: 575 QSFGKLIENVTMTINDSMPHATVPIDMVQREL-GLDPK-NGLIFDVYAQIHADNALYGS L 632
 Q+ +LIE V +IN SMP+ +PID+++ L G++ + G +F+V+ Q+HA N L+G L
 VibF: 2254 QTWQLIEQVKNSINQSMPTDIPIDLIEECLKGVEHETEGHMFEVFIQLHAKNKLHGEL 2313

AngM: 633 QTPNNIPVPYQOILPNKNKSLFGLHFEIMENVIGDERTLR LIVTYQTARYNAKQV 687
 + +QQ+ P+K++S GL FEI+E I ++TIR++++Y + Y+ QV
 VibF: 2314 LLTEGHAI RQQVCPDKSESGIGLQFEILEERIEQQTIRVMMSYMSKHYSAPAQV 2368

B

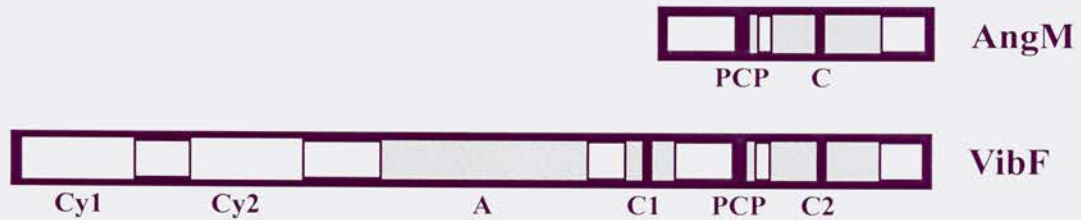


Figure 4.2. Growth in iron limiting conditions and anguibactin production of *V. anguillarum* strains. Ability of *V. anguillarum* strains to grow under iron limitation is expressed as a percentage of the growth in 2 μ M EDDA normalized to the growth in iron-rich conditions (2 μ g ferric ammonium citrate per ml) for each strain. The results are the means of five independent experiments, with the error bars showing the standard deviations. Anguibactin production for each of these strains, as detected on CAS plates, is shown below the graph.

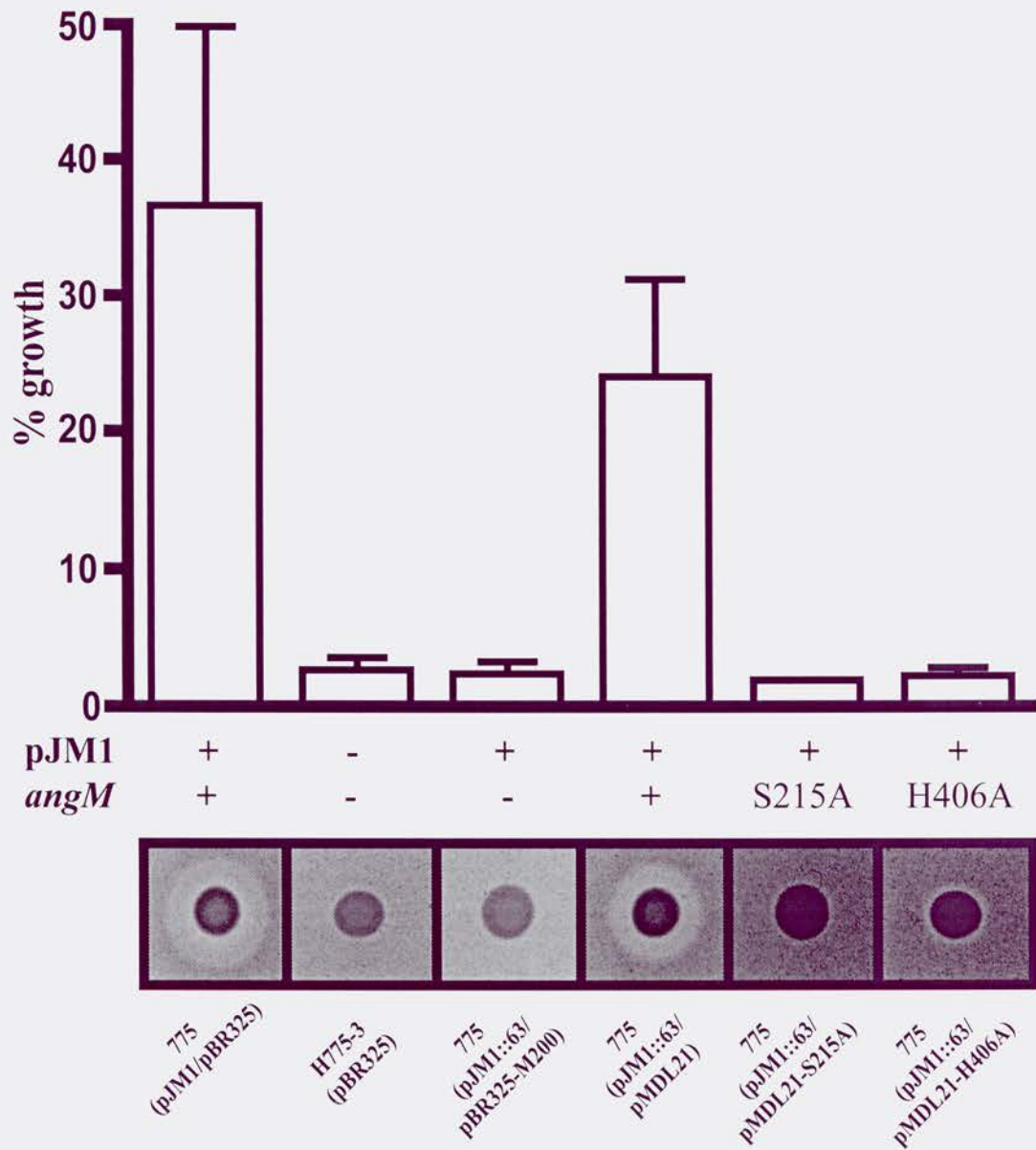


Figure 4.3. CAT assay with fusions of DNA fragments spanning the region between *angM* and the transposase gene, to a promoterless *cat* gene. The fragments cloned in plasmid pKK232-8 upstream of the promoterless *cat* gene are shown on the left-hand side of the figure. On the right-hand side of the figure, the production of CAT protein for each construct is shown as a histogram, with solid bars representing the level of CAT enzyme in iron-rich conditions (2 μ g of ferric ammonium citrate per ml) and the open bars representing the level of CAT enzyme in iron-limiting conditions (0.5 μ M EDDA). The CAT levels plotted are the means of three experiments with the error bars showing the standard deviations. Restriction endonuclease: E, *EcoRI*; A, *AatII*; B, *BstEII*; H, *HpaI*.

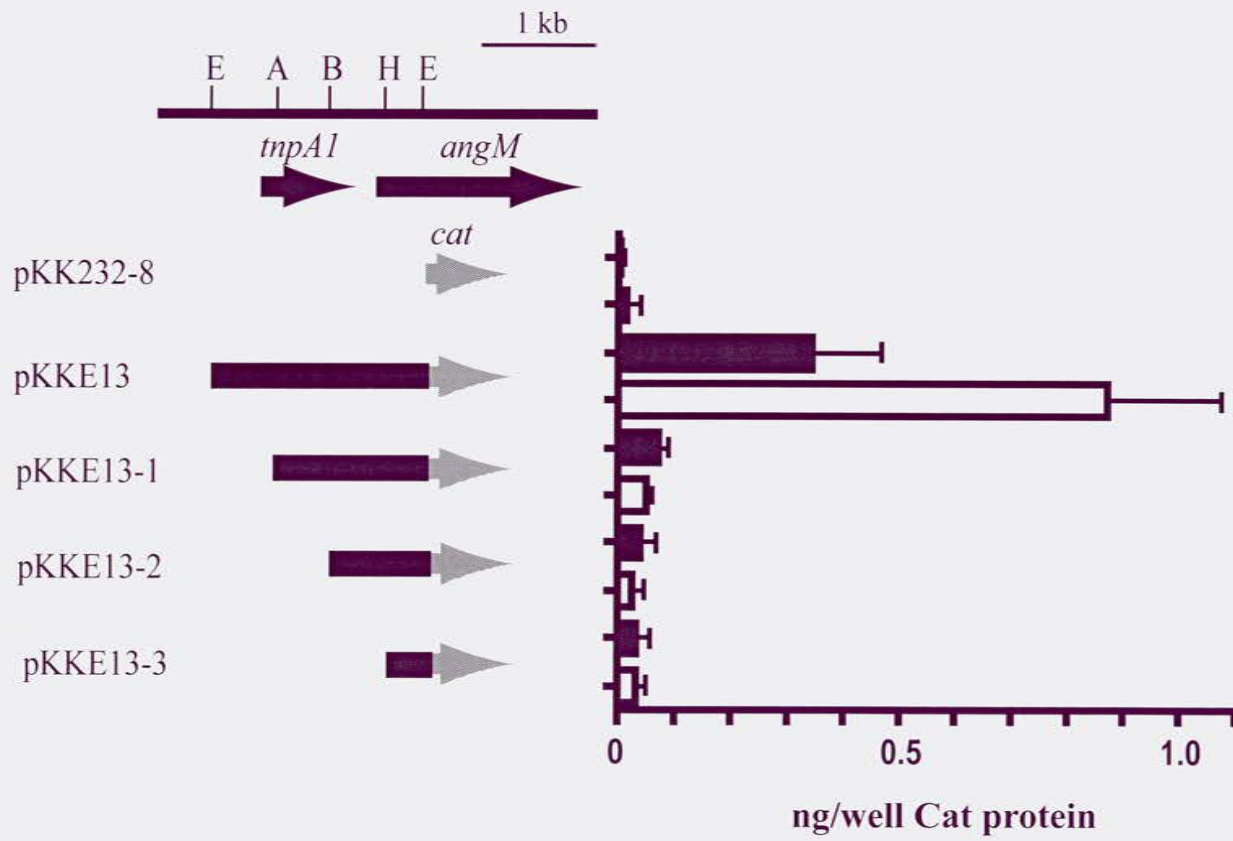
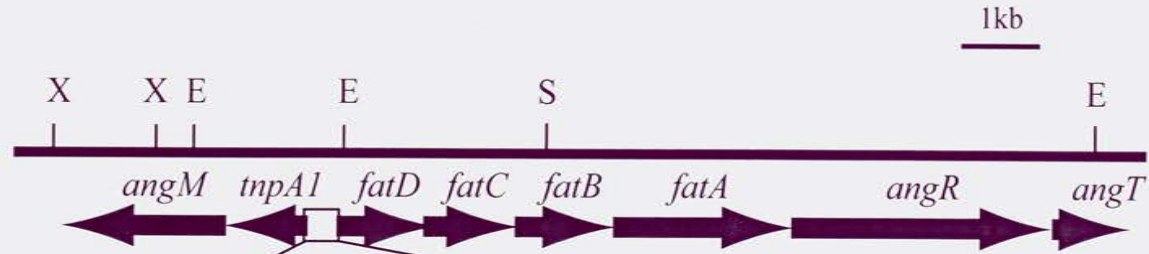


Figure 4.4. Primer extension analysis of the transposase gene promoter region.

Primer extension analysis with a primer at the beginning of the ISV-A1 element transposase gene and RNA obtained from cultures grown in various iron concentrations (lanes 1-4). Lanes G, A, C and T represent the sequence of plasmid pCS25 using primer Seq1762. P1, P2 and P3 are putative transcription start sites for the transposase gene. Supplements to the medium: lane 1, 2 μg ferric ammonium citrate per ml; lane 2, none; lane 3, 3 μM EDDA; lane 4, 6 μM EDDA.



Figure 4.5. Map of a 13 kb DNA region from plasmid pJM1 encoding the *tnpA1* and *angM* genes and the ITB operon. The nucleotide sequence of the region between the *tnpA1* and the *fatD* genes is shown under the map, with the primer (underlined) used in the primer extension experiment of Figure 4.4 and the locations of the putative transcription starts (arrowheads labeled P1, P2 and P3). The -35 and -10 sequences for the P1 product and the opposite orientation -10 and -35 sequences for the ITB mRNA are shown as open boxes, while the Fur binding sites are shown as shaded boxes. Restriction endonucleases: X, *Xho*I; E, *Eco*RI; S, *Sal*I.



```

catgcatctatggctgaatcatctatccaaaacgtaaccgagccacgcttgcacagagcc
gtacgtagataccgacttagtagatagggttttgcattggctcgggtgcgaacgtgtctcgg
W A D I A S D D I W F T V S G R K C L A

ttattgtattccgcccagttagttatcttctttttcgttttaccatgtcaccaccgttc
aataacataaggcgggtcaatcaatagaagaaaaagcgaatgggtacagtggtggcaag
K N Y E A W N T I K K K A K G M

taaccaccataaaggatcagatcacaggacttggaaaaggttcaactgatttaagcaaca
attgggtggtatttcctagctagtgctcctgaaccttttccaagttgactaaattcgttgt
P3 ←┐ P2 ←┐ -35
acgcctttctatgttgtcgatcttatttttataaattatgctgtaattttgcttacaatc
tgcggaagatacaacagctagaataaaaatatttaatacgcgaattaaacgaatgtgtag
-10 -10 ITB mRNA
aagagtaatagtgatagcattgattatcatttagatttacattttccgtcaagttaataa
ttctcattatcactatcgtaaccaatagtaaatctaaatgtaaaaggcagttcaattatt
P1 ←┐ -10 -35
ttttattaagtttaacgatgtattttataactgttgaggctctgctaaatccctgctgtga
aaaataattcaaattgctacataaatattgacaactccgagacgatttagggacgacact

```

Figure 4.6. RNase protection assays. RNase protection assay with a probe specific for the *angM* gene and total RNA isolated from cultures of wild type *V. anguillarum* (lanes 1 and 2) and a Fur-deficient *V. anguillarum* strain (lanes 3 and 4). RNA was obtained under iron-rich conditions (2 μg of ferric ammonium citrate, per ml lanes 1 and 3) or iron-limiting conditions (1 μM EDDA, lanes 2 and 4). The *aroC*-specific riboprobe was included in both RNase protection assays to provide an internal control for the quality of the RNA and the amount of RNA loaded onto the gel, since the *aroC* gene is expressed independently of the iron concentration of the cell.

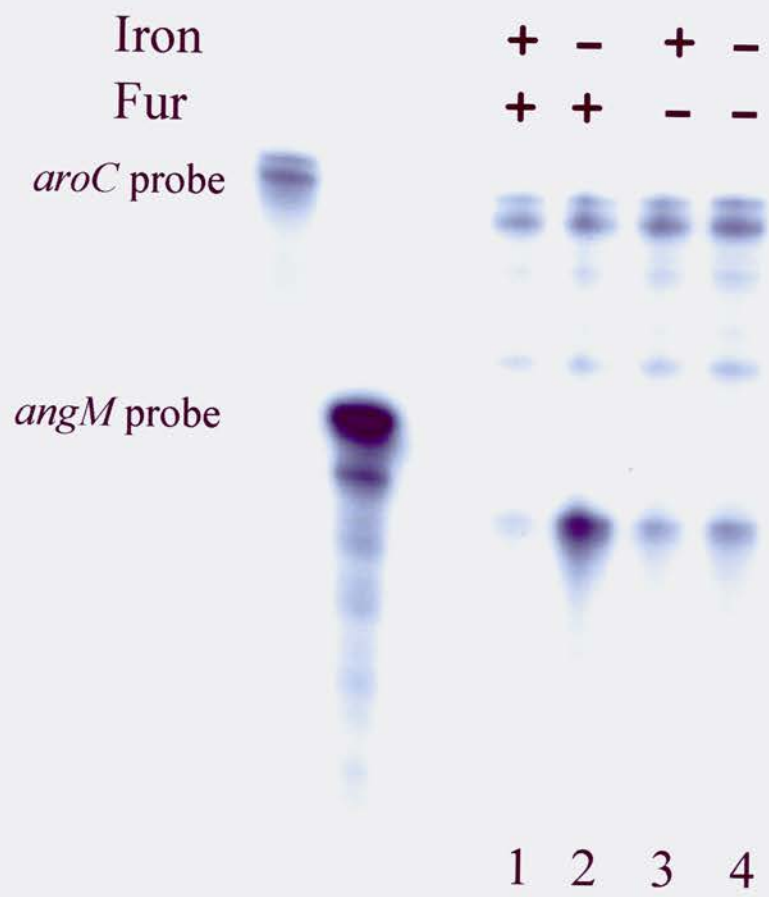
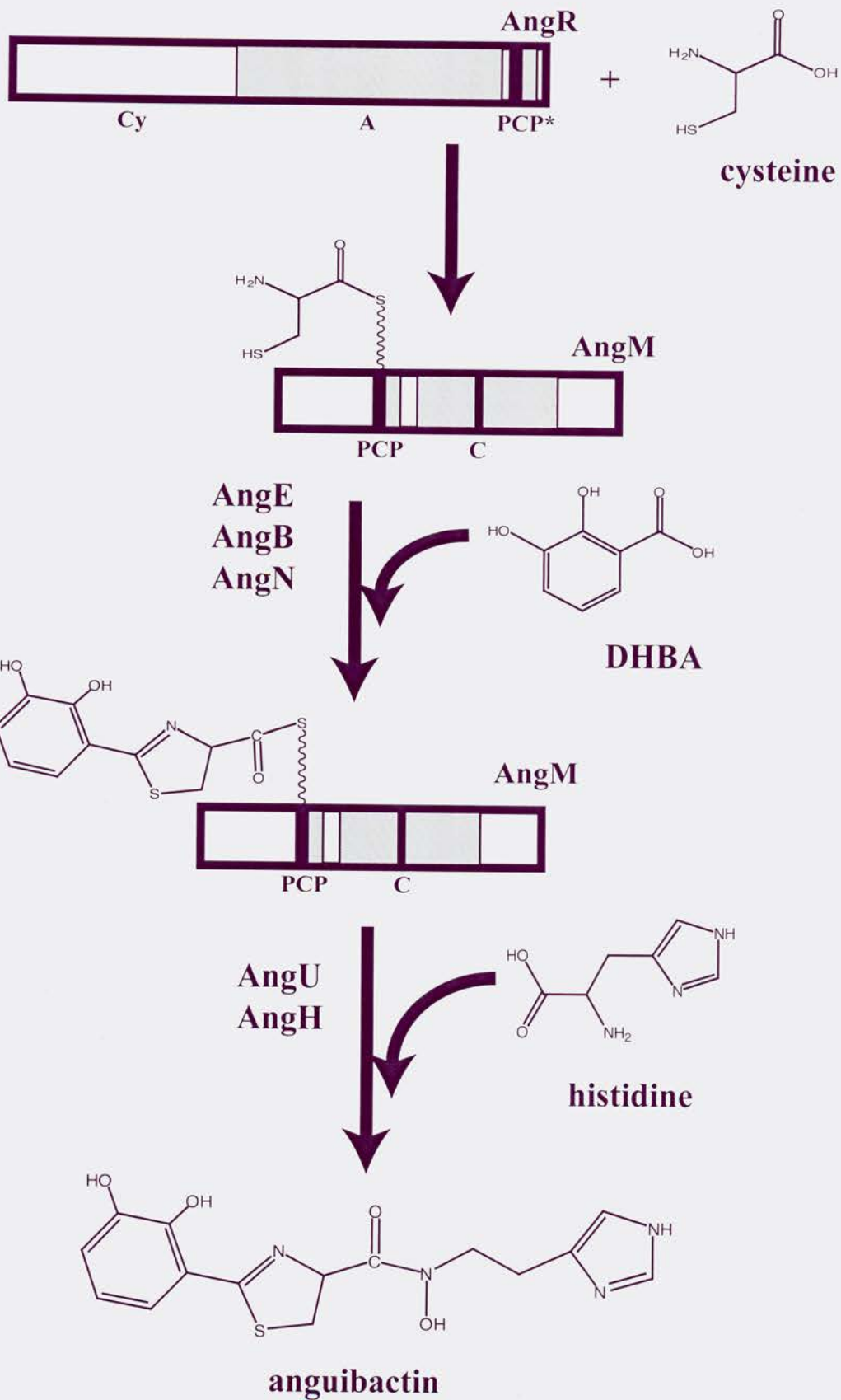


Figure 4.7. Model of the biosynthetic step catalyzed by AngM. The A domain of AngR activates the cysteine, which is then tethered to the PCP domain of AngM. The C domain of AngM catalyzes peptide bond formation between the dihydroxyphenylthiazol (DHPT) group loaded on the PCP domain of AngM and the secondary amine group of hydroxyhistamine. AngE, AngB, AngN, AngU and AngH are other NRPSs and tailoring enzymes that intervene in anguibactin biosynthesis. PCP* indicates the nonfunctional PCP domain of AngR.



CHAPTER 5

**Tandem heterocyclization domains in a nonribosomal
peptide synthetase are essential for siderophore
biosynthesis in *Vibrio anguillarum***

Manuela Di Lorenzo, Michiel Stork, Marcelo E. Tolmasky, and Jorge H. Crosa

Submitted to Journal of Bacteriology

5.0. Abstract

Anguibactin, the siderophore produced by *Vibrio anguillarum* 775, is synthesized via a nonribosomal peptide synthetase (NRPS) mechanism. Most of the genes encoding anguibactin biosynthetic proteins are harbored by the pJM1 plasmid. Complete sequencing of this plasmid identified an *orf* encoding a 108 kDa predicted protein, AngN. In this work we show that AngN is a NRPS that possess two free-standing cyclization domains in tandem and is essential for anguibactin biosynthesis. Substitution by alanine of the aspartic acid residues of each and both domains in separate experiments demonstrated a hierarchy in their functioning during siderophore biosynthesis. Site-directed mutants in both domains (D133A/D575A and D138A/D580A) result in anguibactin-deficient phenotypes underscoring the importance of these two domains in AngN function. These mutations also resulted as expected in a dramatic attenuation of the virulence of *V. anguillarum* 775 highlighting the importance of this gene for the biosynthesis of anguibactin and in the establishment of a septicemic infection in the vertebrate host. Transcription of the *angN* gene is repressed by the Fur protein in the presence of iron and is enhanced by AngR and TAF under iron limitation. Analysis of the sequence at the *angN* promoter demonstrated that it overlaps a putative transposase promoter that transcribes in the opposite direction, thus mirroring the situation described for the *tnp-angM* and iron transport-biosynthesis promoters in a contiguous region of the pJM1 plasmid.

5.1. Introduction

The possession of specialized iron transport systems is crucial for bacteria to override the iron limitation imposed by the host or the environment (23). Pathogenic bacteria have evolved systems, such as siderophores, to scavenge ferric iron from the iron-binding proteins of the host (24, 136). Peptide siderophores are in general low molecular-weight iron chelators (36, 67) that are synthesized by proteins belonging to the nonribosomal peptide synthetase (NRPS) family (40, 52, 106, 134). NRPSs catalyze the formation of a wide variety of peptides, such as antibiotics and siderophores, in the absence of an RNA template (102, 115, 177). These multimodular enzymes work as an enzymatic assembly line in which the order of the modules determines the order of the amino acids in the peptide (103, 159, 178). Each module contains the complete information for an elongation step combining the catalytic functions for the activation of the substrate amino acid (adenylation domain, A), the tethering of the corresponding adenylate to the enzyme-bound 4'-phosphopantetheinyl (4'-PP) cofactor (peptidyl carrier protein domain, PCP) and the formation of the peptide bond by the condensation domain, C (83, 103, 177). In some cases the condensation steps can also be catalyzed by a specialized condensation domain, the cyclization domain (Cy) that converts specific amino acids such as cysteine and threonine to their cyclic derivatives, thiazoline and oxazoline respectively, in the process of peptide bond formation (106, 111, 134, 181).

The bacterial fish pathogen *Vibrio anguillarum* is the causative agent of vibriosis, a highly fatal hemorrhagic septicemic disease in salmonids and other fish including eels (4). Many pathogenic strains of *V. anguillarum* possess a virulence plasmid that encodes an iron-sequestering system that includes a 348-Da siderophore, anguibactin (ω -N-

hydroxy- ω -*N*((2'-(2'',3''-dihydroxyphenyl)thiazolin-4'-yl)carboxy)histamine), and a transport protein system for the binding and transport of iron as a complex with the siderophore anguibactin into the cell cytosol (2, 3, 6, 169). The sequence of the 65 kilobase (kb) virulence plasmid pJM1 of *V. anguillarum* strain 775 has been completed (47) and it revealed that almost all the proteins proposed to be involved in anguibactin biosynthesis are encoded by genes on the plasmid.

One of the genes harbored by the virulence plasmid pJM1, encodes a putative NRPS, AngN, which shows an unusual domain organization with only two cyclization domains in tandem. Transposon insertions in this gene resulted in anguibactin-deficient mutants (169). In this work we present results that demonstrate the role of this gene and the cyclization domains in anguibactin biosynthesis.

5.2. Materials and methods

5.2.1. Bacterial strains and plasmids. Bacterial strains and plasmids used in this study are described in Table 5.1. *V. anguillarum* was grown at 25°C in either trypticase soy broth or agar supplemented with 1% NaCl, TSBS and TSAS respectively. To determine iron uptake characteristics, the strains were grown in M9 minimal medium (144) supplemented with 0.2% Casamino acid, 5% NaCl, the appropriate antibiotics and either various concentration of ethylenediamine-di-(*o*-hydroxyphenyl acetic acid) (EDDA) for iron-limiting condition or 4 µg/ml ferric ammonium citrate for iron-rich conditions. Antibiotic concentrations used for *V. anguillarum* were ampicillin (Ap) 1 mg/ml, tetracycline (Tc) 2.5 µg/ml, rifampicin (Rif) 100 µg/ml, chloramphenicol (Cm) 10 to 15 µg/ml and gentamycin (Gm) 10 µg/ml.

E. coli strains were grown in Luria-Bertani (LB) medium in the presence of the appropriate antibiotics. Antibiotic concentrations used for *E. coli* were Ap 100 µg/ml, Tc 10 µg/ml, Cm 30 µg/ml, Gm 10 µg/ml and trimethopim (Tp) 10 µg/ml.

5.2.2. General methods. Plasmid DNA preparations were performed using the alkaline lysis method (17). Restriction endonuclease digestion of DNA was performed under the conditions recommended by the supplier (Invitrogen, Roche, NEB). Transformations in the *E. coli* strains HB101 and XL1 Blue and other cloning strategies were performed according to standard protocols (144). Plasmids were transferred from *E. coli* to *V. anguillarum* by conjugation as previously described (169).

The Wizard® Plus SV Minipreps (Promega) and Qiaprep® Spin Miniprep Kit (Qiagen) were used to generate sequence quality plasmid DNA. DNA sequencing reactions were carried out by the OHSU-MMI Research Core Facility

(<http://www.ohsu.edu/core>) using a model 377 Applied Biosystems Inc. automated fluorescence sequencer. Sequencing primers were designed using Oligo 6.8® primer analysis software and purchased from the OHSU-MMI Research Core Facility (<http://www.ohsu.edu/core>) and Invitrogen. DNA and protein sequence analysis were carried out at the NCBI using the BLAST network service.

5.2.3. Mobilization of the #120 insertion mutant in *angN* from pJHC-T2612 to the pJM1 plasmid. To generate strain 775(pJM1#120), plasmid pJHC-T2612#120 was transferred to *V. anguillarum* 775 by conjugation. In a second conjugation, plasmid pPH1JI, whose origin of replication is incompatible with the replicon of pJHC-T2612#120, was transferred to the strain obtained from the first conjugation. By plating in the presence of Gm (the resistance marker of pPH1JI) and Ap (the resistance gene harbored by Tn3::HoHo1), it was possible to select for those cells in which the *angN* gene with the Tn3::HoHo1 insertion had replaced the wild type gene on the pJM1 plasmid. The loss of pJHC-T2612 was confirmed by Southern blot hybridization using the pVK102 vector sequence for probing (data not shown).

5.2.4. Construction of the complementing clone. A 3.2 kb fragment containing the *angN* gene was amplified by PCR using the *angN*-F and the *angN*-BamHIR primers (Table 5.2) and pJM1 as a template. Reactions consisted of 2 minutes at 95°C followed by 30 cycles of 1 minute at 95°C, 1 minute at 53°C, and 4 minutes at 72°C followed by a single cycle at 72°C for 10 minutes. The PCR product was cloned in the pCR®-BluntII-TOPO® vector using the Zero Blunt® TOPO® PCR Cloning Kit (Invitrogen) resulting in the pMDL6 plasmid. A *Cla*I-*Bam*HI fragment was subcloned from pMDL6 into the *Cla*I-*Bam*HI sites of pBR325-M200 to generate the pMDL30 plasmid carrying the *angN*

gene. After recloning in pBR325-M200 the entire *angN* gene was sequenced to verify that no mutation was generated in the *angN* gene during amplification or cloning. The pBR325-M200 cloning vector was derived from pBR325 by digestion with *Pst*I, blunting of the ends with T4 DNA polymerase (Gibco) and religation, resulting in a 4-bp deletion leading to the inactivation of the ampicillin resistance gene.

5.2.5. Site-directed mutagenesis. The plasmids pMDL6-D133A, pMDL6-D138A pMDL6-D575A and pMDL6-D580A were generated using the Quickchange™ site-directed mutagenesis kit (Stratagene), plasmid pMDL6 as a template and the primers listed in Table 5.2. The whole procedure was performed according to the manufacturer recommendations, with 16 cycles consisting of: 30 seconds at 95°C followed by 1 minute at 55°C and 16 minutes at 68°C. Plasmids pMDL6-D133A/D575A and pMDL6-D138A/D580A were generated with the same procedure but using plasmids pMDL6-D133A and pMDL6-D138A as templates, respectively. Site-specific mutations were confirmed by DNA sequencing with the appropriate primers. Once mutated, a *Cla*I-*Bam*HI fragment from each derivative was subcloned into the *Cla*I-*Bam*HI sites of pBR325-M200 to generate the plasmids carrying the *angN* derivatives with mutations in the Cy domains listed in Table 5.1. After recloning in pBR325-M200 the entire *angN* mutant genes were sequenced to verify that no other region of *angN* was affected during mutagenesis or cloning.

5.2.6. Growth in iron-limiting conditions and detection of anguibactin. For each mutant and wild type strains we determined the MIC for EDDA by using liquid cultures at increasing concentrations of EDDA in M9 minimal medium at 25°C. From these

analyses we chose a range of concentrations of EDDA to assay for the ability of all the strains to grow in iron-limiting conditions.

The siderophore anguibactin was detected by CAS assay and by bioassays using strains CC9-16 and CC9-8 as previously described (188, 190) with few modifications. For the bioassay experiment each strain was grown in M9 minimal medium supplemented with 0.25 μ M EDDA and after 16 hours the culture volume corresponding to an $OD_{600nm} = 1$ was collected to obtain the supernatant. The supernatants were lyophilized to dryness, resuspended in 500 μ l of methanol and stored at -80°C . Before spotting on the bioassay plates 10 μ l of each sample were dried and resuspended in 3 μ l of water.

5.2.7. Fish infectivity assays. Virulence tests were carried out on juvenile rainbow trout (*Oncorhynchus mykiss*) weighing ca. 2.5-3 g, which were anesthetized with tricaine methane sulfonate (0.1 g/liter). A total of 50 anesthetized fish were inoculated intramuscularly with 0.05 ml of each bacterial dilution, i.e., 50 fish per bacterial dilution. The dilutions were prepared with saline solution from 16 h cultures grown at 25°C in TSBS containing antibiotics for selection of the various plasmids harbored by the strains. The dilutions were prepared to test a range of cell concentrations from 10^1 to 10^7 cells/ml per strain. Therefore, 350 fish were tested per strain. After bacterial challenge, fish were maintained in fresh water at 13°C for 1 month and mortalities were checked daily. Virulence was quantified as the 50% lethal dose (LD_{50}) as determined by the method of Reed and Muench (138).

5.2.8. RNA isolation. A 1:100 inoculum from an overnight culture was grown in minimal medium with appropriate antibiotics. Cultures were grown with 2 μ g of ferric

ammonium citrate per ml (iron-rich) or with EDDA (iron-limiting) supplemented to achieve similar levels of iron-limiting stress for each strain tested (see figure legend). Total RNA was prepared when the culture reached an OD₆₀₀ of 0.3 to 0.5 using the RNeasyTM (Ambion) isolation kit, as previously described (45).

5.2.9. Primer extension. Primer extension experiments were carried out with the synthetic primer PEX-*angN* (Table 5.2), which is complementary to the 5'-end region of the *angN* gene. The primer was end-labeled with T4-polynucleotide kinase (Life Technologies, Inc.) in the presence of [γ -³²P]-ATP and annealed to *V. anguillarum* 775 total RNA (50 μ g). Reverse transcription from the primer by avian myeloblastosis virus reverse transcriptase (Promega) and separation on an urea-PAGE (6%) were carried out as previously described (45). Manual sequencing was performed by the dideoxy chain-termination method using the Sequenase Version 2.0 DNA Sequencing Kit (USB), plasmid pMDL6 as template and the same primer used in the primer extension experiment.

5.2.10. Ribonuclease protection assays. Labeled riboprobes were generated by in vitro transcription of 1 μ g of the linearized DNA with T7 or T3 RNA polymerase (MAXIscript[®] by Ambion) in the presence of [α -³²P]-UTP using as a template pSC50 (linearized with *Bam*HI) for *fatB* and QSH6 (linearized with *Rsa*I) for *aroC*. The template DNA for the *angN* probe was generated by PCR using the two primers *angN*-T7L and *angN*-T7R in which the T7 promoter sequence was added at the 5'-end of the *angN*-T7R primer (Table 5.2). The probes were purified on a 6% polyacrylamide gel. For each probe, the amount corresponding to 4x10⁵ cpm was mixed with each RNA sample (20 μ g). RNase protection assays were performed using the RPA IIITM (Ambion)

kit following the supplier's instructions. The *aroC* riboprobe was used in each reaction as an internal control for the amount and quality of RNA.

5.3. Results

5.3.1. Analysis of the AngN sequence. We have reported the complete sequence of plasmid pJM1 and identified several *orfs* that encode predicted proteins that are part of the iron uptake system (47). *orf10*, named *angN*, is predicted to encode a polypeptide (AngN) of 956 amino acid residues, with a calculated molecular mass of about 108 kDa (GenBank accession number NP943556 and (47)). The predicted AngN amino acid sequence showed significant matches to members of the family of nonribosomal peptide synthetases (NRPSs) such as VibF of *V. cholerae*, PchE and PchF of *Pseudomonas aeruginosa* and HMWP2 of *Yersinia pestis* (25, 68, 134). The similarity that AngN shares with these NRPSs is limited only to the cyclization (Cy) domain of these proteins. Like VibF but differently from the other proteins, the AngN protein possesses two tandem cyclization domains at its N-terminal end with 54% similarity and 35% identity with 927 amino acids of VibF. Figure 5.1 shows the alignment of the amino acid sequence of the entire AngN protein with only the 973 N-terminal amino acids of VibF.

5.3.2. Disruption of the *angN* gene and complementation with a wild type *angN* gene.

To establish the role of this putative NRPS in anguibactin production, we selected from a collection of transposon insertions generated with Tn3::HoHo1 on a cloned region of pJM1, pJHC-T2612, two insertions, #120 and #68. These insertions occurred downstream of the ITB operon in the region of *orf10* (Fig. 5.2) and each mutant was affected in anguibactin biosynthesis (169). DNA sequencing of the #120 and #68 mutants confirmed that these insertions were in *orf10* at 417 bp and 1,913 bp respectively from the 5'-end. Since the insertions were on pJHC-T2612 containing only a partial sequence of pJM1, we had to determine the effect of *angN* mutations on the iron-uptake

system encoded by the whole pJM1 plasmid. Therefore, the Tn3::HoHo1 insertion in mutant #120 was integrated by allelic-exchange onto the pJM1 plasmid resulting in *V. anguillarum* 775(pJM1#120). As expected strain 775(pJM1#120) was unable to grow in iron-limiting conditions at increasing concentrations of the iron chelator ethylenediamine-di-(O-hydroxyphenylacetic acid) (EDDA) since it did not produce anguibactin as detected by CAS (data not shown) and bioassay (Fig. 5.3A and B).

For complementation studies we constructed a clone, pMDL30, containing the complete *angN* gene expressed under the control of the tetracycline resistance gene promoter of the pBR325 vector and tested its ability to restore the growth of the *V. anguillarum* mutant 775(pJM1#120) under iron limitation. Plasmid pMDL30 was introduced into *V. anguillarum* 775(pJM1#120) and growth of the complemented mutant was determined in the presence of increasing concentrations of EDDA. The complemented strain grew as well as the wild type strain 775 under these conditions and produced levels of anguibactin comparable to that of 775 (Fig. 5.3A, strains 1 and 3). Therefore, *angN* plays an essential role in anguibactin biosynthesis and growth under iron limiting conditions.

5.3.3. Effect of site-directed modification of the *angN* gene on anguibactin

production. It has been demonstrated that cyclization domains catalyze peptide bond formation and cyclization of amino acids such as threonine and cysteine (50, 106, 134). In the case of anguibactin it is likely that the thiazoline ring in anguibactin results from the incorporation of the amino acid cysteine in the siderophore. Therefore, it was necessary to determine the functionality of the two Cy domains of AngN in anguibactin biosynthesis. We performed site-directed mutagenesis of the first and second aspartic

acid in the highly conserved motif (DxxxxDxxS). Mutations in each of the aspartic acid residues of Cy domains have been shown to affect the activity of the Cy domains of VibF (106). Both Cy domains of AngN possess the two aspartic acid residues in the Cy motif (**DMIAIDPDS** in Cy₁ and **DALILDARS** in Cy₂). Each aspartic acid residue (shown as bold above) was mutated by site-directed mutagenesis to an alanine in the complementing construct pMDL30 generating four mutant constructs, pCy₁D₁-D133A, pCy₁D₂-D138A, pCy₂D₁-D575A and pCy₂D₂-D580A. Strains containing each plasmid were conjugated with the *angN*-deficient mutant 775(pJM1#120) and the resulting strains tested for their ability to grow in iron-limiting conditions. As shown in Figure 5.3A, the insertion mutant #120 was complemented by the constructs harboring each of the mutated Cy domains (strains 4 to 7) although not as efficiently as with the construct harboring the wild type *angN* gene (strain 3). Furthermore, D to A mutations of each aspartic acid of the second cyclization domain seemed to have a greater effect on the ability to complement the knock-out mutant. The reduced growth in iron-limited medium of each strain perfectly correlated to the amount of anguibactin produced as determined by bioassays (Fig. 5.3B).

Since a mutation in each of the aspartic acids had only a minor effect in anguibactin biosynthesis and growth, we decided to generate double mutations of the two Cy domains. Two plasmid derivatives of pMDL30 were constructed in which the first or the second aspartic acid of each domain, were mutated to an alanine (pCy_{1/2}D₁-D133A/D575A and pCy_{1/2}D₂-D138A/D580A). These two constructs were no longer able to complement the AngN-deficient mutant on pJM1 and no anguibactin could be detected by bioassay (Fig. 5.3A and B, strains 8 and 9).

5.3.4. AngN cyclization domains and the virulence of *V. anguillarum*. Our laboratory has shown that a clear correlation exists between anguibactin production and the multiplication of the bacterium in the fish host (39, 45, 190). Since the mutations in *angN* affected anguibactin production to a different extent, we wanted to determine how this would be reflected in the virulence phenotype of each strain. Experimental infections of rainbow trout were performed with several dilutions of the wild type and the 775(pJM1#120) mutant and this mutant complemented by the constructs harboring wild type or mutant *angN* to calculate the LD₅₀ (138). As expected mutations that resulted in an anguibactin-deficient phenotype (#120 insertion and #120 insertion complemented with the double aspartic acid mutant) had a reduced LD₅₀ as compared to any strain that still produced anguibactin (Fig. 5.3C). Interestingly the LD₅₀ for the mutant in the first Cy domain, although producing reduced levels of anguibactin, was of the same order of magnitude as the LD₅₀ obtained with strain 775(pJM1#120) complemented with the wild type gene (Fig. 5.3C, strains 3 and 4), while the LD₅₀ for the Cy2 mutant strain, which produced even lower amounts of anguibactin, was reduced by one order of magnitude as compared with the two strains above (Fig. 5.3C, strains 3, 4 and 6).

5.3.5. Transcription and regulation of the *angN* gene. Primer extension analysis was performed to determine the transcription start site of the *angN* mRNA using primer PEX-*angN* complementary to the 5'-end of the *angN* gene and RNAs isolated from cultures grown at increasing iron limitation. Two iron-regulated products can be identified upstream of the *angN* gene (Fig. 5.4A and B, P1 and P2) with the first putative transcription start site 143 nt upstream of the start codon. Possible -10 and -35 boxes for

the *angN* promoter and the position of primer PEX-*angN* are indicated in Figure 5.4B with the putative transcription start sites.

From these experiments it can be gathered that expression of the *angN* gene is repressed in iron rich conditions. To confirm this result we performed ribonuclease protection assays with total RNAs obtained from strain 775 cultures grown in iron-rich (minimal medium supplemented with 2 µg/ml of ferric ammonium citrate) and in iron-limiting conditions (minimal medium supplemented with 1.5 µM EDDA and 2 µM EDDA). The RNase protection assay results (Fig. 5.5 panel A, lanes 1 and 2) clearly show that *angN* mRNA is virtually undetected in iron-rich conditions, while *angN* is highly transcribed in iron-limiting conditions. A riboprobe specific for the *aroC*-mRNA was added to each reaction as a control for RNA quality and loading.

In the anguibactin iron uptake system two positive regulators, AngR and TAF, have been identified that regulate expression of genes included in the ITB operon, *fatDCBAangRT* (31, 190). Since the *angN* promoter is adjacent to an ISVA2-transposase gene and transcribed in the opposite orientation, mirroring the organization of the pITBO, we wished to determine whether AngR and/or TAF products also regulate the transcription of *angN*. RNA was extracted from cultures of *angR⁻ taf⁺* and *angR⁺ taf⁻* strains that were grown in iron-limiting conditions (minimal medium supplemented with 0.5 µM EDDA) and RNase protection assay analysis was performed using an *angN* specific probe. We compared the changes in expression of the *angN*-mRNA and the ITB-mRNA using a *fatB*-specific probe. Figure 5.5 shows that AngR and TAF have a similar effect on expression of *angN* (panel A, lanes 3 to 5) as of *fatB* (panel B, lanes 1 to

4) demonstrating that in addition to the ITB operon promoter they can also enhance transcription from the *angN* promoter.

5.4. Discussion

Sequencing of the plasmid pJM1 of *V. anguillarum* resulted in the identification of several genes encoding NRPSs and tailoring enzymes (47). In this work we have characterized one of these genes, *angN*, and established its role in vivo in anguibactin production and in virulence.

As part of this analysis we found that the predicted AngN protein showed homology with the cyclization domain of other NRPSs. AngN consists of two Cy domains in tandem with no associated additional domains and it is the first NRPS so far identified that has two free-standing Cy domains. Each domain has the two aspartic acids residues in the highly conserved motif that have been shown in in vitro experiments with VibF to be essential for the function of Cy domains (106). In this work we have shown that single amino acid substitutions of the conserved aspartic acid in either one of the domains partially abolishes anguibactin production, suggesting the possibility that one wild type Cy domain of AngN is sufficient to catalyze the cyclization reaction. Furthermore, mutations in the aspartic acid residues of both Cy domains (D133A/D575A and D138A/D580A) resulted in cessation of anguibactin biosynthesis demonstrating that these Cy domains are essential for production of anguibactin in vivo. It is of interest that AngR, which plays a role in regulation of the expression of iron transport genes as well as in the production of anguibactin, possesses also a cyclization (Cy) domain (190). However the first aspartic acid residue of the conserved motif is replaced by an asparagine in the Cy domain of AngR. From the results presented in this work the Cy domain of AngR is unable to functionally replace the mutated Cy domains of AngN in anguibactin production.

The unusual domain arrangement of AngN and the results obtained with the mutants affecting only one domain of AngN suggest that AngN is a protein with a redundant catalytic activity, in which each domain is functional independently of the other. However, the lower levels of anguibactin produced by the mutants and the fact that site-directed mutations in either of the two aspartic acid residues in Cy₂ lead to a more dramatic decrease in anguibactin biosynthesis than similar mutations in Cy₁ suggest a different functionality with respect to their operation during anguibactin biosynthesis. This is further supported by the differences in the LD₅₀ of the mutants in the virulence experiments, which seem to be directly correlated with the amount of anguibactin produced by each strain.

It is intriguing that a division of labor by two Cy domains was also demonstrated in an in vitro experiment with VibF (106), an NRPS that in addition to two cyclization domains also has an adenylation, a peptidyl carrier protein and two condensation domains, and thus is not a free standing cyclization enzyme like AngN. From the experiments with VibF it was proposed that the first cyclization domain does the actual cyclization reaction while the second one does the condensation step (106). The in vitro VibF experiments taken together with our in vivo results with the AngN mutants strongly suggest that the reason for the dramatic decrease in anguibactin biosynthesis when Cy₂ is mutated is that this domain might also work on the condensation step in the cyclization reaction. Moreover, sequence alignment of each Cy domain of AngN with other seven Cy domains (VibFCy₁, VibFCy₂, HMWP2Cy₁, HMWP2Cy₂, PchFCy, PchECy and the other Cy domain of AngN) revealed an average of 22.7% identity for Cy₁ and 18.6% identity for Cy₂. The percentage of identity of AngNCy₂ to other Cy domains is

relatively lower than the overall average of 25.4% of the other domains while the similarity shared with VibFCy₂ is significantly higher (32%). Furthermore, the same sequence alignment showed that the amino acid residues that have been shown to be important in cyclization but not in condensation activity of Cy domains (50) were not conserved in the Cy₂ domain of AngN as it was the case for the Cy₂ domain of VibF. Our study together with the results obtained for the two VibF Cy domains and the identification of the residues involved in the cyclization/condensation activity of the Cy domain (50, 106) support the hypothesis that the Cy₂ of AngN is a dedicated condensation domain that forms the peptide bond between DHBA and cysteine prior to the cyclization step catalyzed by its Cy₁ domain.

In this work we also determined that expression of the *angN* gene is negatively regulated by the iron concentration of the culture medium. Analysis of the sequence at the *angN* promoter shows that it overlaps a putative transposase promoter that transcribes in the opposite direction, thus mirroring the situation described for the *tnp-angM* and iron transport-biosynthesis promoters (45). An exciting result was that the *angN* promoter is positively regulated by AngR and TAF, making it another member of the AngR and TAF regulon.

5.5. Acknowledgments

This project was supported by Grants from the National Institute of Health, AI19018 and GM64600, to J.H.C. We are grateful to Christopher T. Walsh for his insightful discussions.

Table 5.1. Strains and plasmids used in this study.

Strain and plasmid	Relevant characteristics	Source or reference
<i>Vibrio anguillarum</i> 775(pJM1)	Wild type	(39)
CC9-16(pJHC9-16)	Anguibactin-deficient, iron transport-proficient	(183)
CC9-8(pJHC9-8)	Anguibactin-deficient, iron transport-deficient	(183)
775(pJM1#120)	775 carrying pJM1 with Tn3::Ho-HoI insertion in <i>angN</i>	This study
<i>Escherichia coli</i> XL1 Blue	<i>recA1, endA1, gyrA46, thi, hsdR17, supE44, relA, lacF' [proAB', lacF', lacZΔM15 Tn10 (Tet^r)]</i>	Stratagene
HB101	<i>supE44 hsd20 (r^{-B} m^{-B}) recA13 ara-14 proA2 lacY1 galK2 rpsL20 xyl-5 mtl-1</i>	(21)
Plasmids		
pJM1	Indigenous plasmid in strain 775	(39)
pJHC-T2612	Recombinant clone carrying a 24 kb region of pJM1 cloned in pVK102, Tc ^r	(169)
pJHC-T2612#120	pJHC-T2612 with a Tn3::Ho-HoI insertion in <i>angN</i> , Tc ^r , Ap ^r	(169)
pJHC9-8	pJM1 derivative carrying only the TAF region	(169)
pJHC9-16	pJM1 derivative carrying TAF and transport genes,	(169)
pPH1JI	Plasmid with RP4 <i>ori</i> , incompatible with pJHC-T2612, Gm ^r	(74)
pRK2073	Helper plasmid for conjugation, Tp ^r , Tra ⁺	(56)
pBluescript SK ⁺	Cloning vector, Ap ^r	Stratagene
pCR [®] -BluntII-TOPO [®]	Cloning vector, Km ^r	Invitrogen
pBR325	Cloning vector, Tc ^r , Cm ^r , Ap ^r	(19)
pBR325-M200	Cloning vector derived from pBR325, Tc ^r , Cm ^r , Ap ^s	(45)
pMDL6	3.2 kb PCR fragment from pJM1 containing the <i>angN</i> gene cloned in pCR [®] -BluntII-TOPO [®]	This study
pMDL6-D133A	pMDL6 with mutation D133A in Cy ₁ domain	This study
pMDL6-D138A	pMDL6 with mutation D138A in Cy ₁ domain	This study
pMDL6-D575A	pMDL6 with mutation D575A in Cy ₂ domain	This study
pMDL6-D580A	pMDL6 with mutation D580A in Cy ₂ domain	This study
pMDL6-D133A/D575A	pMDL6 with mutation D133A in Cy ₁ domain and D575A in Cy ₂ domain	This study
pMDL6-D138A/D580A	pMDL6 with mutation D138A in Cy ₁ domain and D580A in Cy ₂ domain	This study
pMDL30	<i>ClaI</i> - <i>Bam</i> HI fragment from pMDL6 cloned in pBR325-M200	This study
pCy ₁ D ₁ -D133A	<i>ClaI</i> - <i>Bam</i> HI fragment from pMDL6-D133A cloned in pBR325-M200	This study
pCy ₁ D ₂ -D138A	<i>ClaI</i> - <i>Bam</i> HI fragment from pMDL6-D138A cloned in pBR325-M200	This study
pCy ₂ D ₁ -D575A	<i>ClaI</i> - <i>Bam</i> HI fragment from pMDL6-D575A cloned in pBR325-M200	This study
pCy ₂ D ₂ -D580A	<i>ClaI</i> - <i>Bam</i> HI fragment from pMDL6-D580A cloned in pBR325-M200	This study
pCy _{1/2} D ₁ -D133A/D575A	<i>ClaI</i> - <i>Bam</i> HI fragment from pMDL6-D133A/D575A cloned in pBR325-M200	This study
pCy _{1/2} D ₂ -D138A/D580A	<i>ClaI</i> - <i>Bam</i> HI fragment from pMDL6-D138A/D580A cloned in pBR325-M200	This study
pSC50	125 bp <i>Sau</i> 3AI fragment of the <i>fatB</i> gene cloned in pBluescript SK ⁺	(188)
pQSH6	415 bp <i>Sall</i> - <i>ClaI</i> fragment of the <i>aroC</i> gene cloned in pBluescript SK ⁺	(45)

Table 5.2. DNA primers used in this study.

Primer name	Nucleotide sequence ^a
<i>angN</i> -F	5'-ACGACGATTGATGGGTGTAGC-3'
<i>angN</i> - <i>Bam</i> HIR	5'-TTGTATTCACTAT <u>GGATC</u> CTTGC-3'
D133A-F	5'-CGCTTACATATTGATAGCGCTATGATTGCTATTGACCCAG-3'
D133A-R	5'-CTGGGTCAATAGCAATCATAGCGCTATCAATATGTAAGCG-3'
D138A-F	5'-CGATATGATTGCTATTGCCCCAGATAGTTGCCGAG-3'
D138A-R	5'-CTCGGCAACTATCTGGGGCAATAGCAATCATATCG-3'
D575A-F	5'-GTATTTTCTCGCTTTGCTGCATTAATTCTTGATGCTCGCTC-3'
D575A-R	5'-GAGCGAGCATCAAGAATTAATGCAGCAAAGCGAGAAAATAC-3'
D580A-F	5'-CTTTGATGCATTAATTCTTGCTGCTCGCTCCATTGCTTC-3'
D580A-R	5'-GAAGCAATGGAGCGAGCAGCAAGAATTAATGCATCAAAG-3'
PEX- <i>angN</i>	5'-TGCCCATTATCTTTTCTTCC-3'
<i>angN</i> -T7L	5'-CGAAAGTTCTATTATTGATGTT-3'
<i>angN</i> -T7R	5'- <i>ggatc</i> ctaatacgactcactatagggaggAGGTAATAAACTAACGGAGAAT-3'

^a Restriction sites are underlined, base changed from the wt sequence are shown in italics, T7 promoter sequence in lower case

Figure 5.1. Amino acid sequence alignment of AngN from *V. anguillarum* and VibF from *V. cholerae*. The sequence of the highly conserved motif of the Cy domains are underlined. The plusses show conserved amino acid substitutions, while the identical residues are shown between the two protein sequences.

AngN: 1 MSELTPMQAACWFGRKDNQGLGNVASHLYTEFDGENINIDKLNLSALGSLYKRHEMLRLKV 60
 M E+T MQAA W GR+ + L VA+HLY EFDG+ +N L A+ +LY +H MLRL +
 VibF: 1 MKEMTAMQAAYWLGRQHDCLLDGVAAHLYAEFDGQALNRQALTEAVRALYAKHPMLRLAI 60

AngN: 61 NHLGESSIIDVPNHALLEIEDFTHLSPENMHKALIEKRQSWAHQMLDLTQGGQVARFSVSL 120
 G+ I+ + L+++D + P+ + + KRQ HQMLDLTQG S++L
 VibF: 61 TKDGGQKILPLSTFHQLKVDDLSQWKPEVESFVHTKRQRMTHQMLDLTQGNPIEISLTL 120

AngN: 121 LPDNAFRLHIDSMDIAIDPDSRVLIEDLAMLY----ESGASEVKNNP-TFFSWHGMKN 175
 LP+ RLHID+DMIA D S R+L++DL LY E ++++ TFF + +
 VibF: 121 LPEGKHLRHIDADMIACDAQSFRLLVDDLTSLYLEAIEHRLEIIESDVVTFQYLDAAQA 180

AngN: 176 DPILKSQRKSDRAWWKSNNIAPSPSLPFFEPNTN--KAESHHSYSAWLDAEQRTDLITL 233
 D L +++ D+ WW+ L I PSLP+ T+ A S ++ W +R L +
 VibF: 181 DRALAKRKEVDKWWQERLATIPAEPSPYPVPTDAVSANSQRFHWFVTPVERKGLAEV 240

AngN: 234 ARKNNLTPANMLGLFARTLGKATGDETFRINVPTFWRPPIIEGTESLVGDFVNFVLSV 293
 AR+++LT L L LF++ + A + FR+NVPTF R E +GDF N ++ S
 VibF: 241 ARQHHLTLTQLTLALFSQVIANACQERQFRLNVPTFHRGNRSLDIEHTIGDFSNNLIFSA 300

AngN: 294 DMKESKTLLEFCHMVADKMGLLGHSGRYDGVSMRDLSLHHGCTQLAPVVFTSAIDLPSG 353
 D+ ++TLL C A+++ LL H Y GVS+MRDLS G Q +P+VFTS +++
 VibF: 301 DVGTTQTLTLLSQCQTANQLHQLLRHESYSGVSMRDLSRKQGGVQRSPIVFTSGMEMRDE 360

AngN: 354 NLFRRVHKHFGKMDWTISQGSVALDSQVVSIDGGIMINWDVRQEALPKEWTSAMFENF 413
 +FS V +H G+M+W ISQG+ V LD+Q+ GI++NWDVR E + +A+F ++
 VibF: 361 EIFSDHVTQHLGRMNWVISQGAQVTLDAQIAPAYEGILLNWDVRMENFADKIDITLFAHY 420

AngN: 414 VALTKSVISTPDLVAPLDKLPKLVCL---SHFESELTMPQRAYLLGRTTQMPLGGVAM 470
 V L + V P+++ + ++ +L S E LTP+Q+AYLLGR+TQ+ LGGVAM
 VibF: 421 VDLIRCVLHPMMQSVQQIDAQLGYARRESIQEMPLTPLQQAYLLGRSTQIALGGVAM 480

AngN: 471 QETLEHRGTLSSIRHRLSTMVVKYPCLRTFIDSKSLKQVSCQPQVNLAVDLRHRLEK 530
 E E+RG + S+ RL +V P LRT ID + VS C +N +DL+HL +
 VibF: 481 HEFREYRGHIDTQSLHRLLYLVEHIPALRTRIDQEKWIQWVSPCIALNWQAIDLQHLRSR 540

AngN: 531 DKAEELARFRYTYNNHMFDDLQPLWNVTFSL-----SETDTYVFSRFDALILDARSIA 585
 ++A + R Y M DL + W + L E + V + FDALI+D R+ A
 VibF: 541 EQALLAVEPVRQQYQQRMHDLTRSPWQICVVQLPIEEQEESIVLTSFDALIVDGRTHA 600

AngN: 586 SLLVELFDEQAPYIPSF-----DFEPDHEHVQSARAKDEKYWLNKLATVEKSMCFPWHPK 640
 +L L + P I D + S +A+DE YW +KL PW +
 VibF: 601 LILAALLGSEEPDITQVVQNARDTQISISPFASKKAQDEAYWKSCLHPDCPPPALPWKQA 660

AngN: 641 LKSISHSRYSRQSLKIEKETVKKLVRVAGKEGLYKNTLMSVAMEALSSHVCNGQLCVAV 700
 L++I+ SRY R+SL+I KE+V KL R + GL+ N+L+ + ++ LS + V
 VibF: 661 LETITTSRYARESLOPKESVGLNRCGIENGLFLNSLLTATILDVLSYWTTEIGMRVGF 720

AngN: 701 PVL-PMTSANYASQSSFIQTQWNAHQYDFLQRAKTLQVDTLEGLEHLAFSGVDLARVLE 759
 PVL P ++A ++SSF++ + L +A LQ + LE LEHLAFSGVDL R+L
 VibF: 721 PVLIPSSNAIDGNESSFVILEHEKSTLSLLSQASKLQREMLEALEHLAFSGVDLNRLLMN 780

AngN: 760 RCGPAPALPIVITNGLSWPVLSDDASMTLQRGTLQTPQVAMDIRFVAITGGSIMFSVDYA 819
 + A LP+V+TNGLSW L+ + ++TL G+TQTPQVA+DIR +++ S DYA
 VibF: 781 QAPQALVLPVVLTNGLSWKTLNPEDAVTLFDGVTQTPQVALDIRLTYDEQKNLIISFDYA 840

AngN: 820 SEAVADDLVKAILDRIDMILDHVMVETSQYVVQSHKLLPIGRSRVVELVDRDPNESWDIDL 879
 + +L++ +L + L + ++ + + R + D + S D D
 VibF: 841 LAVLETELIREMLSALHHRLSQTSSASLAAPLEPCIDLSHYR----FNSDESASHDCDF 896

AngN: 880 TKRKIFDIYCVIGKEKNNSDSLSLPPFSQLGLRPSHLKQISIDLKELQVDLPVMQLIRC 939
 + ++ + K +L ++QLG Q + L I
 VibF: 897 LAKLAQQLFVRTDKTAVICGEQTLSSYAQLGYARRESIQEMPLTPLQQAYLLGRSTQIAL 956

AngN: 940 RNADDIKDLALQQVDF 956
 + + +D
 VibF: 957 GGVAMHEFREYRGHIDT 973

Figure 5.2. Map of a 17 kb DNA region from the pJM1 plasmid encoding the *angN* gene and the ITB operon. Restriction endonucleases: E, *EcoRI*; S, *SalI*.

Figure 5.3. Growth in iron-limiting conditions, anguibactin production and virulence of the *angN* mutant strains. A. The ability of *V. anguillarum* strains to grow under-iron limitation is expressed as % growth that corresponds to the growth in EDDA normalized to the growth in iron-rich conditions (4 μ g of ferric ammonium citrate per ml) for each strain. Each column for each strain corresponds to concentrations of EDDA, from bottom to top, of 0.5, 0.75 and 1 μ M, respectively. Results are the mean of three independent experiments with the error bars showing the standard error of the mean. B. Measurement of anguibactin production by bioassay in mm of growth. The results shown are the average of three independent experiments with corresponding error. C. Virulence experiments were carried out as described in Material and Methods and the LD₅₀s were calculated by the method of Reed and Muench. ND = not determined

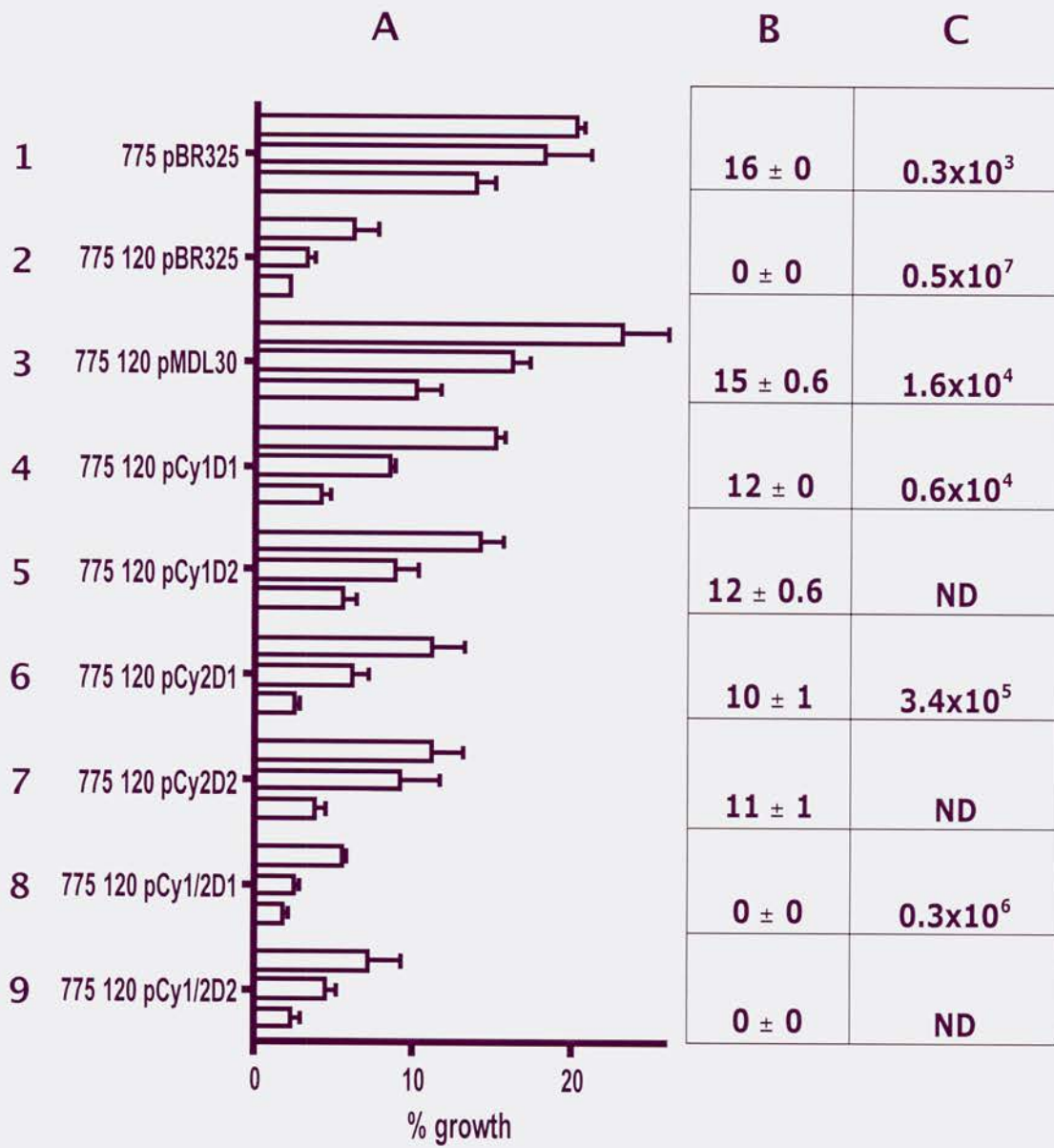


Figure 5.4. Mapping of the transcription start sites of *angN* mRNA. A. Primer extension analysis using a primer at the beginning of the *angN* gene and RNA obtained from cultures grown in iron-rich (lane 1) and in iron-limiting conditions (lane 2 and 3). Lanes G, A, C and T represent the sequence of plasmid pMDL6 using primer PEX-*angN*. P1 and P2 are putative transcription start sites for the *angN* gene. The supplements to the medium were: lane 1, 2 μg of ferric ammonium citrate per ml; lane 2, 1.5 μM EDDA; lane 3, 2 μM EDDA. B. The nucleotide sequence of the region upstream of the *angN* gene is shown with the primer used in the primer extension experiment and the location of the putative transcription starts (arrow heads P1 and P2 and bold letters). The -35 and -10 sequences for the P1 product are shown as open boxes and the ATG for AngN is underlined.



B

```

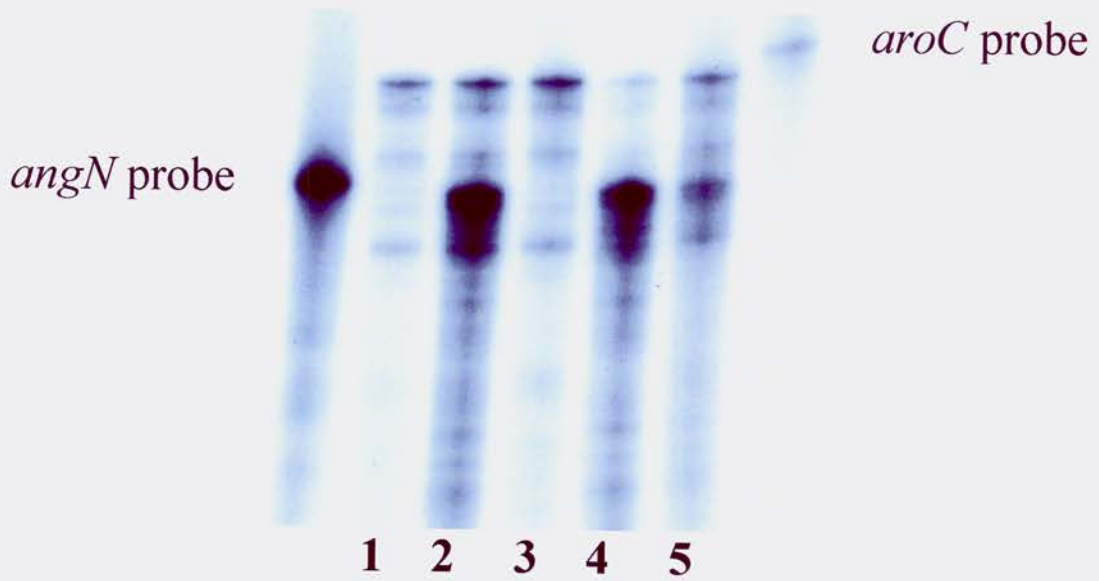
AAAAGGTCAG AGAACCACGG TTGATTAAGG CTTTGTGTGA
      -35
CTGTTCAG TTAGTTGTTT TGTAACGAGG TTTAGGCATG
      -10
      P1
AGGCTACGAC GATTGATGGG TGTAGCCGAT CAGATCGTAG
      P2
CTTCTAGATT TAGTCCATC GATTTAAGCA ACAAAGCCGT
TCAGAGGTGT CGCACTTCGT ACTTGAATCC AAGTCTCTTA
TCTAGTTAAT AATAAGGTTT TTATTGTAAA TGATTATCGT
TTGCAAAATA ATGGGCCTA ACAAATGAAT TGTCACAAA
GTGAAAGCTG ATGAGTGAAT TAACACCAAT GCAGGCTGCA
TGTTGGTTTG GAAGAAAAGA TAATGGGCAA CTAGGCAATG
      c cttottttct attaccgt (PEX-angN)
TTGCTTCTCA CCTTACACC GAATTCGATG GCGAAAATAT

```

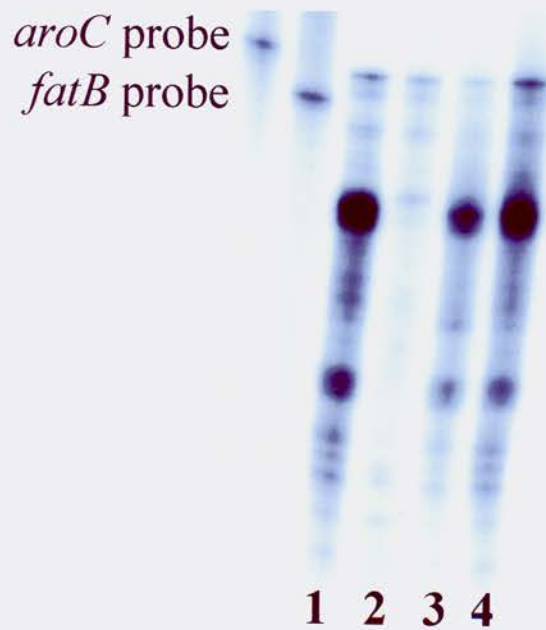
Figure 5.5. Effect of iron, AngR and TAF on transcription of *angN* and *fatB*. A. RNase protection assay using a probe specific for the *angN* gene and total RNA isolated from cultures grown under iron-rich and iron-limiting conditions. *V. anguillarum* wild type (lanes 1, 2 and 4); *V. anguillarum* AngR-deficient strain (lane 3); *V. anguillarum* TAF-deficient strain (lane 5). RNA obtained under: iron-rich conditions, lane 1 (2 μ g of ferric ammonium citrate per ml); iron-limiting conditions, lanes 2 and 4 (1.5 μ M EDDA) and lanes 3 and 5 (0.5 μ M EDDA). B. RNase protection assay with the same RNA used in panel A from the cultures grown under iron-limiting conditions using a *fatB*-specific riboprobe. *V. anguillarum* wild type (lanes 1 and 4); *V. anguillarum* AngR-deficient strain (lane 2); *V. anguillarum* TAF-deficient strain (lane 3). The *aroC*-specific riboprobe is included in both RNase protection assays to provide an internal control for the quality of the RNA and the amount of RNA loaded onto the gel, since the *aroC* gene is expressed independently of the iron concentration of the cell.

A

Iron	+	-	-	-	-
AngR	+	+	-	+	+
TAF	+	+	+	+	-

**B**

AngR	+	-	+	+
TAF	+	+	-	+



CHAPTER 6

Discussion

6.0. Discussion

I will address here the contributions of this work to the field of siderophore biosynthesis and NRPS mechanism of action and suggest future studies that could spawn from my findings.

The sequence of the pJM1 plasmid presented in Chapter 2 represents the first time that an iron metabolic plasmid has been completely sequenced. The analysis of the ORFs found on this plasmid showed that the anguibactin iron transport system is in its majority encoded on pJM1 and that it is the only virulence factor harbored on the plasmid, since no ORFs encoding for additional determinants such as colicins and antibiotic resistances could be identified. The lack of additional traits that could be associated with virulence could be an explanation for the fact that the pJM1-like plasmids are not as widespread as the pColV-K30 family, the only other known type of plasmid that encodes a siderophore-mediated iron acquisition system but also genes for colicins and several antibiotic resistances (185). However, in *V. anguillarum* serotype O1 strains the pJM1-like plasmid evolved to become essential for virulence, solely due to the iron uptake system (37, 45). The finding of this family of plasmids only in the *V. anguillarum* serotype O1 strains could also be a consequence of the inability of pJM1-like plasmids to be transferred from one bacterium to another since no transfer region could be identified by sequencing and annotation. A pJM1-like plasmid could have evolved within the bacterial host, from a replicon already present in the cell by step-wise acquisition of transposons. The bacterial strain containing this newly assembled plasmid could be the ancestor of the serotype O1 strains harboring the pJM1-like plasmids. The modular composition of the pJM1 plasmid as well as the limited variability (mainly the presence of additional insertion sequences)

found in the different plasmids of this family supports this hypothesis. The pJM1 sequence in combination with the growing number of plasmid genomes available offers a wealth of information on the evolution and distribution of these extrachromosomal elements that will be useful in the future for comparative studies with other natural plasmids from environmental and clinical isolates.

The structure of anguibactin, the pJM1-mediated siderophore, is also quite exceptional since it contains three different chemical groups, all possessing iron-chelating properties. Furthermore, this highly compact iron-binding compound is assembled from only one proteinogenic amino acid, cysteine, and two metabolites, DHBA and histamine, that are synthesized exclusively for siderophore production and possess either a carboxylic or an amino group. These features of the two precursors channel the synthesis of anguibactin in only one possible direction with the carboxylic acid capping the N-terminus and the amine functioning as the final acceptor. This simple but unusual structure can be assembled by a limited number of NRPS domains that in this system are distributed in a highly fragmented and original arrangement as determined from my *in silico* analysis.

From the sequence data and the annotation analysis, I proposed a model for the biosynthesis of the siderophore anguibactin that takes into account the current knowledge on NRPSs and peptide synthesis. The pathway based on the pJM1 sequence was the starting point for the work done in this thesis on the single components of the anguibactin assembly line. I will present here the model as proposed at this point taking in account all the conclusions of this thesis. As shown in Figure 6.1 in the proposed pathway, DHBA is activated by AngE and tethered on the ArCP domain of AngB in a similar

manner as it occurs in the vibriobactin and the enterobactin systems of *V. cholerae* and *E. coli*, respectively (52, 61, 79, 105). Using an algorithm designed to predict the identity of the amino acids activated by NRPS A domains based on their amino acid sequences (27), I proposed that the A domain of AngR, possibly the only functional domain of this protein, activates cysteine. Once the activated cysteine is loaded on the PCP domain of AngM, at serine 215, the dihydroxyphenylthiazolyl (DHPT) intermediary is formed in two steps, first amide bond formation between DHBA tethered on the ArCP domain of AngB and the amino group of cysteine followed by cyclodehydration, both catalyzed by the Cy domains of AngN. The final product anguibactin is then released by transfer of DHPT from the PCP domain of AngM to the secondary amine of hydroxyhistamine in a reaction that requires the activity of the AngM C domain. The amine acceptor, hydroxyhistamine, is synthesized from histidine by two tailoring enzymes, AngH, the histidine decarboxylase, and AngU, the histamine monooxygenase.

The predictions made on the basis of anguibactin structure and on the domains found in the biosynthesis proteins were tested using an *in vivo* genetic approach. Mutants that completely obliterated the proteins or that affected only specific residues in the domains were used to determine functionality of each domain. Since all the mutants were tested *in vivo* for their ability to multiply either in a medium depleted of iron or inside the host fish, this study represents a different and novel approach to analyze NRPSs. Biochemical methods are usually applied to study these proteins and their domains with analyses of their functions performed in *in vitro* systems with highly purified components (79, 110, 134). Since both methods provide invaluable information on the mechanisms by which each single domain acts, they should be used in

combination to completely understand how many of the reactions observed in vitro occur also in vivo. This became quite clear in the analysis of the AngB protein domains where the site-directed mutants of the plasmid-encoded protein were used in in vivo and in vitro analyses to test the functionality of each domain (Chapter 3). Loading of the ArCP domain of AngB with the non-specific salicylate monomer could be achieved in vitro but no siderophore production could be measured in vivo when the same substrate was used in cross-feeding experiments of a *V. anguillarum* strain that is not able to produce DHBA but still expresses the ArCP domain. In contrast, anguibactin synthesis could be restored in the same strain when grown in medium supplemented with the natural substrate DHBA. Thus, although the results obtained for the ArCP domain in the in vitro reactions confirmed those in vivo, i.e. that the ArCP domain of the AngBp protein is functional, they clearly posed the question if the ArCP domain can actually be loaded with salicylate within the bacterial cells. I need to point out that from our experiments we could not discard the possibility that salicylate can still be loaded onto the ArCP domain in vivo and the limiting step for the assembly of salicylate in the anguibactin molecule occurs in reactions catalyzed by downstream domains such as the Cy domains of AngN that could be unable to recognize this phenolate as a substrate.

The new approach for the study of NRPS domains used in this thesis could become quite useful in the possible applications that the understanding of this systems have as the final goal. The increasing interest in NRPS systems comes from the fascinating prospect to use these synthetases to assemble alternative bioactive secondary metabolites, such as new antibiotics or bactericidal compounds (78, 115). The ability to tweak sets of domains to incorporate specific monomers in a predetermined order in the

peptide could vary depending which method is used for the biosynthesis. Probably, fewer limitations are encountered in the in vitro versus the in vivo assembly but the use of the latter should be greatly favored since larger yields of product can be obtained from a system working in bacterial cells, an important asset if the final goal is a medical application of the compound.

An additional contribution of this thesis to the field of siderophore biosynthesis comes from the results obtained with the two AngB homologues with respect to anguibactin assembly. Although highly similar, these two proteins showed very different functionality of their ArCP domains in vivo. As discussed in Chapter 3, the chromosomal-encoded ArCP domain is not able to participate in anguibactin production and this could be due to an impairment of this protein to interact with the other proteins of the anguibactin system. Although specific protein-protein interactions have been already suggested to interfere with domain swapping in different systems in several in vitro studies (105, 151, 165), the two AngB proteins are encoded in the same bacterium and more closely related than the previously tested domains were to each other. Furthermore, the recent findings of additional chromosomal and plasmid-encoded gene pairs in the same strain of *V. anguillarum* (7) point to a more complex system of interactions. One of these gene pairs codes for the DHBA-specific A domain and it has been shown that both gene products are proficient in anguibactin production (7). Further analyses are needed to understand the mechanism underlying the different behavior observed in the system specificity of these two domains.

The identification of a functional AngB encoded on the chromosome within a cluster of other DHBA and siderophore biosynthesis genes is an interesting finding both

for the evolution of the iron-uptake systems of *V. anguillarum* species and the future study of the siderophore produced by serotype O1 and O2 strains of *V. anguillarum* that do not carry a pJM1-like plasmid (94). This chromosomal-encoded siderophore that also contains DHBA, can be recognized by the outer membrane receptor for enterobactin but not by that for anguibactin pointing to a structure more similar to the siderophore produced by enteric bacteria than to the siderophore produced by *V. anguillarum* strains (94).

In Chapters 4 and 5, I presented the characterization of two NRPSs with an unusual domain organization. I determined that both AngM and AngN do not even possess a complete module with AngM missing the A domain and AngN harboring the activity for only one step of an elongation round, the cyclization function. Although domain fragmentation has been observed in other systems, it is usually limited to distribution of the domains for activation and tethering of the catecholate or phenolate monomers (79, 105). This is probably a consequence of the fact that the genetic information for the incorporation of these building blocks in very many siderophore systems was acquired as a single gene cluster in which all the enzymatic activity required for the synthesis and assembly of the precursors were present. The only two exceptions to the usual organization of the domains for catechol and phenolic groups (i.e. A and ArCP domains expressed in two independent proteins) were found in the yersiniabactin system where the ArCP domain for DHBA is part of the HMWP2 synthetase N-terminus and in the pyochelin assembly where the tethering domain for salicylate is encoded by the PchE amino terminal end (82, 134). The distribution of domains constituting a single module on distinct polypeptides found in the anguibactin system goes beyond the step of

DHBA incorporation and the activities required for the assembly of the final product are spread over five proteins (including those encoding the A and ArCP domains for DHBA). This is even more striking if we consider that only two modules are required for anguibactin biosynthesis for a total of six domains: it is almost one domain per NRPS. Comparisons with the vibriobactin system showed that the same domains found on AngM, AngN and AngR in *V. anguillarum* are all grouped together in only one polypeptide, the VibF protein from *V. cholerae* (VibF has also an extra C domain, C₁, that was shown to be catalytically non-functional but important for its dimerization) (72, 73, 106). Thus, the highly fragmented system for anguibactin biosynthesis requires a considerable larger number of protein-protein interactions than those needed in the vibriobactin assembly line, to assure the correct processing of the precursors to yield the final molecule of siderophore. Recent findings in the tyrocidine system point to short N-terminal and C-terminal sequences in the NRPS as the intermolecular communication domains between the different synthetases (70, 98). The fragmentation of the anguibactin NRPS domains makes this a rather appealing system to create new module combinations for the production of novel compounds *in vivo*, due to the larger number of units and the better manageability of the protein sizes. Once the extent of the intermolecular communication domains are defined for the proteins of the pJM1 system, each of the anguibactin NRPS could be used as a protein scaffold in which cassettes containing different domains can be swapped for the indigenous domains.

The conclusions on the Cy domains of AngN presented in Chapter 5 are similar to the results obtained for VibF heterocyclization of threonine (104, 106) and they represent the second instance in which two Cy domains in tandem are required for a reaction that in

the yersiniabactin and the pyochelin systems can be performed by a single Cy domain (124, 166). Furthermore, while it can be argued that vibriobactin assembly entails the cyclization of two threonine monomers and thus requires two Cy domains (106), during anguibactin biosynthesis only one heterocyclization step is needed and the presence of two domains with the same functionality seems redundant. Although few residues were identified within the autonomously active domains and these residues were not conserved in those Cy domains that can work only in tandem (50), the question remains open if there is a different mode of action at the molecular level of the two Cy domain kinds.

The anguibactin biosynthetic pathway needs further validation in some of the steps, for example if the A domain of AngR is indeed specific for cysteine and the Cy domain of this same protein is completely obliterated in its function, and additional experiments can be developed to better characterize each domain reaction at a molecular level.

An interesting evolutionary twist to the study of the anguibactin biosynthetic pathway was added by the identification of a highly similar system encoded on the chromosome of the opportunistic human pathogen *Acinetobacter baumannii* (48, 109). The structure of the acinetobactin siderophore differs from anguibactin in that instead of the thiazoline ring of anguibactin generated by cyclization of cysteine there is a methyloxazoline ring in acinetobactin obtained by cyclization of a threonine residue (195). Completing the evolutionary link between these two pathogens it was recently discovered that the outer membrane receptor of each system can recognize and internalize the siderophore produced by the other system (49). Finally, sequencing of the *A. baumannii* gene cluster showed that the domain organization of the acinetobactin genetic

system mirrors topologically that found in the *V. anguillarum* system with minor differences (49, 109). The findings in this thesis can therefore contribute to the analysis of the biosynthetic mechanisms by which acinetobactin is produced. The existence of these two highly related siderophore-mediated iron uptake system in two very distantly related bacteria is interesting not only for the study of their NRPS domains but also from an evolutionary standpoint. As a golden brooch to this section, I would like to add that there have been reports that the human opportunistic pathogen *A. baumannii* was identified as a commensal bacterium in the fish gut (66), which could be the site where the two species met and exchanged genetic information.

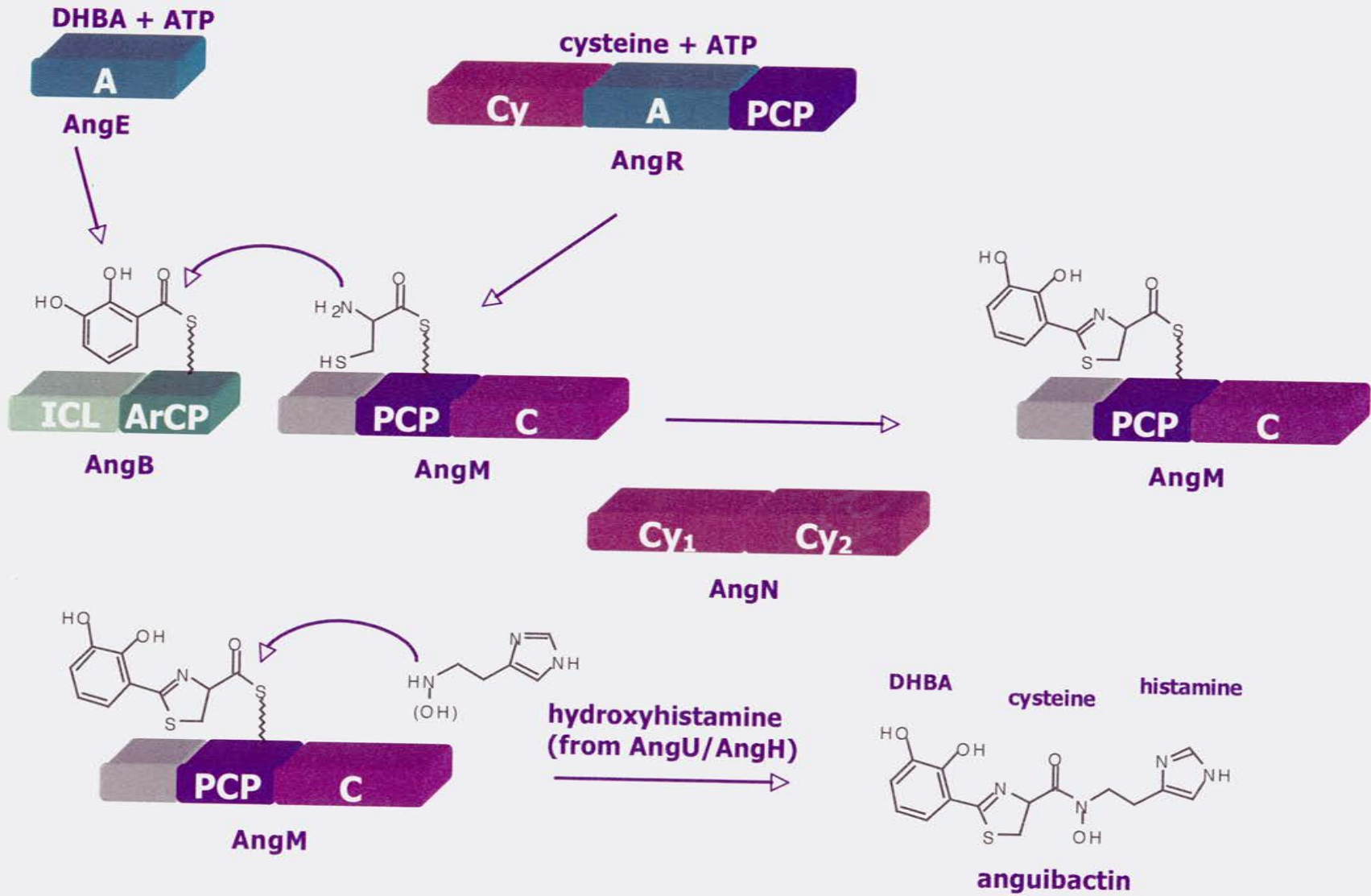
6.1. Summary and conclusions

The studies presented in this thesis identified most of the siderophore biosynthesis genes on the plasmid pJM1 and confirmed that the iron uptake system is the only virulence determinant harbored on the plasmid (Chapter 2). From the analyses of Chapter 2, a model was proposed for the synthesis of anguibactin and the validation of the pathway steps initiated in Chapters 3, 4 and 5. Overall the results from these chapters confirmed the assumptions made from the *in silico* analysis, but also brought new insights on the possible mechanisms of action of NRPS during the assembly of the peptide.

The use of genetics to investigate the functions of the NRPS domains *in vivo* represents a new approach to study the activity of these enzymes and offers to this field an alternative method to exploit the NRPS systems for the production of novel bioactive compounds. As shown in Chapter 3, the combination of *in vitro* and *in vivo* methods can offer the most complete view on the mode of action of each domain and prevent wrong assumptions caused by the limitations of each methodology.

An additional future development of the study of the iron uptake system of *V. anguillarum* comes from the comparison of the biosynthetic machinery of anguibactin with those of other similar siderophores. The many similarities and differences found between the different pathways can be further analyzed to obtain a better understanding of the common mechanisms underlying the synthesis of peptide siderophore and other secondary metabolites.

Figure 6.1. Proposed pathway for anguibactin biosynthesis.



References

1. **Abdallah, M. A., M. Pfestorf, and G. Doring.** 1989. *Pseudomonas aeruginosa* pyoverdinin: structure and function. *Antibiot Chemother* **42**:8-14.
2. **Actis, L. A., W. Fish, J. H. Crosa, K. Kellerman, S. R. Ellenberger, F. M. Hauser, and J. Sanders-Loehr.** 1986. Characterization of anguibactin, a novel siderophore from *Vibrio anguillarum* 775(pJM1). *J Bacteriol* **167**:57-65.
3. **Actis, L. A., S. A. Potter, and J. H. Crosa.** 1985. Iron-regulated outer membrane protein OM2 of *Vibrio anguillarum* is encoded by virulence plasmid pJM1. *J Bacteriol* **161**:736-742.
4. **Actis, L. A., M. E. Tolmasky, and J. H. Crosa.** 1999. Vibriosis, p. 523-557. *In* P. Woo and D. Bruno (ed.), *Fish diseases and disorders. Viral, bacterial, and fungal infections*, vol. 3. Cab International Publishing, Wallingford.
5. **Actis, L. A., M. E. Tolmasky, L. M. Crosa, and J. H. Crosa.** 1995. Characterization and regulation of the expression of FatB, an iron transport protein encoded by the pJM1 virulence plasmid. *Mol Microbiol* **17**:197-204.
6. **Actis, L. A., M. E. Tolmasky, D. H. Farrell, and J. H. Crosa.** 1988. Genetic and molecular characterization of essential components of the *Vibrio anguillarum* plasmid-mediated iron-transport system. *J Biol Chem* **263**:2853-2860.
7. **Alice, A. F., C. S. Lopez, and J. H. Crosa.** 2005. Plasmid- and chromosome-encoded redundant and specific functions are involved in biosynthesis of the siderophore anguibactin in *Vibrio anguillarum* 775: a case of chance and necessity? *J Bacteriol* **187**:2209-2214.

8. **Altschul, S. F., W. Gish, W. Miller, E. W. Myers, and D. J. Lipman.** 1990. Basic local alignment search tool. *J Mol Biol* **215**:403-410.
9. **Arnou, E. L.** 1937. Colorimetric determination of the components of 2,3-dihydroxy-phenylalanine tyrosine mixtures. *J Biol Chem* **118**:531-537.
10. **Baker, H. M., and E. N. Baker.** 2004. Lactoferrin and iron: structural and dynamic aspects of binding and release. *Biometals* **17**:209-216.
11. **Barancin, C. E., J. C. Smoot, R. H. Findlay, and L. A. Actis.** 1998. Plasmid-mediated histamine biosynthesis in the bacterial fish pathogen *Vibrio anguillarum*. *Plasmid* **39**:235-244.
12. **Bashyam, M. D., and S. E. Hasnain.** 2004. The extracytoplasmic function sigma factors: role in bacterial pathogenesis. *Infect Genet Evol* **4**:301-308.
13. **Beare, P. A., R. J. For, L. W. Martin, and I. L. Lamont.** 2003. Siderophore-mediated cell signalling in *Pseudomonas aeruginosa*: divergent pathways regulate virulence factor production and siderophore receptor synthesis. *Mol Microbiol* **47**:195-207.
14. **Becker, K., W. Koster, and V. Braun.** 1990. Iron(III)hydroxamate transport of *Escherichia coli* K12: single amino acid replacements at potential ATP-binding sites inactivate the FhuC protein. *Mol Gen Genet* **223**:159-162.
15. **Berg, D. E.** 1989. Transposon Tn5, p. 185-210. *In* D. E. Berg and M. M. Howe (ed.), *Mobile DNA*. American Society for Microbiology, Washington, D.C.
16. **Bergendahl, V., U. Linne, and M. A. Marahiel.** 2002. Mutational analysis of the C-domain in nonribosomal peptide synthesis. *Eur J Biochem* **269**:620-629.

17. **Birnboim, H. C., and J. Doly.** 1979. A rapid alkaline extraction procedure for screening recombinant plasmid DNA. *Nucleic Acids Res* **7**:1513-1523.
18. **Bobrov, A. G., V. A. Geoffroy, and R. D. Perry.** 2002. Yersiniabactin production requires the thioesterase domain of HMWP2 and YbtD, a putative phosphopantetheinylate transferase. *Infect Immun* **70**:4204-4214.
19. **Bolivar, F.** 1978. Construction and characterization of new cloning vehicles. III. Derivatives of plasmid pBR322 carrying unique *Eco* RI sites for selection of *Eco* RI generated recombinant DNA molecules. *Gene* **4**:121-136.
20. **Borodovsky, M., and M. J.** 1993. GeneMark: parallel gene recognition for both DNA strands. *Comput. Chem.* **17**:123-133.
21. **Boyer, H. W., and D. Roulland-Dussoix.** 1969. A complementation analysis of the restriction and modification of DNA in *Escherichia coli*. *J Mol Biol* **41**:459-472.
22. **Braun, V., R. Gross, W. Koster, and L. Zimmermann.** 1983. Plasmid and chromosomal mutants in the iron(III)-aerobactin transport system of *Escherichia coli*. Use of streptonigrin for selection. *Mol Gen Genet* **192**:131-139.
23. **Braun, V., and H. Killmann.** 1999. Bacterial solutions to the iron-supply problem. *Trends Biochem Sci* **24**:104-109.
24. **Bullen, J. J., and E. Griffiths.** 1999. *Iron and infection*, 2nd ed. John Wiley and Sons Ltd, West Sussex, United Kingdom.
25. **Butterton, J. R., M. H. Choi, P. I. Watnick, P. A. Carroll, and S. B. Calderwood.** 2000. *Vibrio cholerae* VibF is required for vibriobactin synthesis

- and is a member of the family of nonribosomal peptide synthetases. *J Bacteriol* **182**:1731-1738.
26. **Chai, S., T. J. Welch, and J. H. Crosa.** 1998. Characterization of the interaction between Fur and the iron transport promoter of the virulence plasmid in *Vibrio anguillarum*. *J Biol Chem* **273**:33841-33847.
 27. **Challis, G. L., J. Ravel, and C. A. Townsend.** 2000. Predictive, structure-based model of amino acid recognition by nonribosomal peptide synthetase adenylation domains. *Chem Biol* **7**:211-224.
 28. **Chen, Q.** 1995. Ph.D. thesis. Oregon Health & Science University, Portland, Oregon.
 29. **Chen, Q., L. A. Actis, M. E. Tolmasky, and J. H. Crosa.** 1994. Chromosome-mediated 2,3-dihydroxybenzoic acid is a precursor in the biosynthesis of the plasmid-mediated siderophore anguibactin in *Vibrio anguillarum*. *J Bacteriol* **176**:4226-4234.
 30. **Chen, Q., and J. H. Crosa.** 1996. Antisense RNA, Fur, iron, and the regulation of iron transport genes in *Vibrio anguillarum*. *J Biol Chem* **271**:18885-18891.
 31. **Chen, Q., A. M. Wertheimer, M. E. Tolmasky, and J. H. Crosa.** 1996. The AngR protein and the siderophore anguibactin positively regulate the expression of iron-transport genes in *Vibrio anguillarum*. *Mol Microbiol* **22**:127-134.
 32. **Conti, E., T. Stachelhaus, M. A. Marahiel, and P. Brick.** 1997. Structural basis for the activation of phenylalanine in the non-ribosomal biosynthesis of gramicidin S. *Embo J* **16**:4174-4183.

33. **Cornelissen, C. N., and P. F. Sparling.** 1996. Binding and surface exposure characteristics of the gonococcal transferrin receptor are dependent on both transferrin-binding proteins. *J Bacteriol* **178**:1437-1444.
34. **Cornelissen, C. N., and P. F. Sparling.** 2004. Neisseria, p. 256-272. *In* J. H. Crosa, A. R. Mey, and S. M. Payne (ed.), Iron transport in bacteria. ASM Press, Washington D. C.
35. **Craig, N. L.** 1989. Transposon Tn7, p. 211-225. *In* D. E. Berg and M. M. Howe (ed.), Mobile DNA. American Society for Microbiology, Washington, D.C.
36. **Crosa, J. H.** 1989. Genetics and molecular biology of siderophore-mediated iron transport in bacteria. *Microbiol Rev* **53**:517-530.
37. **Crosa, J. H.** 1980. A plasmid associated with virulence in the marine fish pathogen *Vibrio anguillarum* specifies an iron-sequestering system. *Nature* **284**:566-568.
38. **Crosa, J. H.** 1997. Signal transduction and transcriptional and posttranscriptional control of iron-regulated genes in bacteria. *Microbiol Mol Biol Rev* **61**:319-336.
39. **Crosa, J. H., L. L. Hodges, and M. H. Schiewe.** 1980. Curing of a plasmid is correlated with an attenuation of virulence in the marine fish pathogen *Vibrio anguillarum*. *Infect Immun* **27**:897-902.
40. **Crosa, J. H., and C. T. Walsh.** 2002. Genetics and assembly line enzymology of siderophore biosynthesis in bacteria. *Microbiol Mol Biol Rev* **66**:223-249.
41. **Datsenko, K. A., and B. L. Wanner.** 2000. One-step inactivation of chromosomal genes in *Escherichia coli* K-12 using PCR products. *Proc Natl Acad Sci U S A* **97**:6640-6645.

42. **de Lorenzo, V., A. Bindereif, B. H. Paw, and J. B. Neilands.** 1986. Aerobactin biosynthesis and transport genes of plasmid ColV-K30 in *Escherichia coli* K-12. *J Bacteriol* **165**:570-578.
43. **de Lorenzo, V., J. Perez-Martin, L. Escobar, G. Pesole, and G. Bertoni.** 2004. Mode of binding of the Fur protein to target DNA: negative regulation of iron-controlled gene expression, p. 185-196. *In* J. H. Crosa, A. R. Mey, and S. M. Payne (ed.), *Iron transport in bacteria*. ASM Press, Washington D.C.
44. **Debarbieux, L., and C. Wandersman.** 2004. Hemophore-dependent heme acquisition systems, p. 38-47. *In* J. H. Crosa, A. R. Mey, and S. M. Payne (ed.), *Iron transport in bacteria*. ASM Press, Washington D.C.
45. **Di Lorenzo, M., S. Poppelaars, M. Stork, M. Nagasawa, M. E. Tolmasky, and J. H. Crosa.** 2004. A nonribosomal peptide synthetase with a novel domain organization is essential for siderophore biosynthesis in *Vibrio anguillarum*. *J Bacteriol* **186**:7327-7336.
46. **Di Lorenzo, M., M. Stork, A. F. Alice, C. S. Lopez, and J. H. Crosa.** 2004. *Vibrio*, p. 241-255. *In* J. H. Crosa, A. R. Mey, and S. M. Payne (ed.), *Iron transport in bacteria*. ASM Press, Washington D.C.
47. **Di Lorenzo, M., M. Stork, M. E. Tolmasky, L. A. Actis, D. Farrell, T. J. Welch, L. M. Crosa, A. M. Wertheimer, Q. Chen, P. Salinas, L. Waldbeser, and J. H. Crosa.** 2003. Complete sequence of virulence plasmid pJM1 from the marine fish pathogen *Vibrio anguillarum* strain 775. *J Bacteriol* **185**:5822-5830.
48. **Dorsey, C. W., M. E. Tolmasky, J. H. Crosa, and L. A. Actis.** 2003. Genetic organization of an *Acinetobacter baumannii* chromosomal region harbouring

- genes related to siderophore biosynthesis and transport. *Microbiology* **149**:1227-1238.
49. **Dorsey, C. W., A. P. Tomaras, P. L. Connerly, M. E. Tolmasky, J. H. Crosa, and L. A. Actis.** 2004. The siderophore-mediated iron acquisition systems of *Acinetobacter baumannii* ATCC 19606 and *Vibrio anguillarum* 775 are structurally and functionally related. *Microbiology* **150**:3657-3667.
50. **Duerfahrt, T., K. Eppelmann, R. Muller, and M. A. Marahiel.** 2004. Rational design of a bimodular model system for the investigation of heterocyclization in nonribosomal peptide biosynthesis. *Chem Biol* **11**:261-271.
51. **Earhart, C. F.** 2004. Iron uptake via the enterobactin system, p. 133-146. *In* J. H. Crosa, A. R. Mey, and S. M. Payne (ed.), *Iron transport in bacteria*. ASM Press, Washington D.C.
52. **Ehmann, D. E., C. A. Shaw-Reid, H. C. Losey, and C. T. Walsh.** 2000. The EntF and EntE adenylation domains of *Escherichia coli* enterobactin synthetase: sequestration and selectivity in acyl-AMP transfers to thiolation domain cosubstrates. *Proc Natl Acad Sci U S A* **97**:2509-2514.
53. **Emery, T.** 1971. Role of ferrichrome as a ferric ionophore in *Ustilago sphaerogena*. *Biochemistry* **10**:1483-1488.
54. **Faraldo-Gomez, J. D., and M. S. Sansom.** 2003. Acquisition of siderophores in gram-negative bacteria. *Nat Rev Mol Cell Biol* **4**:105-116.
55. **Farrell, D. H., P. Mikesell, L. A. Actis, and J. H. Crosa.** 1990. A regulatory gene, *angR*, of the iron uptake system of *Vibrio anguillarum*: similarity with phage P22 *cro* and regulation by iron. *Gene* **86**:45-51.

56. **Figurski, D. H., and D. R. Helinski.** 1979. Replication of an origin-containing derivative of plasmid RK2 dependent on a plasmid function provided in trans. *Proc Natl Acad Sci U S A* **76**:1648-1652.
57. **Flo, T. H., K. D. Smith, S. Sato, D. J. Rodriguez, M. A. Holmes, R. K. Strong, S. Akira, and A. Aderem.** 2004. Lipocalin 2 mediates an innate immune response to bacterial infection by sequestering iron. *Nature* **432**:917-921.
58. **Frey, J., and H. M. Krisch.** 1985. Omega mutagenesis in gram-negative bacteria: a selectable interposon which is strongly polar in a wide range of bacterial species. *Gene* **36**:143-150.
59. **Furrer, J. L., D. N. Sanders, I. G. Hook-Barnard, and M. A. McIntosh.** 2002. Export of the siderophore enterobactin in *Escherichia coli*: involvement of a 43 kDa membrane exporter. *Mol Microbiol* **44**:1225-1234.
60. **Gaille, C., P. Kast, and D. Haas.** 2002. Salicylate biosynthesis in *Pseudomonas aeruginosa*. Purification and characterization of PchB, a novel bifunctional enzyme displaying isochorismate pyruvate-lyase and chorismate mutase activities. *J Biol Chem* **277**:21768-21775.
61. **Gehring, A. M., K. A. Bradley, and C. T. Walsh.** 1997. Enterobactin biosynthesis in *Escherichia coli*: isochorismate lyase (EntB) is a bifunctional enzyme that is phosphopantetheinylated by EntD and then acylated by EntE using ATP and 2,3-dihydroxybenzoate. *Biochemistry* **36**:8495-8503.
62. **Gehring, A. M., E. DeMoll, J. D. Fetherston, I. Mori, G. F. Mayhew, F. R. Blattner, C. T. Walsh, and R. D. Perry.** 1998. Iron acquisition in plague:

- modular logic in enzymatic biogenesis of yersiniabactin by *Yersinia pestis*. *Chem Biol* **5**:573-586.
63. **Gerdes, K., J. Moller-Jensen, and R. Bugge Jensen.** 2000. Plasmid and chromosome partitioning: surprises from phylogeny. *Mol Microbiol* **37**:455-466.
64. **Gobin, J., C. H. Moore, J. R. Reeve, Jr., D. K. Wong, B. W. Gibson, and M. A. Horwitz.** 1995. Iron acquisition by *Mycobacterium tuberculosis*: isolation and characterization of a family of iron-binding exochelins. *Proc Natl Acad Sci U S A* **92**:5189-5193.
65. **Gonzalez, V., P. Bustos, M. A. Ramirez-Romero, A. Medrano-Soto, H. Salgado, I. Hernandez-Gonzalez, J. C. Hernandez-Celis, V. Quintero, G. Moreno-Hagelsieb, L. Girard, O. Rodriguez, M. Flores, M. A. Cevallos, J. Collado-Vides, D. Romero, and G. Davila.** 2003. The mosaic structure of the symbiotic plasmid of *Rhizobium etli* CFN42 and its relation to other symbiotic genome compartments. *Genome Biol* **4**:R36.
66. **Guardabassi, L., A. Dalsgaard, and J. E. Olsen.** 1999. Phenotypic characterization and antibiotic resistance of *Acinetobacter* spp. isolated from aquatic sources. *J Appl Microbiol* **87**:659-667.
67. **Guerinot, M. L.** 1994. Microbial iron transport. *Annu Rev Microbiol* **48**:743-772.
68. **Guilvout, I., O. Mercereau-Puijalon, S. Bonnefoy, A. P. Pugsley, and E. Carniel.** 1993. High-molecular-weight protein 2 of *Yersinia enterocolitica* is homologous to AngR of *Vibrio anguillarum* and belongs to a family of proteins involved in nonribosomal peptide synthesis. *J Bacteriol* **175**:5488-5504.

69. **Gutteridge, J. M., D. A. Rowley, and B. Halliwell.** 1981. Superoxide-dependent formation of hydroxyl radicals in the presence of iron salts. Detection of 'free' iron in biological systems by using bleomycin-dependent degradation of DNA. *Biochem J* **199**:263-265.
70. **Hahn, M., and T. Stachelhaus.** 2004. Selective interaction between nonribosomal peptide synthetases is facilitated by short communication-mediating domains. *Proc Natl Acad Sci U S A* **101**:15585-15590.
71. **Heinrichs, D. E., and K. Poole.** 1996. PchR, a regulator of ferripyochelin receptor gene (*fptA*) expression in *Pseudomonas aeruginosa*, functions both as an activator and as a repressor. *J Bacteriol* **178**:2586-2592.
72. **Hillson, N. J., C. J. Balibar, and C. T. Walsh.** 2004. Catalytically inactive condensation domain C1 is responsible for the dimerization of the VibF subunit of vibriobactin synthetase. *Biochemistry* **43**:11344-11351.
73. **Hillson, N. J., and C. T. Walsh.** 2003. Dimeric structure of the six-domain VibF subunit of vibriobactin synthetase: mutant domain activity regain and ultracentrifugation studies. *Biochemistry* **42**:766-775.
74. **Hirsch, P. R., and J. E. Beringer.** 1984. A physical map of pPH1JI and pJB4JI. *Plasmid* **12**:139-141.
75. **Holmstrom, K., and L. Gram.** 2003. Elucidation of the *Vibrio anguillarum* genetic response to the potential fish probiont *Pseudomonas fluorescens* AH2, using RNA-arbitrarily primed PCR. *J Bacteriol* **185**:831-842.
76. **Hornig, Y. T., S. C. Deng, M. Daykin, P. C. Soo, J. R. Wei, K. T. Luh, S. W. Ho, S. Swift, H. C. Lai, and P. Williams.** 2002. The LuxR family protein SpnR

- functions as a negative regulator of N-acylhomoserine lactone-dependent quorum sensing in *Serratia marcescens*. *Mol Microbiol* **45**:1655-1671.
77. **Jalal, M., D. Hossain, D. van der Helm, J. Sanders-Loehr, L. A. Actis, and J. H. Crosa.** 1989. Structure of anguibactin, a unique plasmid-related bacterial siderophore from the fish pathogen *Vibrio anguillarum*. *Journal of the American Chemical Society* **111**:292-296.
78. **Katz, L., and R. McDaniel.** 1999. Novel macrolides through genetic engineering. *Med Res Rev* **19**:543-558.
79. **Keating, T. A., C. G. Marshall, and C. T. Walsh.** 2000. Reconstitution and characterization of the *Vibrio cholerae* vibriobactin synthetase from VibB, VibE, VibF, and VibH. *Biochemistry* **39**:15522-15530.
80. **Keating, T. A., C. G. Marshall, and C. T. Walsh.** 2000. Vibriobactin biosynthesis in *Vibrio cholerae*: VibH is an amide synthase homologous to nonribosomal peptide synthetase condensation domains. *Biochemistry* **39**:15513-15521.
81. **Keating, T. A., C. G. Marshall, C. T. Walsh, and A. E. Keating.** 2002. The structure of VibH represents nonribosomal peptide synthetase condensation, cyclization and epimerization domains. *Nat Struct Biol* **9**:522-526.
82. **Keating, T. A., D. A. Miller, and C. T. Walsh.** 2000. Expression, purification, and characterization of HMWP2, a 229 kDa, six domain protein subunit of Yersiniabactin synthetase. *Biochemistry* **39**:4729-4739.

83. **Keating, T. A., and C. T. Walsh.** 1999. Initiation, elongation, and termination strategies in polyketide and polypeptide antibiotic biosynthesis. *Curr Opin Chem Biol* **3**:598-606.
84. **Kleckner, N.** 1989. Transposon *Tn10*, p. 227-268. *In* D. E. Berg and M. M. Howe (ed.), *Mobile DNA*. American Society for Microbiology, Washington, D.C.
85. **Kleinkauf, H., and H. Von Dohren.** 1996. A nonribosomal system of peptide biosynthesis. *Eur J Biochem* **236**:335-351.
86. **Konz, D., and M. A. Marahiel.** 1999. How do peptide synthetases generate structural diversity? *Chem Biol* **6**:R39-48.
87. **Koster, W.** 1991. Iron(III) hydroxamate transport across the cytoplasmic membrane of *Escherichia coli*. *Biol Met* **4**:23-32.
88. **Koster, W. L., L. A. Actis, L. S. Waldbeser, M. E. Tolmasky, and J. H. Crosa.** 1991. Molecular characterization of the iron transport system mediated by the pJM1 plasmid in *Vibrio anguillarum* 775. *J Biol Chem* **266**:23829-23833.
89. **Krewulak, K. D., R. S. Peacock, and H. J. Vogel.** 2004. Periplasmic binding proteins involved in bacterial iron uptake, p. 113-129. *In* J. H. Crosa, A. R. Mey, and S. M. Payne (ed.), *Iron transport in bacteria*. ASM Press, Washington D.C.
90. **Kwong, S. M., C. C. Yeo, and C. L. Poh.** 2001. Molecular analysis of the pRA2 partitioning region: ParB autoregulates *parAB* transcription and forms a nucleoprotein complex with the plasmid partition site, *parS*. *Mol Microbiol* **40**:621-633.
91. **L'Abée-Lund, T. M., and H. Sorum.** 2002. A global non-conjugative Tet C plasmid, pRAS3, from *Aeromonas salmonicida*. *Plasmid* **47**:172-181.

92. **Lambalot, R. H., A. M. Gehring, R. S. Flugel, P. Zuber, M. LaCelle, M. A. Marahiel, R. Reid, C. Khosla, and C. T. Walsh.** 1996. A new enzyme superfamily - the phosphopantetheinyl transferases. *Chem Biol* **3**:923-936.
93. **Larsen, R. A., T. E. Letain, and K. Postle.** 2003. In vivo evidence of TonB shuttling between the cytoplasmic and outer membrane in *Escherichia coli*. *Mol Microbiol* **49**:211-218.
94. **Lemos, M. L., P. Salinas, A. E. Toranzo, J. L. Barja, and J. H. Crosa.** 1988. Chromosome-mediated iron uptake system in pathogenic strains of *Vibrio anguillarum*. *J Bacteriol* **170**:1920-1925.
95. **Lin, D. C., and A. D. Grossman.** 1998. Identification and characterization of a bacterial chromosome partitioning site. *Cell* **92**:675-685.
96. **Linne, U., S. Doekel, and M. A. Marahiel.** 2001. Portability of epimerization domain and role of peptidyl carrier protein on epimerization activity in nonribosomal peptide synthetases. *Biochemistry* **40**:15824-15834.
97. **Linne, U., and M. A. Marahiel.** 2000. Control of directionality in nonribosomal peptide synthesis: role of the condensation domain in preventing misinitiation and timing of epimerization. *Biochemistry* **39**:10439-10447.
98. **Linne, U., D. B. Stein, H. D. Mootz, and M. A. Marahiel.** 2003. Systematic and quantitative analysis of protein-protein recognition between nonribosomal peptide synthetases investigated in the tyrocidine biosynthetic template. *Biochemistry* **42**:5114-5124.
99. **Litwin, C. M., T. W. Rayback, and J. Skinner.** 1996. Role of catechol siderophore synthesis in *Vibrio vulnificus* virulence. *Infect Immun* **64**:2834-2838.

100. **Liu, J., N. Quinn, G. A. Berchtold, and C. T. Walsh.** 1990. Overexpression, purification, and characterization of isochorismate synthase (EntC), the first enzyme involved in the biosynthesis of enterobactin from chorismate. *Biochemistry* **29**:1417-1425.
101. **Mahren, S., S. Enz, and V. Braun.** 2002. Functional interaction of region 4 of the extracytoplasmic function sigma factor FecI with the cytoplasmic portion of the FecR transmembrane protein of the *Escherichia coli* ferric citrate transport system. *J Bacteriol* **184**:3704-3711.
102. **Marahiel, M. A.** 1992. Multidomain enzymes involved in peptide synthesis. *FEBS Lett* **307**:40-43.
103. **Marahiel, M. A., T. Stachelhaus, and H. D. Mootz.** 1997. Modular Peptide Synthetases Involved in Nonribosomal Peptide Synthesis. *Chem Rev* **97**:2651-2674.
104. **Marshall, C. G., M. D. Burkart, T. A. Keating, and C. T. Walsh.** 2001. Heterocycle formation in vibriobactin biosynthesis: alternative substrate utilization and identification of a condensed intermediate. *Biochemistry* **40**:10655-10663.
105. **Marshall, C. G., M. D. Burkart, R. K. Meray, and C. T. Walsh.** 2002. Carrier protein recognition in siderophore-producing nonribosomal peptide synthetases. *Biochemistry* **41**:8429-8437.
106. **Marshall, C. G., N. J. Hillson, and C. T. Walsh.** 2002. Catalytic mapping of the vibriobactin biosynthetic enzyme VibF. *Biochemistry* **41**:244-250.

107. **Mazoy, R., and M. L. Lemos.** 1996. Identification of heme-binding proteins in the cell membranes of *Vibrio anguillarum*. FEMS Microbiol Lett **135**:265-270.
108. **McDougall, S., and J. B. Neilands.** 1984. Plasmid- and chromosome-coded aerobactin synthesis in enteric bacteria: insertion sequences flank operon in plasmid-mediated systems. J Bacteriol **159**:300-305.
109. **Mihara, K., T. Tanabe, Y. Yamakawa, T. Funahashi, H. Nakao, S. Narimatsu, and S. Yamamoto.** 2004. Identification and transcriptional organization of a gene cluster involved in biosynthesis and transport of acinetobactin, a siderophore produced by *Acinetobacter baumannii* ATCC 19606T. Microbiology **150**:2587-2597.
110. **Miller, D. A., L. Luo, N. Hillson, T. A. Keating, and C. T. Walsh.** 2002. Yersiniabactin synthetase: a four-protein assembly line producing the nonribosomal peptide/polyketide hybrid siderophore of *Yersinia pestis*. Chem Biol **9**:333-344.
111. **Miller, D. A., and C. T. Walsh.** 2001. Yersiniabactin synthetase: probing the recognition of carrier protein domains by the catalytic heterocyclization domains, Cy1 and Cy2, in the chain-initiating HWMP2 subunit. Biochemistry **40**:5313-5321.
112. **Milton, D. L., A. Norqvist, and H. Wolf-Watz.** 1992. Cloning of a metalloprotease gene involved in the virulence mechanism of *Vibrio anguillarum*. J Bacteriol **174**:7235-7244.
113. **Milton, D. L., R. O'Toole, P. Horstedt, and H. Wolf-Watz.** 1996. Flagellin A is essential for the virulence of *Vibrio anguillarum*. J Bacteriol **178**:1310-1319.

114. **Moore, C. H., L. A. Foster, D. G. Gerbig, Jr., D. W. Dyer, and B. W. Gibson.** 1995. Identification of alcaligin as the siderophore produced by *Bordetella pertussis* and *B. bronchiseptica*. *J Bacteriol* **177**:1116-1118.
115. **Mootz, H. D., D. Schwarzer, and M. A. Marahiel.** 2002. Ways of assembling complex natural products on modular nonribosomal peptide synthetases. *Chembiochem* **3**:490-504.
116. **Mourino, S., C. R. Osorio, and M. L. Lemos.** 2004. Characterization of heme uptake cluster genes in the fish pathogen *Vibrio anguillarum*. *J Bacteriol* **186**:6159-6167.
117. **Nahlik, M. S., T. P. Fleming, and M. A. McIntosh.** 1987. Cluster of genes controlling synthesis and activation of 2,3-dihydroxybenzoic acid in production of enterobactin in *Escherichia coli*. *J Bacteriol* **169**:4163-4170.
118. **O'Toole, R., D. L. Milton, P. Horstedt, and H. Wolf-Watz.** 1997. RpoN of the fish pathogen *Vibrio (Listonella) anguillarum* is essential for flagellum production and virulence by the water-borne but not intraperitoneal route of inoculation. *Microbiology* **143 (Pt 12)**:3849-3859.
119. **O'Toole, R., D. L. Milton, and H. Wolf-Watz.** 1996. Chemotactic motility is required for invasion of the host by the fish pathogen *Vibrio anguillarum*. *Mol Microbiol* **19**:625-637.
120. **Ogura, T., and A. J. Wilkinson.** 2001. AAA+ superfamily ATPases: common structure--diverse function. *Genes Cells* **6**:575-597.

121. **Olsen, J. E., and J. L. Larsen.** 1990. Restriction fragment length polymorphism of the *Vibrio anguillarum* serovar O1 virulence plasmid. *Appl Environ Microbiol* **56**:3130-3132.
122. **Ozenberger, B. A., M. S. Nahlik, and M. A. McIntosh.** 1987. Genetic organization of multiple *fep* genes encoding ferric enterobactin transport functions in *Escherichia coli*. *J Bacteriol* **169**:3638-3646.
123. **Parsons, J. F., K. Calabrese, E. Eisenstein, and J. E. Ladner.** 2003. Structure and mechanism of *Pseudomonas aeruginosa* PhzD, an isochorismatase from the phenazine biosynthetic pathway. *Biochemistry* **42**:5684-5693.
124. **Patel, H. M., J. Tao, and C. T. Walsh.** 2003. Epimerization of an L-cysteinyll to a D-cysteinyll residue during thiazoline ring formation in siderophore chain elongation by pyochelin synthetase from *Pseudomonas aeruginosa*. *Biochemistry* **42**:10514-10527.
125. **Payne, S. M., and A. R. Mey.** 2004. Pathogenic *Escherichia coli*, *Shigella*, and *Salmonella*, p. 199-218. In J. H. Crosa, A. R. Mey, and S. M. Payne (ed.), *Iron transport in bacteria*. ASM Press, Washington D.C.
126. **Pedersen, K., T. Tiainen, and J. L. Larsen.** 1996. Plasmid profiles, restriction fragment length polymorphisms and O-serotypes among *Vibrio anguillarum* isolates. *Epidemiol Infect* **117**:471-478.
127. **Perkins-Balding, D., A. Rasmussen, and I. Stojiljkovic.** 2004. Bacterial heme and hemoproteins receptors, p. 66-85. In J. H. Crosa, A. R. Mey, and S. M. Payne (ed.), *Iron transport in bacteria*. ASM Press, Washington D.C.

128. **Picardeau, M., J. R. Lobry, and B. J. Hinnebusch.** 2000. Analyzing DNA strand compositional asymmetry to identify candidate replication origins of *Borrelia burgdorferi* linear and circular plasmids. *Genome Res* **10**:1594-1604.
129. **Poirot, O., E. O'Toole, and C. Notredame.** 2003. Tcoffee@igs: A web server for computing, evaluating and combining multiple sequence alignments. *Nucleic Acids Res* **31**:3503-3506.
130. **Poirot, O., K. Suhre, C. Abergel, E. O'Toole, and C. Notredame.** 2004. 3DCoffee@igs: a web server for combining sequences and structures into a multiple sequence alignment. *Nucleic Acids Res* **32**:W37-40.
131. **Pollack, J. R., and J. B. Neilands.** 1970. Enterobactin, an iron transport compound from *Salmonella typhimurium*. *Biochem Biophys Res Commun* **38**:989-992.
132. **Postle, K., and R. A. Larsen.** 2004. The TonB, ExbB, and ExbD proteins, p. 96-112. *In* J. H. Crosa, A. R. Mey, and S. M. Payne (ed.), *Iron transport in bacteria*. ASM Press, Washington D.C.
133. **Quadri, L. E.** 2000. Assembly of aryl-capped siderophores by modular peptide synthetases and polyketide synthases. *Mol Microbiol* **37**:1-12.
134. **Quadri, L. E., T. A. Keating, H. M. Patel, and C. T. Walsh.** 1999. Assembly of the *Pseudomonas aeruginosa* nonribosomal peptide siderophore pyochelin: In vitro reconstitution of aryl-4, 2-bisthiazoline synthetase activity from PchD, PchE, and PchF. *Biochemistry* **38**:14941-14954.
135. **Quadri, L. E., P. H. Weinreb, M. Lei, M. M. Nakano, P. Zuber, and C. T. Walsh.** 1998. Characterization of Sfp, a *Bacillus subtilis* phosphopantetheinyl

- transferase for peptidyl carrier protein domains in peptide synthetases.
Biochemistry **37**:1585-1595.
136. **Ratledge, C., and L. G. Dover.** 2000. Iron metabolism in pathogenic bacteria.
Annu Rev Microbiol **54**:881-941.
137. **Raymond, K. N., and E. A. Dertz.** 2004. Biochemical and physical properties of siderophores, p. 3-17. *In* J. H. Crosa, A. R. Mey, and S. M. Payne (ed.), Iron transport in bacteria. ASM Press, Washington D.C.
138. **Reed, L. J., and H. Muench.** 1938. A simple method of estimating fifty per cent endpoints. The American Journal of Hygiene **27**.
139. **Roche, E. D., and C. T. Walsh.** 2003. Dissection of the EntF condensation domain boundary and active site residues in nonribosomal peptide synthesis. Biochemistry **42**:1334-1344.
140. **Rusnak, F., J. Liu, N. Quinn, G. A. Berchtold, and C. T. Walsh.** 1990. Subcloning of the enterobactin biosynthetic gene *entB*: expression, purification, characterization, and substrate specificity of isochorismatase. Biochemistry **29**:1425-1435.
141. **Sadrzadeh, S. M., and J. Bozorgmehr.** 2004. Haptoglobin phenotypes in health and disorders. Am J Clin Pathol **121 Suppl**:S97-104.
142. **Salinas, P. C., and J. H. Crosa.** 1995. Regulation of *angR*, a gene with regulatory and biosynthetic functions in the pJM1 plasmid-mediated iron uptake system of *Vibrio anguillarum*. Gene **160**:17-23.

143. **Salinas, P. C., L. S. Waldbeser, and J. H. Crosa.** 1993. Regulation of the expression of bacterial iron transport genes: possible role of an antisense RNA as a repressor. *Gene* **123**:33-38.
144. **Sambrook, J., and D. W. Russell.** 2001. *Molecular Cloning: A Laboratory Manual*, 3rd ed. Cold Spring Harbor Laboratory Press, Cold Spring Harbor, NY.
145. **Schaible, U. E., and S. H. Kaufmann.** 2004. Iron and microbial infection. *Nat Rev Microbiol* **2**:946-953.
146. **Schiewe, M. H., J. H. Crosa, and E. J. Ordal.** 1977. Deoxyribonucleic acid relationships among marine vibrios pathogenic to fish. *Can J Microbiol* **23**:954-958.
147. **Schlumbohm, W., T. Stein, C. Ullrich, J. Vater, M. Krause, M. A. Marahiel, V. Kruft, and B. Wittmann-Liebold.** 1991. An active serine is involved in covalent substrate amino acid binding at each reaction center of gramicidin S synthetase. *J Biol Chem* **266**:23135-23141.
148. **Schryvers, A. B., and S. Gray-Owen.** 1992. Iron acquisition in *Haemophilus influenzae*: receptors for human transferrin. *J Infect Dis* **165 Suppl 1**:S103-104.
149. **Schryvers, A. B., and I. Stojiljkovic.** 1999. Iron acquisition systems in the pathogenic *Neisseria*. *Mol Microbiol* **32**:1117-1123.
150. **Schwarzer, D., H. D. Mootz, U. Linne, and M. A. Marahiel.** 2002. Regeneration of misprimed nonribosomal peptide synthetases by type II thioesterases. *Proc Natl Acad Sci U S A* **99**:14083-14088.

151. **Schwarzer, D., H. D. Mootz, and M. A. Marahiel.** 2001. Exploring the impact of different thioesterase domains for the design of hybrid peptide synthetases. *Chem Biol* **8**:997-1010.
152. **Schwyn, B., and J. B. Neilands.** 1987. Universal chemical assay for the detection and determination of siderophores. *Anal Biochem* **160**:47-56.
153. **Seliger, S. S., A. R. Mey, A. M. Valle, and S. M. Payne.** 2001. The two TonB systems of *Vibrio cholerae*: redundant and specific functions. *Mol Microbiol* **39**:801-812.
154. **Serino, L., C. Reimmann, H. Baur, M. Beyeler, P. Visca, and D. Haas.** 1995. Structural genes for salicylate biosynthesis from chorismate in *Pseudomonas aeruginosa*. *Mol Gen Genet* **249**:217-228.
155. **Smith, J. L.** 2004. The physiological role of ferritin-like compounds in bacteria. *Crit Rev Microbiol* **30**:173-185.
156. **Staab, J. F., and C. F. Earhart.** 1990. EntG activity of *Escherichia coli* enterobactin synthetase. *J Bacteriol* **172**:6403-6410.
157. **Stachelhaus, T., A. Huser, and M. A. Marahiel.** 1996. Biochemical characterization of peptidyl carrier protein (PCP), the thiolation domain of multifunctional peptide synthetases. *Chem Biol* **3**:913-921.
158. **Stachelhaus, T., H. D. Mootz, V. Bergendahl, and M. A. Marahiel.** 1998. Peptide bond formation in nonribosomal peptide biosynthesis. Catalytic role of the condensation domain. *J Biol Chem* **273**:22773-22781.
159. **Stein, T., J. Vater, V. Kruff, A. Otto, B. Wittmann-Liebold, P. Franke, M. Panico, R. McDowell, and H. R. Morris.** 1996. The multiple carrier model of

- nonribosomal peptide biosynthesis at modular multienzymatic templates. *J Biol Chem* **271**:15428-15435.
160. **Stephan, H., S. Freund, W. Beck, G. Jung, J. M. Meyer, and G. Winkelmann.** 1993. Ornibactins--a new family of siderophores from *Pseudomonas*. *Biometals* **6**:93-100.
161. **Stephens, D. L., M. D. Choe, and C. F. Earhart.** 1995. *Escherichia coli* periplasmic protein FepB binds ferrienterobactin. *Microbiology* **141 (Pt 7)**:1647-1654.
162. **Stohl, E. A., J. P. Brockman, K. L. Burkle, K. Morimatsu, S. C. Kowalczykowski, and H. S. Seifert.** 2003. *Escherichia coli* RecX inhibits RecA recombinase and coprotease activities in vitro and in vivo. *J Biol Chem* **278**:2278-2285.
163. **Stork, M., M. Di Lorenzo, S. Mourino, C. R. Osorio, M. L. Lemos, and J. H. Crosa.** 2004. Two *tonB* systems function in iron transport in *Vibrio anguillarum*, but only one is essential for virulence. *Infect Immun* **72**:7326-7329.
164. **Stork, M., M. Di Lorenzo, T. J. Welch, L. M. Crosa, and J. H. Crosa.** 2002. Plasmid-mediated iron uptake and virulence in *Vibrio anguillarum*. *Plasmid* **48**:222-228.
165. **Suo, Z.** 2005. Thioesterase portability and peptidyl carrier protein swapping in Yersiniabactin synthetase from *Yersinia pestis*. *Biochemistry* **44**:4926-4938.
166. **Suo, Z., C. T. Walsh, and D. A. Miller.** 1999. Tandem heterocyclization activity of the multidomain 230 kDa HMWP2 subunit of *Yersinia pestis* yersiniabactin

- synthetase: interaction of the 1-1382 and 1383-2035 fragments. *Biochemistry* **38**:17000.
167. **Thariath, A., D. Socha, M. A. Valvano, and T. Viswanatha.** 1993. Construction and biochemical characterization of recombinant cytoplasmic forms of the IucD protein (lysine:N6-hydroxylase) encoded by the pColV-K30 aerobactin gene cluster. *J Bacteriol* **175**:589-596.
168. **Theil, E. C.** 2003. Ferritin: at the crossroads of iron and oxygen metabolism. *J Nutr* **133**:1549S-1553S.
169. **Tolmasky, M. E., L. A. Actis, and J. H. Crosa.** 1988. Genetic analysis of the iron uptake region of the *Vibrio anguillarum* plasmid pJM1: molecular cloning of genetic determinants encoding a novel trans activator of siderophore biosynthesis. *J Bacteriol* **170**:1913-1919.
170. **Tolmasky, M. E., L. A. Actis, and J. H. Crosa.** 1995. A histidine decarboxylase gene encoded by the *Vibrio anguillarum* plasmid pJM1 is essential for virulence: histamine is a precursor in the biosynthesis of anguibactin. *Mol Microbiol* **15**:87-95.
171. **Tolmasky, M. E., L. A. Actis, and J. H. Crosa.** 1993. A single amino acid change in AngR, a protein encoded by pJM1-like virulence plasmids, results in hyperproduction of anguibactin. *Infect Immun* **61**:3228-3233.
172. **Tolmasky, M. E., L. A. Actis, A. E. Toranzo, J. L. Barja, and J. H. Crosa.** 1985. Plasmids mediating iron uptake in *Vibrio anguillarum* strains isolated from turbot in Spain. *J Gen Microbiol* **131 (Pt 8)**:1989-1997.

173. **Tolmasky, M. E., and J. H. Crosa.** 1995. Iron transport genes of the pJM1-mediated iron uptake system of *Vibrio anguillarum* are included in a transposonlike structure. *Plasmid* **33**:180-190.
174. **Tolmasky, M. E., and J. H. Crosa.** 1984. Molecular cloning and expression of genetic determinants for the iron uptake system mediated by the *Vibrio anguillarum* plasmid pJM1. *J Bacteriol* **160**:860-866.
175. **Tolmasky, M. E., P. C. Salinas, L. A. Actis, and J. H. Crosa.** 1988. Increased production of the siderophore anguibactin mediated by pJM1-like plasmids in *Vibrio anguillarum*. *Infect Immun* **56**:1608-1614.
176. **Tolosano, E., and F. Altruda.** 2002. Hemopexin: structure, function, and regulation. *DNA Cell Biol* **21**:297-306.
177. **von Dohren, H., R. Dieckmann, and M. Pavela-Vrancic.** 1999. The nonribosomal code. *Chem Biol* **6**:R273-279.
178. **von Dohren, H., U. Keller, J. Vater, and R. Zocher.** 1997. Multifunctional Peptide Synthetases. *Chem Rev* **97**:2675-2706.
179. **Waldbeser, L. S., Q. Chen, and J. H. Crosa.** 1995. Antisense RNA regulation of the *fatB* iron transport protein gene in *Vibrio anguillarum*. *Mol Microbiol* **17**:747-756.
180. **Waldbeser, L. S., M. E. Tolmasky, L. A. Actis, and J. H. Crosa.** 1993. Mechanisms for negative regulation by iron of the *fatA* outer membrane protein gene expression in *Vibrio anguillarum* 775. *J Biol Chem* **268**:10433-10439.
181. **Walsh, C. T., H. Chen, T. A. Keating, B. K. Hubbard, H. C. Losey, L. Luo, C. G. Marshall, D. A. Miller, and H. M. Patel.** 2001. Tailoring enzymes that

- modify nonribosomal peptides during and after chain elongation on NRPS assembly lines. *Curr Opin Chem Biol* **5**:525-534.
182. **Walsh, C. T., and C. G. Marshall.** 2004. Siderophore biosynthesis in bacteria, p. 18-37. *In* J. H. Crosa, A. R. Mey, and S. M. Payne (ed.), *Iron transport in bacteria*. ASM Press, Washington D.C.
183. **Walter, M. A., S. A. Potter, and J. H. Crosa.** 1983. Iron uptake system mediated by *Vibrio anguillarum* plasmid pJM1. *J Bacteriol* **156**:880-887.
184. **Warner, P. J., P. H. Williams, A. Bindereif, and J. B. Neilands.** 1981. ColV plasmid-specific aerobactin synthesis by invasive strains of *Escherichia coli*. *Infect Immun* **33**:540-545.
185. **Waters, V. L., and J. H. Crosa.** 1991. Colicin V virulence plasmids. *Microbiol Rev* **55**:437-450.
186. **Weber, T., R. Baumgartner, C. Renner, M. A. Marahiel, and T. A. Holak.** 2000. Solution structure of PCP, a prototype for the peptidyl carrier domains of modular peptide synthetases. *Structure Fold Des* **8**:407-418.
187. **Weinberg, E. D.** 1993. The development of awareness of iron-withholding defense. *Perspect Biol Med* **36**:215-221.
188. **Welch, T. J., S. Chai, and J. H. Crosa.** 2000. The overlapping *angB* and *angG* genes are encoded within the trans-acting factor region of the virulence plasmid in *Vibrio anguillarum*: essential role in siderophore biosynthesis. *J Bacteriol* **182**:6762-6773.

189. **Wertheimer, A. M., M. E. Tolmasky, L. A. Actis, and J. H. Crosa.** 1994. Structural and functional analyses of mutant Fur proteins with impaired regulatory function. *J Bacteriol* **176**:5116-5122.
190. **Wertheimer, A. M., W. Verweij, Q. Chen, L. M. Crosa, M. Nagasawa, M. E. Tolmasky, L. A. Actis, and J. H. Crosa.** 1999. Characterization of the *angR* gene of *Vibrio anguillarum*: essential role in virulence. *Infect Immun* **67**:6496-6509.
191. **Williams, P. H., and N. H. Carbonetti.** 1986. Iron, siderophores, and the pursuit of virulence: independence of the aerobactin and enterochelin iron uptake systems in *Escherichia coli*. *Infect Immun* **51**:942-947.
192. **Wolf, M. K., and J. H. Crosa.** 1986. Evidence for the role of a siderophore in promoting *Vibrio anguillarum* infections. *J Gen Microbiol* **132 (Pt 10)**:2949-2952.
193. **Wooldridge, K. G., and P. H. Williams.** 1993. Iron uptake mechanisms of pathogenic bacteria. *FEMS Microbiol Rev* **12**:325-348.
194. **Wyckoff, E. E., J. A. Stoebner, K. E. Reed, and S. M. Payne.** 1997. Cloning of a *Vibrio cholerae* vibriobactin gene cluster: identification of genes required for early steps in siderophore biosynthesis. *J Bacteriol* **179**:7055-7062.
195. **Yamamoto, S., N. Okujo, and Y. Sakakibara.** 1994. Isolation and structure elucidation of acinetobactin, a novel siderophore from *Acinetobacter baumannii*. *Arch Microbiol* **162**:249-254.

196. **Yeh, E., R. M. Kohli, S. D. Bruner, and C. T. Walsh.** 2004. Type II thioesterase restores activity of a NRPS module stalled with an aminoacyl-S-enzyme that cannot be elongated. *ChemBiochem* **5**:1290-1293.